12-12-2017 9:30 AM

Hydrodeoxygenation of Anisole in a Novel Externally Agitated Reactor

Brett Pomeroy, *The University of Western Ontario*

Supervisor: Dominic Pjontek, *The University of Western Ontario*

A thesis submitted in partial fulfillment of the requirements for the Master of Engineering Science degree in Chemical and Biochemical Engineering

Abstract

Bio-oil upgrading via hydrodeoxygenation (HDO) was investigated using anisole, a model compound, in a novel Externally Agitated (EA) reactor which is expected to enhance gas-liquid-solid mixing. Operating conditions were established based on anisole HDO with 10 wt.% Ni on silica, γ-alumina, and δ-alumina while varying temperatures between 160 to 280^{o}C, and reaction times between 30 – 90 minutes. Mild temperatures of 220^{o}C and 45 minutes for reaction time with γ-alumina were selected for subsequent work since γ-alumina demonstrated the highest HDO activity. HDO was then investigated with varying Ni-Cu and Ni loadings. Despite the improved reducibility from copper addition, monometallic Ni catalysts had higher cyclohexane yields, whereas conversion and coke varied based on total metal loading. Increasing Ni loading from 2 – 10 wt.% improved hydrogenation but deoxygenation to cyclohexane remained constant. Lanthanum promotion to Ni and Ni-Cu catalysts improved reducibility, however, lowered conversion and cyclohexane yields, and increased coke formation.

Keywords

Bio-oil upgrading, hydrodeoxygenation, catalysis, transition metal, bifunctional catalyst, hydrogenation, model compound, promoter

Co-Authorship Statement

Chapter 3

Article Title: Anisole Hydrodeoxygenation over Low Loading Ni and Ni-Cu Catalysts in a Novel Externally Agitated Reactor
Authors: Brett Pomeroy, Dongmin Yun, Jose Herrera, Dominic Pjontek
Status: To be submitted
Contributions: Brett Pomeroy conducted all experimental work, analyzed the data and wrote the manuscript. Dongmin Yun helped in catalyst preparation and analysis. Jose Herrera provided assistance throughout the project and review drafts. The project was supervised by Dominic Pjontek who provided technical advice and reviewed the drafts for this work.

Chapter 4

Article Title: Anisole Hydrodeoxygenation over Lanthanum Promoted Ni and Ni-Cu Catalysts in a Novel Externally Agitated Reactor
Authors: Brett Pomeroy, Dominic Pjontek
Status: To be submitted
Contributions: Brett Pomeroy conducted all experimental work, analyzed the data and wrote the manuscript. The project was supervised by Dominic Pjontek who provided technical advice and reviewed the drafts for this work.

Acknowledgements

First and foremost, I would like to express immense gratitude to my supervisor Dr. Dominic Pjontek for his endless guidance and support throughout the entirety of my master's program. I appreciate his endless knowledge and assistance in this thesis writing.

I would like to thank Dr. Jose Herrera for his experimental advice and allowing me access to his lab and equipment to conduct various catalyst characterization. Also, I would like to thank Dongmin Yun for his assistance with catalyst preparation and gas chromography methods. I would like to thank Fang Cao for carrying out TGA analysis of spent catalysts and Reddy Kandlakuti for performing BET and ICP analysis.

I would also like to thank the members of the University Machine Shop (UMS) with the construction and installing of the EA reactor, as well as Tom Johnson of ICFAR for his help with the reactor setup and all related technical problems.

I would like to finally thank my family, specifically my parents Laurie and Bud Pomeroy, for their unconditional love and support over these past two years.

Table of Contents

List of Tables

List of Figures

Chapter 1

1.1 Introduction

As energy demands are projected to increase by 48% over the next 20 years, primarily from a rise in transportation and public access in developing countries, there is a growing need for sustainable energy sources that are renewable and more environmentally friendly than currently used fossil fuels (U.S. Energy Information Administration, 2017). Non-renewable fossil fuel reserves such as natural gas, coal, and petroleum oil represent the majority total global energy supply with reports as high as 86%; however, these are being depleted at an alarming rate and sustainable alternatives must be found to ensure global energy security (BP Statistical Review of World Energy, 2017). In addition to energy supply, the concern for global warming due to excessive green house gas (GHG) and CO_2 emissions, for which fossil fuels are a main contributor, further hastens the necessity for carbon neutral methods of energy and chemical production, and a drastic shift away from non-renewable resources. Research into renewable energies from biomass has been widespread to resolve these issues of fossil fuel usage, yet current reports show biomass supports only approximately 10% of the worlds energy demand (Rosillo-Calle, 2016). Biomass has progressively been considered as a promising renewable substitute for biofuel and chemical production due to its availability, reduced environmental impact and GHG emissions, and carbon neutrality compared to petroleum (Mante et al., 2011). Although promising, the viability of biomass is not without its challenges. More efficient conversion technologies, reduced processing costs, and reliable as well as cost effective feedstocks are necessary before biomass can be considered a feasible alternative to fossil fuels (Chakraborty et al., 2012; Sims et al., 2010).

Biofuels can be divided into two main categories, first or second generation, depending on the feedstock it is derived from. First-generation biofuels, which represent most current bioethanol and biodiesel production, use biomass feedstocks that are considered edible, such as sugarcane, corn, soybeans, and oilseeds including canola and palm. Bioethanol is generally made through fermentation of glucose from sugars and starches, while biodiesel is made via esterification/ transesterification of fatty acids and oils, with upwards of 95% from edible vegetable oils (Yusuf et al., 2011). This is undesirable as these crops compete for food availability, require high amounts of land and water, and represent a small fraction of biomass (Alonso et al., 2010). More favourable

second-generation or “advanced” biofuels use non-edible feedstocks such as lignocellulosic biomass, woody crops and sawdust, as well as agricultural and municipal waste which do not compete with food resources and represent a larger portion of biomass (Lynd, 1996). Lignocellulosic biomass has shown promise as a reliable feedstock due to its abundance as a biomass feedstock, no overlap with food and land availability, fast growing, and extremely low cost (J. Kumar & Reetu, 2015). There are major difficulties, however, when it comes to refining and purifying as current technologies are limited in efficiently breaking up lignocellulosic biomass into its fundamental parts for downstream processing and upgrading (Saini et al., 2015).

Lignocellulosic biomass is composed of three components; lignin, cellulose, and hemicellulose, each having individual properties and applications. The main component is cellulose, a polysaccharide of β-glycosidic linked glucose monomers that comprises approximately 40 to 50 wt.% of lignocellulosic biomass (Mante et al., 2011). Due to a large amount of hydrogen bonds between molecules, cellulose is highly resistant to degradation by hydrolysis and is usually separated from other lignocellulosic fractions for more effective glucose separation and use in bioethanol production (Demirbaş, 2005). Hemicellulose comprises approximately 15 to 30 wt.% of all lignocellulosic biomass, is amorphous and composed of a variety of randomly arranged C5 and C6 monosaccharides, mostly containing xylose but also some glucose. Unlike cellulose, hemicellulose is more easily degraded during hydrolysis and the separated pentoses and hexoses can also be fermented for bioethanol (Harmsen & Huijgen, 2010). Finally, lignin consists of approximately 15 to 30 wt.% of the biomass and is rich in oxygenated aromatic species, mainly 3 phenolic molecules; p – coumaryl alcohol, coniferyl alcohol, and sinapyl alcohol (Galkin & Samec, 2016). Since lignin is a major contributor to plant stability and structure, it surrounds hemicellulose and cellulose and must be separated to be able to access the interior carbohydrate fractions. Until recently, lignin has generally been considered a waste product with only about 2% of lignin is currently recovered for use in chemical or biofuel production, whereas the remainder is burned for energy generation (Alonso et al., 2012). With an annual production of approximately 300 billion tonnes, this presents an untapped renewable resource with a huge potential for high valued chemical and biofuel production (Laurichesse & Avérous, 2014).

1.2 Pyrolysis Bio-oil Upgrading

Proposed methods for the conversion of lignocellulosic biomass to transportation biofuels and chemical intermediates involve a combination of thermochemical and/or biochemical processes. Thermochemical methods that have been shown to be conceivable strategies for biofuel and chemical production include liquefaction, gasification, hydrolysis, and pyrolysis.

Liquefaction involves thermal decomposition of biomass under increased pressures typically between 4 and 20 MPa, moderate temperatures approximately 200°C to 370°C, and residence times of a few hours (Elliott et al., 1991). A major advantage of the liquefaction method is the ability to process high moisture feedstocks, eliminating the need for drying typically involved in pyrolysis and gasification methods (Peterson et al., 2008). Although liquefaction produces a higher quality bio-oil with lower oxygen content when compared to pyrolysis, the higher operating pressures increase operating costs and product yields are lower relative to pyrolysis, reducing its applicability (He & Wang, 2012).

Syngas formation via gasification followed by Fischer-Tropsch, to make diesel-ranged hydrocarbons, or methanol synthesis has also been demonstrated for biomass. Gasification involves incomplete combustion of biomass at temperatures between 700 – 900ºC, leading to gas yields of approximately 85%, mainly consisting of hydrogen, carbon monoxide, methane, and carbon dioxide (Molino et al., 2016). Gasification can use almost any lignocellulosic feedstock, including waste material that are generally unfit for other conversion methods; however, heat and energy requirements are significant and high quality and clean syngas is difficult to obtain (Sikarwar et al., 2016).

Hydrolysis of polysaccharides extracted from cellulose and hemicellulose involves cleaving β-glycosidic bonds between sugar molecules to form monosaccharides and a range of partially hydrolyzed oligomers, which can then be further processed or fermented. These reactions are usually carried out using acid or base catalysts, depending on the sugars present, at temperatures between 100°C and 300°C (Chheda et al., 2007). Although hydrolysis is efficient at producing highly selective chemical intermediates and hydrocarbons once sugars are separated, the costly and complex pretreatments necessary to isolate the sugars have limited its full utilization (Mahmood et al., 2015).

Finally, pyrolysis involves thermal decomposition in the absence of oxygen at temperatures of approximately 500°C, atmospheric pressures with an inert gas such as nitrogen, varying residence times, with the possibility to condense the resulting vapours (Bridgwater, 2012). Pyrolysis products are a combination of solids, including ash and biochar, non-condensable gases, and liquids/condensed vapours commonly referred as bio-oil. Pyrolysis product yields generally depend on feedstock, temperature, vapor residence time, and reactor configuration (Alonso et al., 2010). Bio-oil yields can be maximized (upwards of around 75 wt.%) by limiting residence times to less than 2 seconds, enforcing heating rates greater than 1000°C/s, and rapid condensation of the product vapours (Bridgwater, 2015). Feedstock pretreatment consisting of drying and grinding to form fine particles, control requirements for operating conditions, and the need for downstream processing increases costs and complexity for pyrolysis (Mohan et al., 2006; Bridgwater, 2012).

The main issue for the previous biomass conversion methods is discovering low-cost processing technologies as current approaches require large amounts of energy and involve multiple complex steps to complete (Gandarias & Arias, 2013). Pyrolysis has been shown to be a promising technique by utilizing all biomass components (unlike hydrolysis), ease of transportation and storage of liquid products (rather than gases), reduced operating pressures and higher yields (when compared to liquefaction) (Huynh, et al., 2015).

Prior to recent interests for liquid fuel production from sustainable resources, slow pyrolysis was conventionally performed for biochar production, where lower heating rates and longer vapour residence times between 5 – 30 minutes are implemented (Bridgwater, 1999). Produced vapours continue to react due to the residence time, resulting in higher biochar and gas yields when compared to fast pyrolysis (Mohan et al., 2006). By controlling reaction temperatures around 500^{o}C with fast heating rates and short vapour residence times of only a few seconds, liquid yields can be optimized in fast pyrolysis, which is more desirable for bio-oil production (Bridgwater, 2012). An example of product yields with increasing reaction temperature is shown in Figure 1.1a. Many reactor configurations have been considered and implemented for effective fast pyrolysis to achieve the necessary high heating rates, controlled reaction temperatures, short residence times, and rapid cooling to isolate pyrolysis vapours. The most common type of commercialized reactor are fluidized beds due to their ease of operation and scale-up, though limited by the effective heat transfer through biomass particles and large amounts of carrier gas

(Bridgwater, 1999). Figure 1.1b shows the typical layout of a pyrolysis fluidized bed system. Globally recognized fast pyrolysis processes include Ensyn with two circulating fluidized beds with capacities of 1500kg/h, Bio-alternative with a 2000 kg/h fixed bed bed plant, and THEE with a smaller bubbling fluidized bed plant capable of 500 kg/h (Kumar & Nanda, 2016).

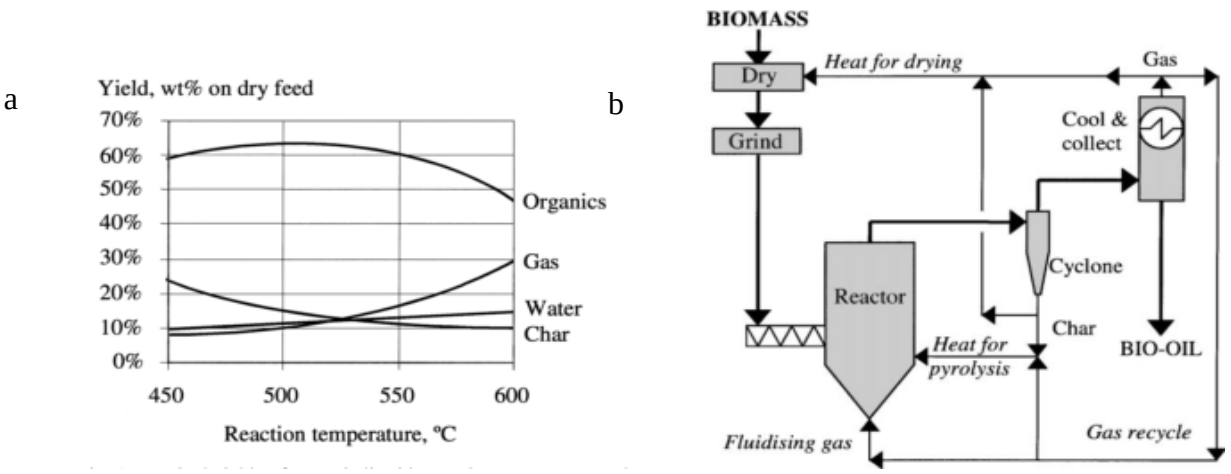

Figure 1.1 a) Product yields from fast pyrolysis in relation to reaction temperature and b) typical layout of a pyrolysis fluidized bed system (Bridgwater, 1999)

It is presently acknowledged that the conversion of pyrolysis bio-oils to biofuels as a replacement for gasoline or diesel in the transportation sector is not economically favourable. The relatively low cost of crude oil, high feedstock costs, and expensive or inefficient current refining processes lead biofuel production to be financially uncompetitive compared to current petroleum hydroprocessing (Wright et al., 2010; Kumar et al., 2016; De Wild et al., 2014). The production of high-value chemicals from bio-oils within the bio-refinery concept has nonetheless recently been investigated as a way to improve the economic viability of biomass pyrolysis (Butler et al., 2011; Cherubini, 2010). The aromaticity of lignocellulosic biomass provides the potential as a renewable replacement for several valuable phenolic compounds, such as benzene, toluene, and xylene (BXT) which are chemical building blocks and are almost entirely sourced from fossil sources (Laurichesse & Avérous, 2014). The remaining bio-oil components after extraction of selected high-value chemicals can then be upgraded to transportation fuels. Recent interests have focused on the production of biofuels for aviation and marine uses. Fuel is reported to be the largest operating cost for commercial airlines, accounting for 29% in 2014 (Radich, 2015). By blending even a small percentage of biofuel to conventional aviation fuels, green house gas emissions could

be drastically reduced in the global aviation industry (Jiménez-Díaz et al., 2017). Furthermore, typical marine fuels are of lower quality compared to diesel used for road transport, requiring less refining to convert bio-oils to suitable marine fuels (Chong & Bridgwater, 2017).

The principal difference between petroleum-derived fuels and pyrolysis oil is the high oxygen content in the latter. The increased amount of oxygen in pyrolysis oil, including up to 40 wt.%, imposes problems when attempting to implement biomass-derived oil as a liquid fuel or blending with conventional crude oils, which commonly have less than 2 wt. % of oxygen (Furimsky, 2000). Oxygenated compounds and water content lead to undesirable properties such as low heating values, thermal instability, high acidity and corrosiveness, increased viscosity, and immiscibility with crude oils due to polar and hydrophilic compounds (Ardiyanti et al., 2016). A property comparison between bio-oil and crude oil is provided in Table 1.1. Effective techniques to lower the oxygen content of biomass-derived pyrolysis oils, known as bio-oil "upgrading", are required to make it a more suitable component for traditional fuels.

Table 2.1 Property comparison between typical bio-oil and crude oil. (Oasmaa & Czernik, 1999; Mortensen et al., 2011)

Property	Bio-oil	Crude Oil
Moisture Content (wt%)	25	0.1
pH	~3	-
Elemental Analysis		
C (wt%)	55-65	83-86
H (wt%)	5-7	11-14
O (wt%)	30-40	<1
N (wt%)	0-0.2	<1
HHV (MJ/kg)	16-19	44
Viscosity at 50^{o}C (cP)	40 – 100	180
Char (wt%)	0-0.2	1

Zeolite cracking and catalytic hydrodeoxygenation (HDO) have primarily been investigated as potential catalytic upgrading methods to reduce the oxygen-content of pyrolysis oils. Cracking via zeolites takes place without the need of hydrogen as a reducing gas and expels oxygen in the form of carbon dioxide and water at atmospheric pressures and temperatures between

300 to 600^{o}C (He & Wang, 2012). Requiring no external hydrogen source and atmospheric pressures greatly lowers costs, making zeolite cracking appealing; however, it has been suggested unfeasible with current technologies due to low yields or approximately 20 wt.%, and excessive carbon formation, with some reports as high as 40 wt.% (Balat et al., 2009). Catalytic hydrodeoxygenation requires large amounts of hydrogen at elevated pressures, increasing upgrading costs, though the higher yields and existing technologies in petroleum hydrotreatment as a starting points makes this method more desirable (Bulushev & Ross, 2011).

Catalytic hydrodeoxygenation has been identified as a preferred upgrading method due to experience with existing petroleum hydrotreating technologies (Zacher et al., 2014). Hydrodeoxygenation of pyrolysis oil typically involves a heterogeneous catalyst, high hydrogen pressures (up to 200 MPa), and temperatures ranging from 200 to 400^{o}C, where oxygen is removed primarily as water with minimal carbon dioxide and carbon monoxide (Mortensen et al., 2013). Reactions include hydrocracking, cracking, and hydrogenation occurring alongside hydrodeoxygenation, shown in Figure 1.2 where reaction conditions, catalyst, and reactor configuration can modify extent of the previous reactions (Mortensen et al., 2011). Decarboxylation and decarbonylation are endothermic side reactions forming CO_2 and CO, respectively, which are undesired as they lower the overall carbon content of the upgraded product (Srifa et al., 2015). The extent of possible reactions makes bio-oil upgrading a challenging process to achieve the desired deoxygenation levels without reducing the overall carbon content and minimizing the use of costly hydrogen gas.

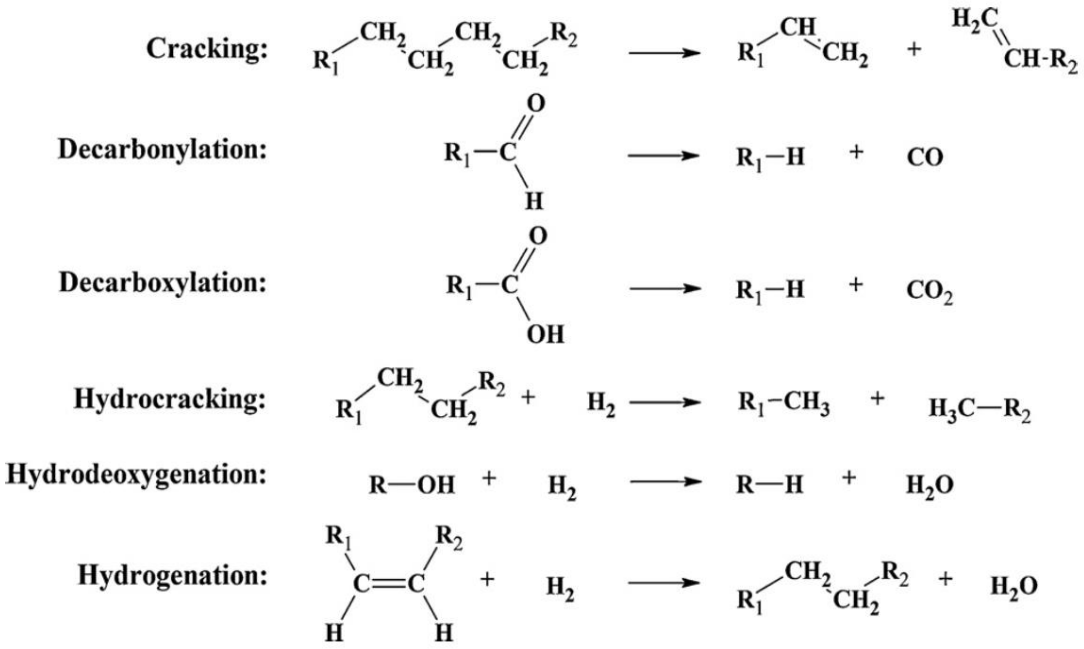

Figure 1.2 Main reactions related to catalytic bio-oil upgrading (Mortensen et al., 2011)

Although catalytic hydrodeoxygenation has been recognized as an effective method for bio-oil upgrading, major challenges remain for effective catalyst formulations and reactor configurations. The objective is to identify inexpensive catalysts that are highly active for deoxygenation reactions at mild conditions (temperatures <300^{o}C and pressures <10 MPa) and with long catalytic lifespan by being resistant to coke formation, the main cause of catalyst deactivation (Mortensen et al., 2013). Pacific Northwest National Laboratory (PNNL), experienced in biofuel research, reported a maximum catalyst lifespan of approximately 100 hours on stream using a sulfided ruthenium catalyst in a fixed-bed reactor, until excessive coke formation lead to reactor plugging and complete catalyst deactivation (Elliott et al., 2012).

Crude pyrolysis bio-oil is a complex mixture of highly oxygenated hydrocarbons resulting from depolymerization and fragmentation reactions of the three building blocks of lignocellulosic biomass (i.e., cellulose, hemicellulose, and lignin) and highly influenced by feedstock and pyrolysis conditions (Mohan et al., 2006). Over 400 compounds have been idenfied in pyrolytic bio-oils, consisting of acids, esters, alcohols, ketones, aldehydes, and phenols, which are typically aromatic in nature (Huber et al., 2006). Other issues arise with storage of pyrolysis oils due to compounds being thermally unstable, polymerizing under air and forming high molecular weight resins which undergo phase seperation over time. Bio-char frequently contained within bio-oils is difficult to remove and can agglomerate and plug reactors, which can be further problematic during upgrading experiments (Bridgwater, 2012). Due to complications when conducting studies with actual bio-oil, model compounds are frequently used to simplify the analysis as well as provide more details into reaction mechanisms and kinetics. Phenolic compounds such as guaiacol, phenol and anisole are typically selected as appropriate model compounds as they comprise a large fraction (30-40%) of bio-oils produced from lignocellulosic biomass, and their C-O bond is difficult to break (Foster et al., 2012; Massoth et al., 2006). Anisole was selected as the model compound for this study as it is of intermediate complexity between phenol and guaiacol. Compared to guaiacol with two separate functional groups, anisole forms fewer possible products during HDO and thus, is easier to identify specific reaction mechanisms that are present. It is important to note that model compounds can provide valuable insights and be effective for screening purposes in HDO studies; however, limitations and difficulties can arise when extrapolating to actual pyrolysis bio-oils.

Reaction pathways that have been observed for HDO of anisole typically involve one of two main routes, resulting in a deoxygenated product of either cyclohexane or benzene. An overview of the major reaction pathways that have been observed for HDO of anisole is presented in figure 1.3.

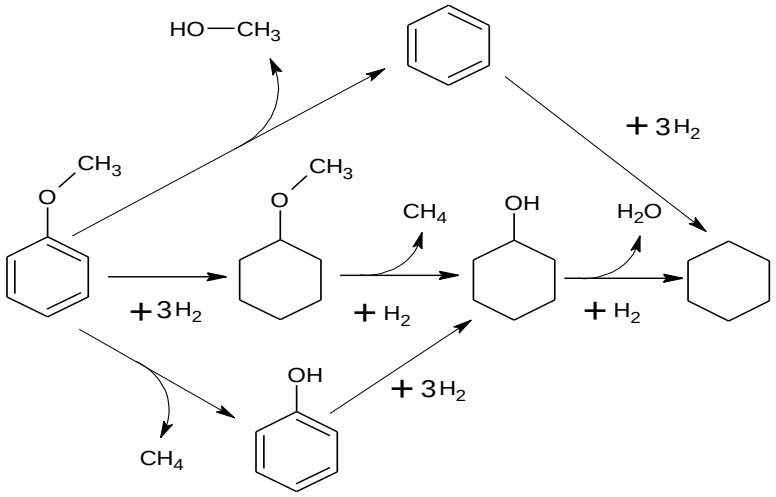

Figure 1.3. Overview of reaction pathways present for HDO of anisole.

One reaction pathway involves an initial hydrogenation of the aromatic ring followed by deoxygenation to form cyclohexane (Khromova et al., 2014). The other reaction pathway consists of a direct deoxygenation to form benzene, where some studies have reported it to remain benzene, or can also be further hydrogenated to form cyclohexane (Wang et al., 2017; Smirnov et al., 2014). Few reports have also reported the formation of phenol following HDO of anisole, however, this is rare as it is typically hydrogenated to form cyclohexanol (Zhu et al., 2011; Sankaranarayanan et al., 2015). Studies are unclear which parameters influence the dominate reaction pathway, where some reports have proposed the presence of two separate active sites that facilitate the occurrence of each reaction pathway (Khromova et al., 2014). Other reports have indicated reaction temperature to influence whether hydrogenation or deoxygenation occurs initially (Robinson et al., 2016). Benzene content increased when reaction temperature increased from 200°C to 280°C (Zhang et al., 2016). Nonetheless, it is more likely to break the bond of the ether in anisole on the methyl side instead of the aromatic ring side due to a lower bond dissociation energy, thus forming cyclohexanol instead of benzene (Wang et al., 2017). Furthermore, hydrogenation of the aromatic ring is necessary at lower temperatures to weaken the C-O bond, requiring less energy to break in cyclohexanol relative to phenol (Robinson et al., 2016).

1.3 Catalysts

Catalyst studies initially focused on sulfided hydrodesulfurization (HDS) catalysts that had been used extensively for petroleum hydrotreating, where unlike bio-oil, has a high content of sulfur (Ryymin et al., 2009; Popov et al., 2013; (Marchal et al., 1996; Louwers et al., 1993). Examples of such catalysts include sulfided CoMo and NiMo supported on alumina, which demonstrated similar mechanisms for oxygen removal as observed for sulfur removal (Huber & Corma, 2007). It is predicted that vacant sulfur sites on the outside of the molybdenum-sulfur phase, formed from the release of H_2S in a hydrogen environment, are the main active sites for HDO and HDS. Nickel or cobalt are added as promoters which donate electrons to Mo, weakening the Mo-S bond and increasing the number of vacant sulfur sites (Romero et al., 2010). It was observed that sulfided catalysts deactivated rapidly due to sulfur stripping from the catalyst, thus requiring an external sulfur source (i.e. H_2S) for regeneration. Bio-oil has minimal concentrations of sulfur, hence needing sulfur addition and contamination of the upgraded product (Huynh et al., 2015). Sulfided catalysts were also reported susceptible to water deactivation, a major by-product of HDO, as well as coke formation (Jin et al., 2014).

Noble metals have also been studied as promising bio-oil upgrading catalysts as they have been shown effective for hydrogen activation and deoxygenation under milder conditions and lower metal loadings (He & Wang, 2012). Reports comparing <1 wt.% of Rh, Pd, and Pt supported on zirconia and silica against traditional sulfided 14 wt.% NiMo and CoMo supported on silica showed noble metals to be more active for both hydrogenation at 100^{o}C, for 5 hours, and HDO of guaiacol at 300^{o}C for 3 hours (Gutierrez et al., 2009). Another study demonstrated hydrogenation and HDO of a model compound and actual bio-oil, with Pd, Pt, Rh, and Ru supported on active carbon, with Ru having superior performance (Mu et al., 2014). Near complete guaiacol HDO was observed with Pt supported on active carbon in an acidic environment at a mild temperature of 200^{o}C with a reaction time of 2 hours (Guvenatam et al., 2014). Although noble metals have shown potential for HDO, their high cost, limited availability, and sensitivity to poisoning are key issues in their application (Mortensen et al., 2011).

Finally, transition metal catalysts such as nickel, copper, iron, and cobalt have also been studied for HDO applications. Though not as active noble metals, their lower cost and availability

make them attractive. Nickel has been extensively studied due to its availability, low cost, high hydrogen activity and evidence for hydrogenolysis of C-O bonds (Sánchez-cárdenas et al., 2016). Transition metal catalysts should be bifunctional, where an oxide support allows activation of the oxygenated molecule and the transition metal facilitates hydrogen dissociation and donation for C=C saturation and C-O cleavage, as demonstrated in Figure 1.4 (Mortensen et al., 2011). Both active sites must be near one another to be effective for HDO, which often can not occur by transition metals alone. Several studies have demonstrated its ability to carry out successful HDO activity of both model compounds and actual bio-oil; however, they typically require higher operating temperatures (>250°C) and high metal loadings (>20 wt.%), relative to noble metal catalysts, to be effective, reducing the cost advantage. For example, Bykova et al. observed a significant degree of conversion and hydrodeoxygenation of guaiacol with ~60 wt.% Ni and NiCu supported on SiO_2, ZrO_2, and Al_2O_3 in a batch reactor at 320^{o}C (Bykova et al., 2011). Ni and NiCu catalysts with total metal loadings of 90 wt.% supported on SiO_2 resulted in 100% anisole conversion with ~15% HDO at 280^{o}C in a batch reactor (Khromova et al., 2014). Furthermore, anisole HDO in a continuous fixed bed reactor at 300^{o}C and fast pyrolysis oil in a batch reactor at 350^{o}C were successful with Ni and NiCu supported on δ-Al_2O_3 with total metal loadings of 20 wt.% (Ardiyanti et al., 2012).

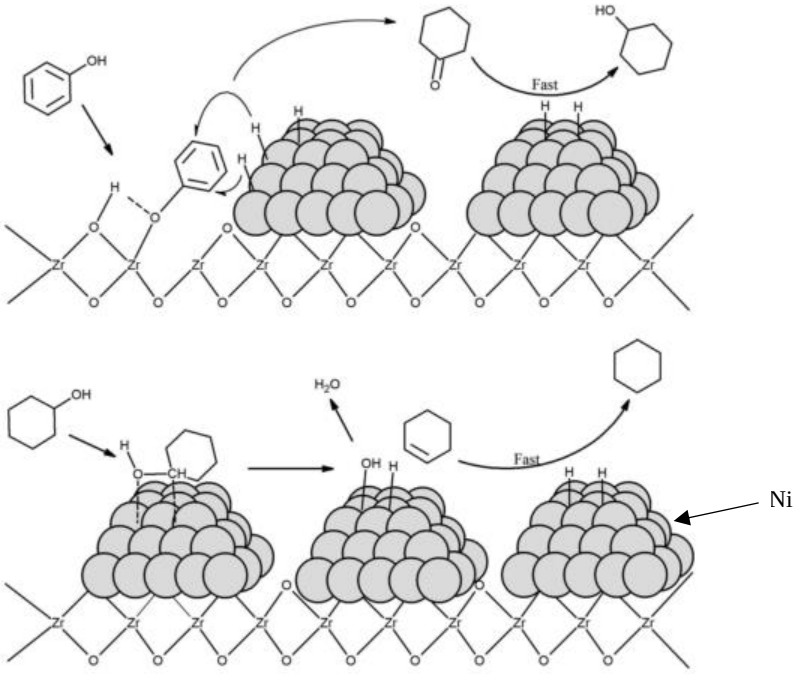

Figure 1.4 Proposed Mechanism for HDO of Phenol over Ni/ZrO_2 (Mortensen et al., 2013)

Another metal may be added, known as a promoter, to enhance the performance and stability of the catalyst during certain reactions. Several studies have shown the beneficial impact of combining two distinct metals to cooperatively carry out HDO, known as bimetallic catalysts, where one metal is the active component and the other enhances either the activity, selectivity, or stability of the first metal (Khromova et al., 2014). Sulfided Ni, Mo, and NiMo catalysts supported on alumina were studied for HDO of rapeseed oil in a fixed bed reactor. Catalyst activity and hydrocarbon formation decreased in the order of $NiMo/Al_2O_3$ > Mo/Al_2O_3 > Ni/Al_2O_3 demonstrating a synergistic effect of the bimetallic catalyst (Kubička & Kaluža, 2010). Substitution of nickel with cobalt supported on HZSM-5 was shown to be effective in improving deoxygenation rates and lessening coke deposits in both phenol and pyrolysis oil in relation to monometallic Ni by enhancing nickel dispersion and lowering the surface acidity of the catalyst (Huynh et al., 2015).

The use of copper has been widely established as an advantageous promoter as studies have demonstrated that small amounts of copper can considerably impact the overall catalyst performance. Lee et al. observed an increase in catalyst activity and stability, as well as reduced carbon deposits, during methane reforming with the addition of only 1 wt.% of Cu to an alumina-supported nickel catalyst (Lee et al., 2004). HDO experiments have shown copper addition, specifically to nickel-based catalysts, enhanced reaction activity by increasing nickel dispersion, improving the degree of reducibility (Yang et al, 2009), and weakening the interaction effects between nickel and the support (Smirnov et al., 2014). Studies comparing monometallic and bimetallic noble metals supported on ZrO_2 were performed for the HDO of guaiacol in a batch reactor. Bimetallic RhPd and RhPt catalysts resulted in higher conversion and HDO activity in comparison to monometallic Pd and Pt; however, when PdPt were combined, it demonstrated inferior conversion and HDO activity than monometallic Pt and Pd (Gutierrez et al., 2009).

The catalyst support material can influence a range of properties, including metal dispersion, acidity, stability, and even activity and selectivity towards certain products. One of the most widely studied supports for applications has been alumina, due its relatively low cost, availability, and its high surface area (Carre et al., 2008). Materials with large surface areas improve metal dispersion over the catalyst surface, enhancing thermal stability and providing additional active sites for reactions to take place (He et al., 2015). The acidity of alumina supports

has been linked to promote coke precursors that lead to carbon deposits and catalyst deactivation (Bui et al., 2011; Huuska, 1986). Coking was observed to be almost four times higher for guaiacol HDO when sulfided CoMo catalysts were supported on alumina rather than silica or activated carbon (Centeno et al., 1994). The impact of acidic supports, such as alumina, can be reduced by using more neutral alternatives, such as silica, zirconia, and titania. Silica has been broadly implemented as a practical support for its moderate thermal stability, high surface area, and availability (Yao et al., 2013; Smirnov et al., 2014; Jin et al., 2014). Activated carbon has also recently been explored as an alternative and has shown to be active in HDO reactions, specifically with noble metals, due to its high porosity and surface area (Ferrari et al., 2002; Ferrari et al., 2001).

Deactivation of catalysts can result from several occurrences, namely through poisoning by water or nitrogen, sintering, and/or coking. The catalyst composition, feed, and reaction conditions can play an important factor in rate of catalyst deactivation, although carbon formation via coking has been deemed the most troublesome. Catalyst deactivation can be considered as the primary challenge when optimizing HDO catalyst. As mentioned earlier, 100 operational hours on stream with a Ru/C catalyst have been achieved in a fixed bed reactor, though this is still far the requirements to make bio-oil hydrotreating sustainable and economically feasible (D. C. Elliott et al., 2012). Carbon deposits that form on the catalyst surface, typically from polymerization and polycondensation reactions, plug pores and block available active sites, reducing catalyst activity (Furimsky, 2000). It has been suggested that aromatics and alkenes obtained from lignocellulosic biomass have a greater association with carbon formation, increasing interactions with the catalyst surface compared to saturated hydrocarbons. Oxygenated compounds with higher oxygen content have also been reported to have higher affinity to coking through polymerization reactions (Mortensen et al., 2011; Venderbosch et al., 2010). Minimizing carbon deposition has therefor been a central focus for bio-oil HDO.

1.4 Catalytic Hydrotreating Reactors

Operating conditions for HDO have been widely investigated to limit cracking reactions, stabilize compounds, and extend catalyst lifetime by preventing carbon deposits. Lower

temperatures are thought to decrease coke formation and cracking reactions, which are undesirable as they decrease the yield of upgraded products (Elliot et al., 2009). Observations generally show that higher reaction temperatures result in higher HDO by providing energy to break resilient C-O bonds and adjusting product selectivity (Xinghua Zhang et al., 2013). High hydrogen pressures are typically implemented around 100 – 200 bars to ensure hydrogen in the liquid phase, maximizing the hydrogen contact with the catalyst. Elevated pressures however increases the operating and capital costs of HDO (Mortensen et al., 2011).

Several research groups have investigated a two-stage HDO process. The first step is an initial hydrotreating step at low temperatures (<300^{o}C) to stabilize highly reactive compounds and functional groups that are susceptible to polymerization at higher temperatures. The second hydrocracking step occurs at higher temperatures (>350^{o}C) to maximise HDO efficiency (Parapati et al., 2014). Elliot et al. studied HDO of pyrolysis oil from pine sawdust in a bench-scale continuous-flow fixed-bed reactor with sulfide molybdenum catalysts. HDO activity with oxygen content below 3 wt.% for the upgraded bio-oil and reduced coking occurrence were demonstrated in the hydrocracking stage, enabling catalyst time on stream upwards of 90 hours (D. C. Elliott et al., 2012).

Current reactors for HDO studies typically use magnetically stirred batch or fixed bed reactors. Impeller systems do not have ideal mixing conditions and tend to have heat and mass transfer limitations between the gas and liquid phases (Dickey, 2015). Attempts to address these limitations include using impellers with a hollow shaft to induce better mixing and mass transfer as well as adding baffles to the reactor walls to improve agitation while stirring (de Miguel Mercader et al., 2011). Fixed bed reactors can suffer from reactor plugging and fouling from carbon deposits due to uneven distribution of bio-oil over the catalyst bed, requiring careful control over gas and liquid flow rates during operation (Elliott et al., 2009). Temperature uniformity is also needed to prevent hotspots from exothermic HDO reactions that can increase the relative temperature by 60^{o}C in certain areas, leading to carbon deposition and rapid catalyst deactivation (Elliott, 2013). Improved catalyst agitation and gas-liquid-solid mixing is anticipated to reduce carbon deposit formation and prevent reactor plugging; however, mechanical stability of the catalyst and potential lower deoxygenation activity compared to fixed bed setups must be considered (Rana et al., 2007; Elliott, 2013).

Proper mixing between the gas, liquid, and solid phases is vital for catalytic HDO reactions. Since reactions take place on the catalyst surface, effective gas-liquid hydrogen mass transfer is required to limit unwanted side reactions and maximize hydrogenation activity (Mortensen et al., 2011). Impeller systems may lack sufficient mixing between the gas-liquid phases, impacting mass and heat transfer and increasing coke formation. The externally agitated (EA) reactor was designed as an alternative bench-scale reactor for catalyst screening of gas-liquid-solid reactions, including bio-oil HDO. The agitation method was based on a previous gasification study (Latifi et al., 2015). The external agitation method was selected to improve mixing between the gas, liquid and solid phases, while removing catalyst mechanical limitations imposed by attrition from impeller systems. Reduced mass transfer limitations are expected to improve hydrogen solubility by increasing the gas-liquid interfacial area. Enhanced heat transfer should also improve internal temperature uniformity, reducing hot spots and heat distribution from exothermic HDO reactions, minimizing cracking and coking reactions.

1.5 Thesis Objectives

Bio-oil upgrading from lignocellulosic biomass has demonstrated potential as a renewable alternative for fuels and chemicals with benefits to pollution and reduced greenhouse gas emissions, without competing with food sources (Gandarias & Arias, 2013). HDO has been demonstrated as an effective bio-oil upgrading method to reduce oxygen content; however, current HDO processes are economically unfeasible due to low efficiency, poor quality, and expensive catalysts with short lifespans due to deactivation and coking (Furimsky, 2000). The main objectives of the presented thesis are summarized as follows:

- Validate the externally agitated reactor on hydrodeoxygenation of anisole as a model compound using a baseline 10 wt.% Ni while varying support material, reaction temperature, and reaction time. This will identify appropriate operating conditions for subsequent HDO experiments that will investigate catalyst optimization where impacts on conversion and product selectivity will be more apparent. In addition, comparisons will be made between the EA reactor and a mechanically stirred batch reactor on HDO activity.

- Investigate the impact of a promoter on low loading Ni catalysts that is expected to increase reducibility to enhance hydrogenation and deoxygenation activity during HDO. The addition of copper was selected as an appropriate promoter.
- Study how changes to support acidity with the addition of a basic promoter has on HDO performance and coke formation tendencies. The addition of lanthanum as a basic promoter to Ni and Ni-Cu catalysts was chosen.

References

Alonso, D. M., Bond, J. Q., & Dumesic, J. A. (2010). Catalytic conversion of biomass to biofuels. *Green Chemistry*, 12, 1493–1513. https://doi.org/10.1039/c004654j

Alonso, D. M., Wettstein, S. G., Dumesic, J. A., Alonso, D. M., Wettstein, G., & Dumesic, J. A. (2012). Bimetallic catalysts for upgrading of biomass to fuels and chemicals. *Chem. Soc. Rev.* *41*(24). https://doi.org/10.1039/c2cs35188a

Ardiyanti, A. R., Bykova, M. V., Khromova, S. A., Yin, W., Venderbosch, R. H., Yakovlev, V. A., & Heeres, H. J. (2016). Ni-Based Catalysts for the Hydrotreatment of Fast Pyrolysis Oil. *Energy & Fuels*, https://doi.org/10.1021/acs.energyfuels.5b02223

Ardiyanti, A. R., Khromova, S. A., Venderbosch, R. H., Yakovlev, V. A., & Heeres, H. J. (2012). Catalytic hydrotreatment of fast-pyrolysis oil using non-sulfided bimetallic Ni-Cu catalysts on a δ-Al 2O 3 support. *Applied Catalysis B: Environmental*, *117–118*, 105–117. https://doi.org/10.1016/j.apcatb.2011.12.032

Balat, M., Balat, M., Kirtay, E., & Balat, H. (2009). Main routes for the thermo-conversion of biomass into fuels and chemicals. Part 1: Pyrolysis systems. *Energy Conversion and Management*, *50*(12), 3147–3157. https://doi.org/10.1016/j.enconman.2009.08.014

Bridgwater, A.V., Carson, P., Coulson, M. (2015). A comparison of fast and slow pyrolysis liquids from mallee. *Int. J. Global Energy Issues*, 27. https://doi.org/10.1504/IJGEI.2007.013655

Bridgwater, A. V., Meier, D., & Radlein, D. (1999). An overview of fast pyrolysis of biomass. *Organic Geochemistry*, *30*(12), 1479–1493. https://doi.org/10.1016/S0146-6380(99)00120-5

Bridgwater, a. V. (2012). Review of fast pyrolysis of biomass and product upgrading. *Biomass and Bioenergy*, *38*, 68–94. https://doi.org/10.1016/j.biombioe.2011.01.048

Bui, V. N., Laurenti, D., Delichre, P., & Geantet, C. (2011). Hydrodeoxygenation of guaiacol. Part II: Support effect for CoMoS catalysts on HDO activity and selectivity. *Applied Catalysis B: Environmental*, *101*(3–4), 246–255. https://doi.org/10.1016/j.apcatb.2010.10.031

Bulushev, D. A., & Ross, J. R. H. (2011). Catalysis for conversion of biomass to fuels via pyrolysis and gasification: A review. *Catalysis Today*, *171*(1), 1–13. https://doi.org/10.1016/j.cattod.2011.02.005

Butler, E., Devlin, G., Meier, D., & McDonnell, K. (2011). A review of recent laboratory research and commercial developments in fast pyrolysis and upgrading. *Renewable and Sustainable Energy Reviews*, *15*(8), 4171–4186. https://doi.org/10.1016/j.rser.2011.07.035

Bykova, M. V., Bulavchenko, O. a., Ermakov, D. Y., Lebedev, M. Y., Yakovlev, V. a., & Parmon, V. N. (2011). Guaiacol hydrodeoxygenation in the presence of Ni-containing catalysts. *Catalysis in Industry*, *3*(1), 15–22. https://doi.org/10.1134/S2070050411010028

Centeno, A., Laurent, E., & Delmon, B. (1994). Influence of the Support of CoMo Sulfide Catalysts and of the Addition of Potassium and Platinum on the Catalytic Performances for the Hydrodeoxygenation of Carbonyl, Carboxyl, and Guaiacol-Type Molecules. *Journal of Catalysis*, *154*, 288–298.

Chakraborty, S., Aggarwal, V., Mukherjee, D., & Andras, K. (2012). Biomass to biofuel: a review on production technology. *Asia-Pacific Journal of Chemical Engineering*, *7*, 254–262. https://doi.org/10.1002/apj.1642

Cherubini, F. (2010). The biorefinery concept: Using biomass instead of oil for producing energy and chemicals. *Energy Conversion and Management*, *51*(7), 1412–1421. https://doi.org/10.1016/j.enconman.2010.01.015

Chheda, J. N., Huber, G. W., & Dumesic, J. A. (2007). Liquid-phase catalytic processing of biomass-derived oxygenated hydrocarbons to fuels and chemicals. *Angewandte Chemie - International Edition*, *46*(38), 7164–7183. https://doi.org/10.1002/anie.200604274

Chong, K. J., & Bridgwater, A. V. (2017). Fast Pyrolysis Oil Fuel Blend for Marine Vessels. *Environmental Progress & Sustainable Energy*, *36*(3), 677–684. https://doi.org/10.1002/ep.12402

de Miguel Mercader, F., Groeneveld, M. J., Kersten, S. R. a., Geantet, C., Toussaint, G., Way, N. W. J., Hogendoorn, K. J. a. (2011). Hydrodeoxygenation of Pyrolysis Oil Fractions: Process Understanding and Quality Assessment Through Co-processing in Refinery Units. *Energy & Environmental Science*, *4*, 985. https://doi.org/10.1039/c0ee00523a

De Wild, P. J., Huijgen, W. J. J., & Gosselink, R. J. A. (2014). Lignin pyrolysis for profitable lignocellulosic biorefineries. *Biofuels, Bioproducts and Biorefining*, *8*(5), 645–657. https://doi.org/10.1002/bbb.1474

Demirbaş, A. (2005). Bioethanol from Cellulosic Materials: A Renewable Motor Fuel from Biomass. *Energy Sources*, *27*(4), 327–337. https://doi.org/10.1080/00908310390266643

Dickey, D. S. (2015). Tackling difficult mixing problems. *Chemical Engineering Progress*, *111*(8), 35–42.

Elliott, D. C., Beckman, D, Bridgwater, A. V. (1991). Reviews Developments in Direct Thermochemical Liquefaction of. *Energy and Fuels*, *5*, 399–410.

Elliott, D. C. (2013). Transportation fuels from biomass via fast pyrolysis and hydroprocessing. *Wiley Interdisciplinary Reviews: Energy and Environment*, *2*(5), 525–533. https://doi.org/10.1002/wene.74

Elliott, D. C., Hart, T. R., Neuenschwander, G. G., Rotness, L. J., Olarte, M. V., Zacher, A. H., & Solantausta, Y. (2012). Catalytic hydroprocessing of fast pyrolysis bio-oil from pine sawdust. *Energy and Fuels*, *26*(6), 3891–3896. https://doi.org/10.1021/ef3004587

Elliott, D., Hart, T., Neuenschwander, G., Rotness, L., & Zacher, A. (2009). Catalytic Hydroprocessing of Biomass Fast Pyrolysis Bio-oil to Produce Hydrocarbon Products. *American Institute of Chemical Engineers*, *28*, 441–449. https://doi.org/10.1002/ep

Ferrari, M., Bosmans, S., Maggi, R., Delmon, B., & Grange, P. (2001). CoMo / carbon hydrodeoxygenation catalysts : influence of the hydrogen sulfide partial pressure and of the sulfidation temperature. *Catalysis Today*, *65*, 257–264. https://doi.org/10.1016/S0920-5861(00)00559-9

Ferrari, M., Delmon, B., & Grange, P. (2002). Influence of the active phase loading in carbon supported molybdenum – cobalt catalysts for hydrodeoxygenation reactions. *Microporous and Mesoporous Materials*, *56*, 279–290.

Foster, A. J., Do, P. T. M., & Lobo, R. F. (2012). The synergy of the support acid function and the metal function in the catalytic hydrodeoxygenation of m-cresol. *Topics in Catalysis*, *55*(3–4), 118–128. https://doi.org/10.1007/s11244-012-9781-7

Furimsky, E. (2000). Catalytic hydrodeoxygenation. *Applied Catalysis A: General*, *199*(2), 147–190. https://doi.org/10.1016/S0926-860X(99)00555-4

Galkin, M. V., & Samec, J. S. M. (2016). Lignin Valorization through Catalytic Lignocellulose Fractionation: A Fundamental Platform for the Future Biorefinery. *ChemSusChem*, *9*(13), 1544–1558. https://doi.org/10.1002/cssc.201600237

Gandarias, I., & Arias, P. L. (2013). Hydrotreating Catalytic Processes for Oxygen Removal in the Upgrading of Bio-Oils and Bio-Chemicals. *Liquid, Gaseous, and Solid Biofuels-Conversion Techniques*, 327–356. https://doi.org/10.5772/50479

Gutierrez, A., Kaila, R. K., Honkela, M. L., Slioor, R., & Krause, A. O. I. (2009). Hydrodeoxygenation of guaiacol on noble metal catalysts. *Catalysis Today*, *147*(3–4), 239–246. https://doi.org/10.1016/j.cattod.2008.10.037

Guvenatam, B., Osman, K., Heeres, E., Pidko, E., & Hensen, E. (2014). HDO of mono- and dimeric lignin model compounds on noble metal catalysts. *Catalysis Today*. 233, 83-91. http://dx.doi.org/10.1016/j.cattod.2013.12.011

Harmsen, P., & Huijgen, W. (2010). Literature Review of Physical and Chemical Pretreatment Processes for Lignocellulosic Biomass, *Food and Biobased Research.* (September), 1–49.

He, S. S., Zhang, L., He, S. S., Mo, L., Zheng, X., Wang, H., & Luo, Y. (2015). Ni / SiO 2 Catalyst Prepared with Nickel Nitrate Precursor for Combination of CO2 Reforming and Partial Oxidation of Methane : Characterization and Deactivation Mechanism Investigation. *Journal of Nanomaterials*, *2015*. http://dx.doi.org/10.1155/2015/659402

He, Z., & Wang, X. (2012). Hydrodeoxygenation of model compounds and catalytic systems for pyrolysis bio-oils upgrading. *Catalysis for Sustainable Energy*, *1*, 28–52. https://doi.org/10.2478/cse-2012-0004

Huber, G. W., & Corma, A. (2007). Synergies between bio- and oil refineries for the production of fuels from biomass. *Angewandte Chemie - International Edition*, *46*(38), 7184–7201. https://doi.org/10.1002/anie.200604504

Huber, G. W., Iborra, S., & Corma, A. (2006). Synthesis of transportation fuels from biomass: Chemistry, catalysts, and engineering. *Chemical Reviews*, *106*(9), 4044–4098. https://doi.org/10.1021/cr068360d

Huuska, M. K. (1986). Effect of catalyst composition on the hydrogenolysis of anisole. *Polyhedron*, *5*(1–2), 233–236. https://doi.org/10.1016/S0277-5387(00)84915-3

Huynh, T. M., Armbruster, U., Nguyen, L. H., & Nguyen, D. A. (2015). Hydrodeoxygenation of Bio-Oil on Bimetallic Catalysts: From Model Compound to Real Feed, *Journal of Sustainable Bioenergy Systems.* 5, 151–160. http://dx.doi.org/10.4236/jsbs.2015.54014

Jiménez-Díaz, L., Caballero, A., Pérez-Hernández, N., & Segura, A. (2017). Microbial alkane production for jet fuel industry: motivation, state of the art and perspectives. *Microbial Biotechnology*, *10*(1), 103–124. https://doi.org/10.1111/1751-7915.12423

Jin, S., Xiao, Z., Li, C., Chen, X., Wang, L., Xing, J., … Liang, C. (2014). Catalytic hydrodeoxygenation of anisole as lignin model compound over supported nickel catalysts. *Catalysis Today*, *234*, 125–132. https://doi.org/10.1016/j.cattod.2014.02.014

Khromova, S. A., Smirnov, A. A., Bulavchenko, O. A., Saraev, A. A., Kaichev, V. V., Reshetnikov, S. I., & Yakovlev, V. A. (2014). Anisole hydrodeoxygenation over Ni-Cu bimetallic catalysts: The effect of Ni/Cu ratio on selectivity. *Applied Catalysis A: General*, *470* (2014), 261–270. https://doi.org/10.1016/j.apcata.2013.10.046

Kubička, D., & Kaluža, L. (2010). Deoxygenation of vegetable oils over sulfided Ni, Mo and NiMo catalysts. *Applied Catalysis A: General*, *372*(2), 199–208. https://doi.org/10.1016/j.apcata.2009.10.034

Kumar, J., & Reetu, S. (2015). Lignocellulosic agriculture wastes as biomass feedstocks for second-generation bioethanol production : concepts and recent developments. *Biotechnology.* 337–353. https://doi.org/10.1007/s13205-014-0246-5

Kumar, M., Olajire Oyedun, A., & Kumar, A. (2016). A review on the current status of various hydrothermal technologies on biomass feedstock. *Renewable and Sustainable Energy Reviews*, *81*(May 2017), 1742–1770. https://doi.org/10.1016/j.rser.2017.05.270

Kumar, V., & Nanda, M. (2016). Biomass Pyrolysis-Current status and future directions. *Energy Sources, Part A: Recovery, Utilization and Environmental Effects*, *38*(19), 2914–2921. https://doi.org/10.1080/15567036.2015.1098751

Latifi, M., Berruti, F., & Briens, C. (2015). Thermal and catalytic gasification of bio-oils in the Jiggle Bed Reactor for syngas production. *International Journal of Hydrogen Energy*, *40*(17), 5856–5868. https://doi.org/10.1016/j.ijhydene.2015.02.088

Laurichesse, S., & Avérous, L. (2014). Chemical modification of lignins: Towards biobased polymers. *Progress in Polymer Science*, *39*(7), 1266–1290. https://doi.org/10.1016/j.progpolymsci.2013.11.004

Lee, J., Lee, E., Joo, O., & Jung, K. (2004). Stabilization of Ni / Al2O3 catalyst by Cu addition for CO 2 reforming of methane. *Applied Catalysis. 269*, 1–6. https://doi.org/10.1016/j.apcata.2004.01.035

Louwers, S. P. A., Craje, M. W. J., Vanderkraan, A. M., Geantet, C., & Prins, R. (1993). The Effect of Passivation on the Activity and Structure of Sulfided Hydrotreating Catalysts. *Journal of Catalysis*. https://doi.org/10.1006/jcat.1993.1355

Lynd, L. (1996). Overview and evaluation of fuel ethanol from cellulosic biomass: Technology, economics, the environment, and policy. *Annu. Rev. Energy Environ.*, *21*, 403–465.

Mahmood, N., Yuan, Z., Schmidt, J., & Xu, C. C. (2015). Hydrolytic depolymerization of hydrolysis lignin: Effects of catalysts and solvents. *Bioresource Technology*, *190*, 416–419. https://doi.org/10.1016/j.biortech.2015.04.074

Mante, Ofei D; Agblevor, F. A. (2011). Catalytic conversion of biomass to biofuels. *Biomass Conv. Bioref.*, *1*, 203–215. https://doi.org/10.1007/s13399-011-0020-4

Marchal, N., Mignard, S., & Kasztelan, S. (1996). Aromatics Saturation by Sulfided Nickel-molybdenum hydrotreating catalysts. *Catalysis Today*, *29*, 203–207.

Massoth, F. E., Politzer, P., Concha, M. C., Murray, J. S., Jakowski, J., & Simons, J. (2006). Catalytic hydrodeoxygenation of methyl-substituted phenols: Correlations of kinetic parameters with molecular properties. *Journal of Physical Chemistry B*, *110*(29), 14283–14291. https://doi.org/10.1021/jp057332g

Mohan, D., Pittman, C. U., & Steele, P. H. (2006). Pyrolysis of wood/biomass for bio-oil: A critical review. *Energy and Fuels*, *20*(3), 848–889. https://doi.org/10.1021/ef0502397

Molino, A., Chianese, S., & Musmarra, D. (2016). Biomass gasification technology: The state of the art overview. *Journal of Energy Chemistry*, *25*(1), 10–25. https://doi.org/10.1016/j.jechem.2015.11.005

Mortensen, P. M., Grunwaldt, J. D., Jensen, P. A., & Jensen, A. D. (2013). Screening of catalysts for hydrodeoxygenation of phenol as a model compound for bio-oil. *ACS Catalysis*, *3*(8), 1774–1785. https://doi.org/10.1021/cs400266e

Mortensen, P. M., Grunwaldt, J. D., Jensen, P. A., Knudsen, K. G., & Jensen, A. D. (2011). A review of catalytic upgrading of bio-oil to engine fuels. *Applied Catalysis A: General*, *407*(1–2), 1–19. https://doi.org/10.1016/j.apcata.2011.08.046

Mu, W., Ben, H., Du, X., Zhang, X., Hu, F., Liu, W., … Deng, Y. (2014). Noble metal catalyzed aqueous phase hydrogenation and hydrodeoxygenation of lignin-derived pyrolysis oil and related model compounds *Bioresource Tech.* https://doi.org/10.1016/j.biortech.2014.09.067

Oasmaa, A., & Czernik, S. (1999). Fuel oil quality of biomass pyrolysis oils-state of the art for the end users. *Fuel and Energy Abstracts*, *13*, 914–921. https://doi.org/10.1016/S0140-6701(00)96592-5

Parapati, D., Guda, V., Penmetsa, V., Steele, P. H., & Tanneru, S. (2014). Single Stage Hydroprocessing of Pyrolysis Oil in a Continuous Packed-Bed Reactor. *Environmental Progress and Sustainable Energy*, *33*(3), 726–731. https://doi.org/10.1002/ep

Peterson, A. A., Vogel, F., Lachance, R. P., Fröling, M., Antal, Jr., M. J., & Tester, J. W. (2008). Thermochemical biofuel production in hydrothermal media: A review of sub- and supercritical water technologies. *Energy & Environmental Science*, *1*(1), 32. https://doi.org/10.1039/b810100k

Popov, A., Kondratieva, E., Mariey, L., Goupil, J. M., El Fallah, J., Gilson, J. P. (2013). Bio-oil hydrodeoxygenation: Adsorption of phenolic compounds on sulfided (Co)Mo catalysts. *Journal of Catalysis*, *297*, 176–186. https://doi.org/10.1016/j.jcat.2012.10.005

Radich, T. (2015). The Flight Paths for Biojet Fuel. *Independent Statistics & Analy*, 18. Retrieved from http://www.eia.gov/workingpapers/pdf/flightpaths_biojetffuel.pdf

Rana, M. S., Sámano, V., Ancheyta, J., & Diaz, J. A. I. (2007). A review of recent advances on process technologies for upgrading of heavy oils and residua. *Fuel*, *86*, 1216–1231. https://doi.org/10.1016/j.fuel.2006.08.004

Romero, Y., Richard, F., & Brunet, S. (2010). Hydrodeoxygenation of 2-ethylphenol as a model compound of bio-crude over sulfided Mo-based catalysts: Promoting effect and reaction mechanism. *Applied Catalysis B: Environmental*, *98*(3–4), 213–223. https://doi.org/10.1016/j.apcatb.2010.05.031

Rosillo-Calle, F. (2016). A review of biomass energy - shortcomings and concerns. *Journal of Chemical Technology and Biotechnology*, *91*(7), 1933–1945. https://doi.org/10.1002/jctb.4918

Ryymin, E. M., Honkela, M. L., Viljava, T. R., & Krause, A. O. I. (2009). Insight to sulfur species in the hydrodeoxygenation of aliphatic esters over sulfided NiMo/γ-Al2O3 catalyst. *Applied Catalysis A: General*, *358*(1), 42–48. https://doi.org/10.1016/j.apcata.2009.01.035

Saini, J. K., Saini, R., & Tewari, L. (2015). Lignocellulosic agriculture wastes as biomass feedstocks for second-generation bioethanol production: concepts and recent developments. *3 Biotech*, *5*(4), 337–353. https://doi.org/10.1007/s13205-014-0246-5

Sánchez-cárdenas, M., Medina-valtierra, J., Kamaraj, S., Rafael, R., Ramírez, M., & Sánchez-olmos, L. A. (2016). γ-Al2O3 in Oleic Acid Hydrodeoxygenation to Produce n-Alkanes. https://doi.org/10.3390/catal6100156

Sikarwar, V. S., Zhao, M., Clough, P., Yao, J., Zhong, X., Memon, M. Z., Fennell, P. S. (2016). An overview of advances in biomass gasification. *Energy Environ. Sci.*, *9*(10), 2939–2977. https://doi.org/10.1039/C6EE00935B

Sims, R. E. H., Mabee, W., Saddler, J. N., & Taylor, M. (2010). An overview of second generation biofuel technologies. *Bioresource Technology*, *101*(6), 1570–1580. https://doi.org/10.1016/j.biortech.2009.11.046

Smirnov, a. a., Khromova, S. a., Bulavchenko, O. a., Kaichev, V. V., Saraev, a. a., Reshetnikov, S. I., Yakovlev, V. a. (2014). Effect of the Ni/Cu ratio on the composition and catalytic properties of nickel-copper alloy in anisole hydrodeoxygenation. *Kinetics and Catalysis*, *55*(1), 69–78. https://doi.org/10.1134/S0023158414010145

Srifa, A., Viriya-empikul, N., Assabumrungrat, S., & Faungnawakij, K. (2015). Catalytic behaviors of Ni/γ-Al2O3 and Co/γ-Al2O3 during the hydrodeoxygenation of palm oil. *Catal. Sci. Technol.*, *5*(7), 3693-. https://doi.org/10.1039/C5CY00425J

Venderbosch, R. H., Ardiyanti, A. R., Wildschut, J., Oasmaa, A., & Heeres, H. J. (2010). Stabilization of biomass-derived pyrolysis oils. *Journal of Chemical Technology and Biotechnology*, *85*(5), 674–686. https://doi.org/10.1002/jctb.2354

Wright, M. M., Daugaard, D. E., Satrio, J. A., & Brown, R. C. (2010). Techno-economic analysis of biomass fast pyrolysis to transportation fuels. *Fuel*, *89*, 2–10. https://doi.org/10.1016/j.fuel.2010.07.029

Yang, R., Li, X., Wu, J., Zhang, X., & Zhang, Z. (2009). Promotion effects of copper and lanthanum oxides on nickel/gamma-alumina catalyst in the hydrotreating of crude 2-ethylhexanol. *Journal of Physical Chemistry C*, *113*(41), 17787–17794. https://doi.org/10.1021/jp9053296

Yao, L., Zhu, J., Peng, X., Tong, D., & Hu, C. (2013). Comparative study on the promotion effect of Mn and Zr on the stability of Ni / SiO 2 catalyst for CO 2 reforming of methane. *International Journal of Hydrogen Energy*, *38*(18), 7268–7279. https://doi.org/10.1016/j.ijhydene.2013.02.126

Yusuf, N. N. A. N., Kamarudin, S. K., & Yaakub, Z. (2011). Overview on the current trends in biodiesel production. *Energy Conversion and Management*, *52*(7), 2741–2751. https://doi.org/10.1016/j.enconman.2010.12.004

Zacher, A., Olarte, M., & Santosa, D. (2014). A review and perspective of recent bio-oil hydrotreating research. *Green Chemistry*, *16*(2), 491-515. https://doi.org/10.1039/c3gc41382a

Zhang, X., Wang, T., Ma, L., Zhang, Q., Huang, X., & Yu, Y. (2013). Production of Cyclohexane from Lignin Degradation Compounds over Ni ZrO2 SiO2 catalysts. *Applied Energy*. 112, 533-538. http://dx.doi.org.10.1016/j.apenergy.2013.04.077

Chapter 2

Validation and Optimization of EA Reactor for HDO Reactions with Inexpensive Transition Metal Catalysts

2.1 Introduction

Catalytic hydrodeoxygenation (HDO) has been identified as an effective upgrading method to convert pyrolysis bio-oils into suitable biofuels with enhanced properties and better heating values (Bridgwater, 2012). Research is needed to reduce operating costs, improve deoxygenation rates and reduce catalyst deactivation before HDO of biomass-derived oils becomes a viable alternative for petroleum-based chemicals and fuels (Absi-Halabi et al., 1991; Mahamulkar et al., 2016).

Typical reactor configurations that have been implemented for liquid-phase HDO studies include mechanically stirred batch autoclaves and continuous packed-bed reactors. Continuous packed-bed systems can be beneficial for longer studies compared to batch reactors as they are not limited by chemical equilibrium and offer better kinetic control, but are more costly and highly susceptible to fouling and reactor plugging via coking (Venderbosch, et al., 2010; Zarchin et al., 2015; Huynh et al., 2016). Batch reactors have widely been used to screen potential catalyst compositions and operating conditions as they are easy and relatively inexpensive to operate (Mortensen et al., 2013; Huynh et al., 2013; Wildschut et al., 2009). Poor mixing of the gas-liquid-solid phases can be problematic in batch reactors and can impose mass and heat transfer limitations. When catalyst is completely submerged in a surplus of liquid solvent with poor mixing, the reaction may be limited by hydrogen diffusion to the catalyst. The restriction of hydrogen in contact with the catalyst can also increase the prevalence of coking (Pandey & Kim, 2011). Additionally, the small gas-liquid interfacial area would restrict the solubility of hydrogen gas into the liquid solvent, further exacerbating any mass transfer limitations (Sugai et al., 2014; Sotowa, 2014; Sobieszuk et al., 2011). The EA reactor was developed to combine the simplicity and ease of a batch system with the improved three-phase mixing and greater interfacial area, expected in an ebullated bed configuration, to conduct complementary HDO studies for current impeller batch systems.

Since the reaction takes place on the catalyst surface, it is necessary to ensure good mixing between all four phases (gas-liquid-liquid-solid) to increase the contact time of reactants and catalyst. However, many studies rely on mechanically stirred batch reactors to enforce good mixing, although they do not have the most ideal mixing conditions and can lead to potential mass transfer limitations. The EA reactor was developed to address the poor mixing reported in batch reactors mixed by an impeller (Dickey, 2015). The EA reactor helps increase the interfacial area between the gas and liquid phases, thus resulting in increased diffusion of hydrogen into the liquid solvent and decreasing the boundary layer between the gas and liquid compared to the mechanically stirred batch reactor (Mercader et al., 2011).

Using a baseline of 10 wt.% Ni, preliminary HDO tests of anisole were used to identify appropriate operating conditions for future catalyst optimization experiments. Nickel-based catalysts were selected since they have been shown effective for HDO, have a relatively low cost and are available, while also extensively studied for HDO in batch reactors, providing considerable data for comparison. (Navalikhina & Krylov, 2001; Calles et al., 2009). Many studies have implemented high nickel loadings of 20 wt.% (Ardiyanti et al., 2012), 60 wt.% (Bykova et al., 2011), and even 90 wt.% (Smirnov et al., 2014); therefore, a lower 10 wt.% of nickel was chosen as a baseline to investigate the performance of the EA reactor and further reduce costs associated with catalyst compositions. Anisole conversion and liquid product selectivity were analyzed with variations to support material, reaction time, and reaction temperature while maintaining a constant hydrogen pressure. Comparisons were also performed between the EA reactor and a mechanically stirred batch reactor under equivalent operating conditions and catalyst compositions to determine the improvements, if any, the EA reactor may have on anisole HDO activity.

2.2 Material and Methods

2.2.1 Catalyst Preparation

All catalysts were prepared by incipient wetness impregnation using aqueous solutions of $Ni(NO_3)_2 \cdot 6H_2O$ obtained from Sigma-Aldrich (Steinheim, Germany). Spherical γ-alumina particles (1.7mm diameter, K2476) and spherical δ-alumina particles (1.5mm diameter, M8928) were provided by Sasol (Hamburg, Germany). The alumina spheres were crushed, sieved, and the 200-425µm particle size fraction was used for impregnation. Silica powder (Davisil®, Grade 633,

pore size 60Å, 200-425 mesh) was obtained from Sigma-Aldrich (Steinheim, Germany). Nickel precursor amounts were added to achieve the desired 10 wt.% and dissolved in water equal to the pore volume of the crushed support. Following impregnation, catalyst samples were dried overnight in an oven at 100°C, then calcined in dry air (Praxair, Ultra-Zero) at 400°C for 3 hours with a heating rate of 10°C/min and a flowrate of 10mL/min. Catalysts were reduced with 3.5MPa of hydrogen (Praxair, Ultra-High Purity (UHP)) at 400°C for 2 hours in the reactor prior to HDO reactions.

2.2.3 Experimental Setup and Catalyst Testing Procedure

Catalytic hydrodeoxygenation reactions of anisole were carried out in a 100mL stainless steel high-pressure and temperature batch reactor (model 4793 Parr) attached to a pneumatic actuator providing external agitation. The agitation method of the EA reactor was based on a previous system at ICFAR which investigated gasification at elevated temperatures and atmospheric pressures (Latifi et al., 2015). A schematic of the reactor setup is provided in Figure 2.1. A catalyst mass of 0.1g was added to the reactor, sealed, and vacuum purged with nitrogen three times to ensure removal of air. The reactor was then pressurized with hydrogen gas at room temperature to 3.5 MPa prior to the reduction. Catalysts were reduced for a total of 2 hours (t = 0 when heater was turned on at room temperature) with a heating rate of 12°C/min until a final temperature of 400°C. After 2 hours, the reactor was cooled in hydrogen atmosphere at an approximate rate of 5°C/min until approximately 40°C. A summary of the operating conditions implemented for HDO of anisole is presented in Table 2.1.

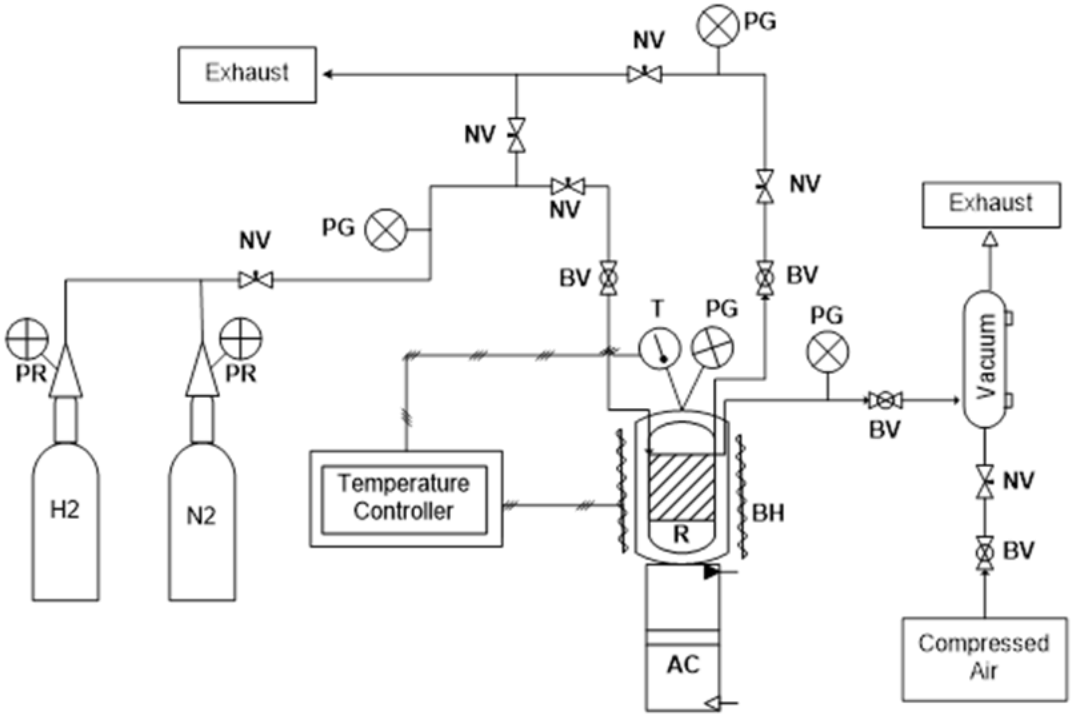

Figure 2.1 Schematic of the EA reactor (BV=ball valve, NV=needle valve, R=reactor, PR=pressure regulator, BH=band heater, AC=actuator, PG=pressure gauge, T=thermocouple).

Table 2.1 Operating conditions implemented for HDO of anisole.

Parameter	**Value**	**Units**
Reduction time	120	minutes
Reduction temperature	400	°C
Initial Hydrogen Pressure (at 25°C)	3.5	MPa
Reaction Temperature	160 - 280	°C
Reaction Time	30 - 120	minutes

The liquid reactant contained 1.2ml of anisole (99%, Fischer Scientific), 20ml of n-decane (99%, Fischer Scientific), and 0.4ml of n-dodecane (99%, Fischer Scientific) used as internal standard for chromatographic analysis. After the reduction and cooling step, the reactor was depressurized and the liquid reactant was injected into the reactor using a syringe through a septum to prevent exposing the reactor to air. Hydrogen was then flowed through the reactor to ensure no

residual air was present. The reactor was then pressurized to 3.5 MPa of hydrogen at 40°C. This amount of hydrogen ensured a H:O ratio of approximately 10:1 for anisole. Reaction time started from 40°C (t = 0), when the heater was initiated, the reactor was heated to the desired reaction temperature at a 12°C/min heating rate and then held at reaction temperature until the desired reaction time. External agitation was initiated at t = 0. The external reactor had a frequency of 3 Hz and an amplitude of 10cm. The reactor was then fan cooled to 40°C.

2.2.4 Product Analysis

Liquid samples were collected and identified by Gas Chromatography (Agilent 7890A) using a HP-5MS column (Agilent, 30m x 0.250mm x 0.25µm film thickness) coupled to a MS detector (Agilent 5975C MSD) and quantified using Flame Ionization Detector (FID). The GC-MS system was calibrated using liquid standards of methoxycyclohexane (99%, Alfa Aesar), cyclohexanol (99%, Alfa Aesar), and cyclohexane (99%, Alfa Aesar). Anisole conversion was determined as:

$$x = \left(1 - \frac{C_A}{C_A^0}\right) \cdot 100\% \quad (1)$$

where C_A represents the concentration of anisole in the product and C_A^0 is the concentration of anisole initially introduced into the reactor. Liquid product selectivity was calculated as:

$$s_i(mol\%) = \frac{n_{product\ i}}{n_{anisole\ converted}} \cdot 100\% \quad (2)$$

where $n_{product\ i}$ is the number of moles of product i and $n_{anisole\ converted}$ is the number of moles of converted anisole. Liquid product selectivity is normalized based on the total liquid products formed, and does not consider anisole that was not converted.

2.3 Results

2.3.1 Reaction Time

Figures 2.2 and 2.3 presents the anisole conversion and product selectivity at 280°C when reaction times varied from 30 minutes to 120 minutes for catalysts supported by silica and γ-alumina, respectively. When reaction time varied for the silica supported catalyst, anisole conversion remained constant at 100% with product selectivity consisting of approximately 95% methoxycyclohexane and 5% cyclohexane (Figure 2.2). When γ-alumina was the support, conversion was 83% at 30 minutes and then increased to 100% for reaction times of 60 minutes and 120 minutes. Product selectivity varied similarly to conversion where cyclohexane selectivity was 86% at a reaction time of 30 minutes, and subsequently increased to 100% once reaction time lengthened to 60 minutes and above.

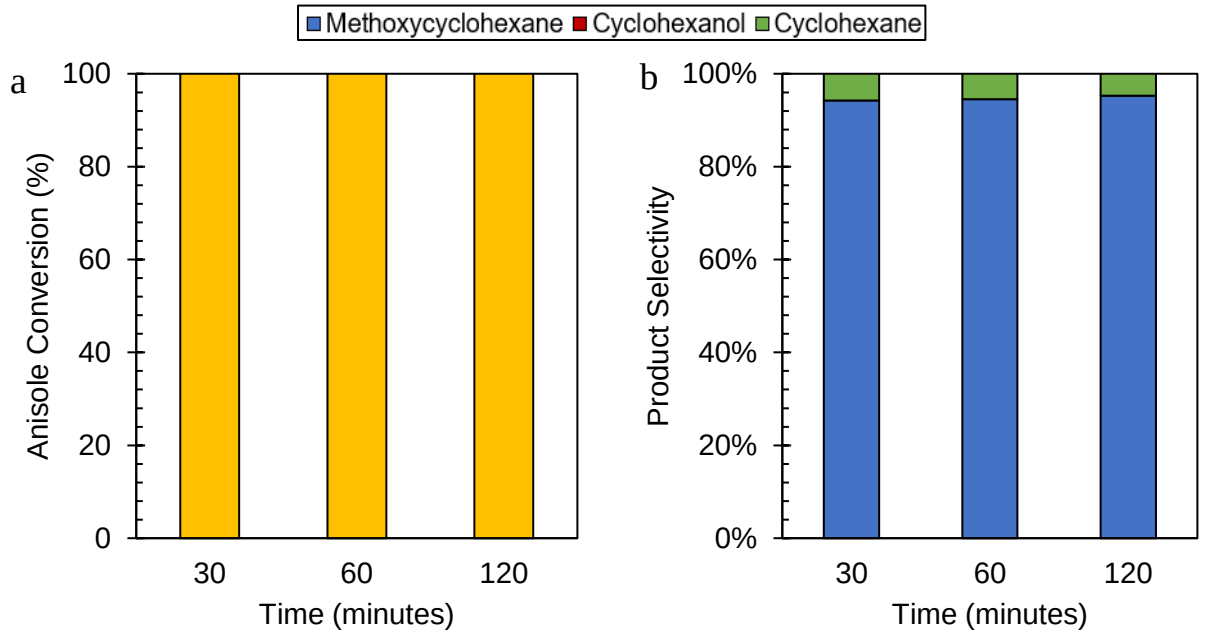

Figure 2.2. a) Conversion and b) product selectivity with varied reaction time on catalytic activity at 280°C, an initial hydrogen pressure of 3.5MPa, and 0.1g of 10 wt.% Ni supported on silica (reduced at 400°C for 2h).

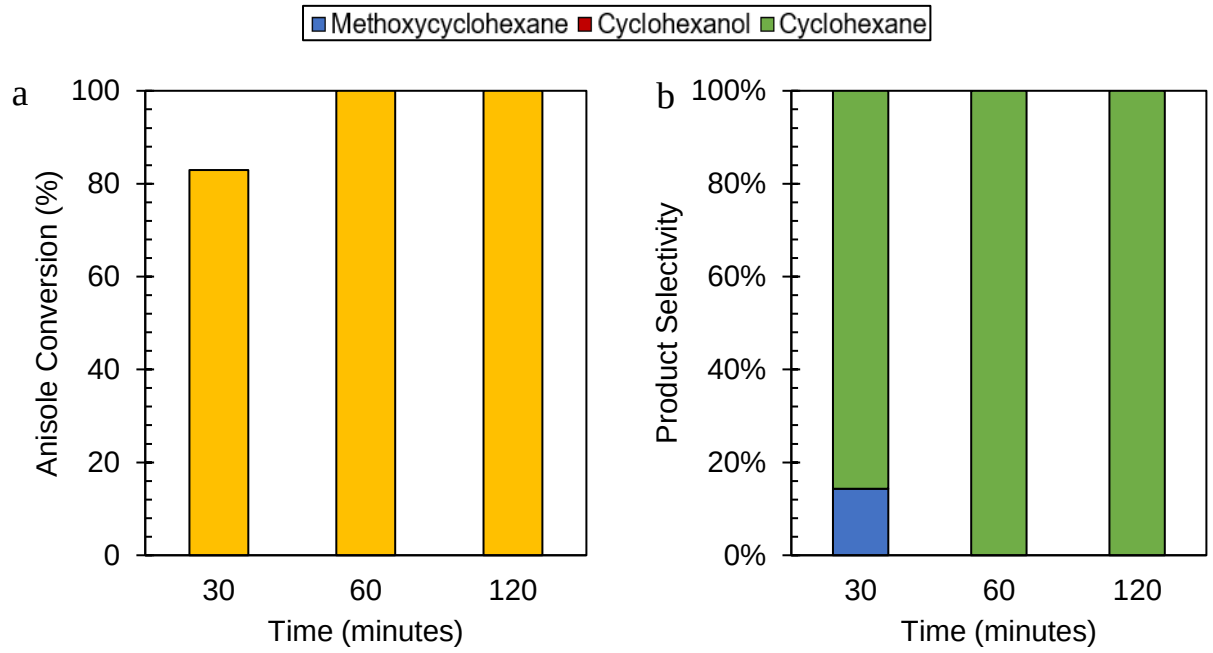

Figure 2.3. a) Conversion and b) product selectivity with varied reaction time on catalytic activity at 280°C, an initial hydrogen pressure of 3.5MPa, and 0.1g of 10 wt.% Ni supported on γ-alumina (reduced at 400°C for 2h).

2.3.2 Reaction Temperature

Figure 2.4 shows the anisole conversion and product selectivity at a reaction time of 60 minutes when reaction temperature varied from 180°C to 280°C with silica as the support. Figure 2.5 shows the anisole conversion and product selectivity at a reaction time of 60 minutes when reaction temperature varied from 160°C to 280°C with γ-alumina as the support. Once again, silica demonstrated high anisole conversion in the form of hydrogenation, yet deoxygenation activity was limited significantly with only 15% cyclohexane selectivity when reaction temperature was at our highest reaction temperature of 280°C (Figure 2.4b). When γ-alumina was the support, anisole conversion and product selectivity were affected by reaction temperature significantly more than silica, increasing almost linearly with increasing reaction temperature. Anisole conversion increased from 17% at 160°C to 100% at 280°C (Figure 2.5). Product selectivity varied significantly with reaction temperature where cyclohexane was undetected at 160°C and gradually increased to complete deoxygenation (100% conversion and cyclohexane selectivity) at 280°C. Furthermore, cyclohexanol was only detectable at 220°C with 13% selectivity.

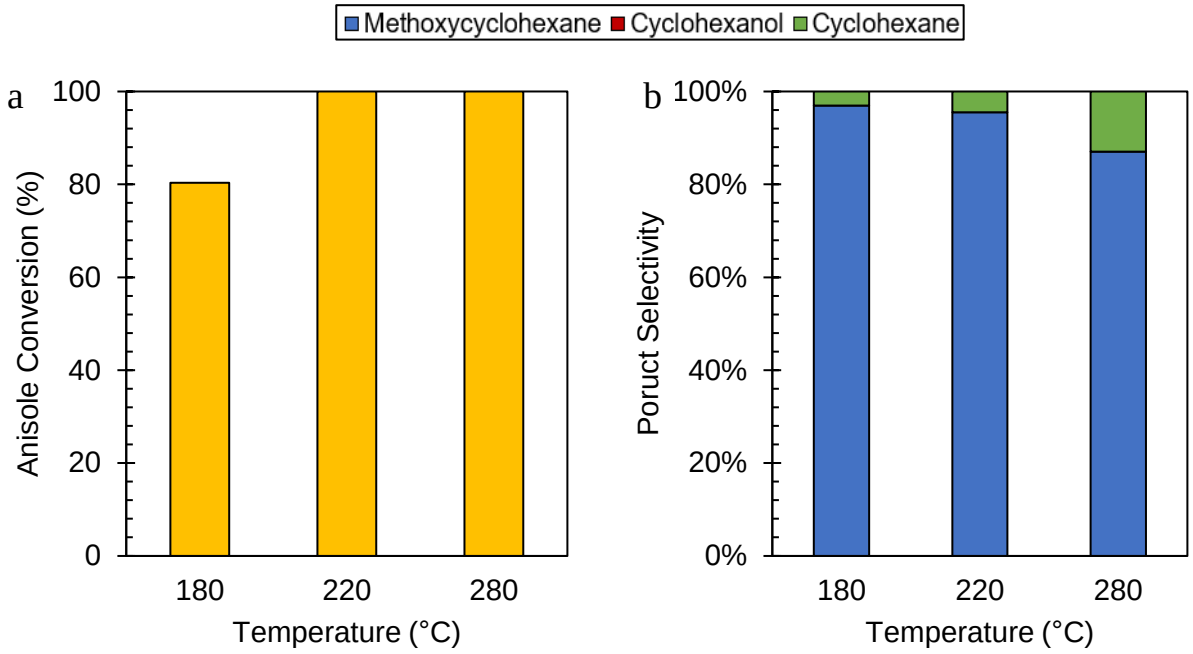

Figure 2.4. a) Conversion and b) product selectivity with varied reaction temperature at 60 minutes, an initial hydrogen pressure of 3.5MPa, and 0.1g of 10 wt.% Ni supported on silica (reduced at 400°C for 2h).

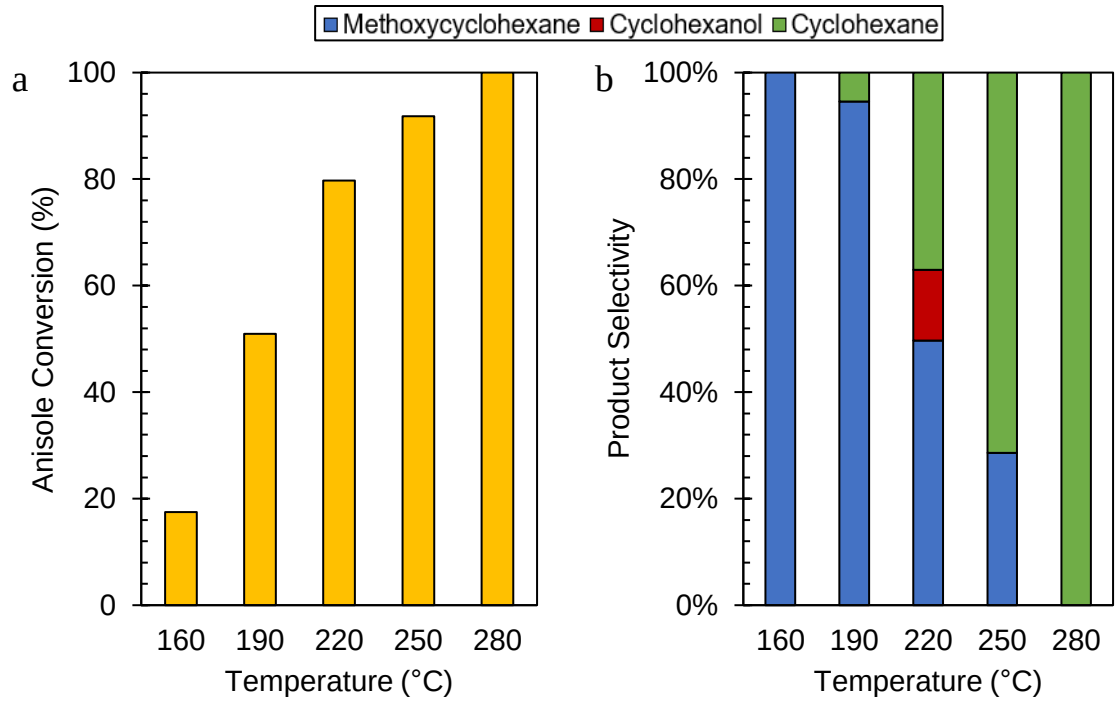

Figure 2.5. a) Conversion and b) product selectivity with varied reaction temperature at 60 minutes, an initial hydrogen pressure of 3.5MPa, and 0.1g of 10 wt.% Ni supported on γ-alumina (reduced at 400°C for 2h).

2.3.3 Support

Figures 2.6 and 2.7 present anisole conversion and product selectivity at 220°C and a reaction time of 60 minutes and 120 minutes, respectively, while varying the supports. Figure 2.8 presents the anisole conversion and product selectivity at a reaction temperature of 280°C and a reaction time of 60 minutes when support was varied. More acidic γ- and δ- alumina supports were selected based on the observed low deoxygenation activities of the silica support in early experiments. The γ-alumina support is commonly used in HDO studies due to its high acidity, while some studies have implemented δ-alumina instead due to its higher thermal stability and lower acidity (Ardiyanti et al., 2012). The reduced acidity of δ-alumina has been predicted to reduce catalyst deactivation by limiting coke formation on support acid sites, potentially enhancing catalytic activity (Carre et al., 2008). Anisole conversion was continuously 100% for all supports at both 220°C and 280°C, although deoxygenation activity varied greatly between supports. For example, cyclohexane selectivity only improved from 5% at 220°C to 12% at 280°C with a constant reaction time of 60 minutes (Figures 2.6 and 2.8). When δ-alumina was the support, cyclohexane selectivity remained relatively consistent at 220°C at approximately 16% even when reaction time was doubled from 60 minutes to 120 minutes (Figures 2.6 and 2.7). However, deoxygenation significantly improved to 71% when reaction temperature was increased to 280°C (Figure 2.8). With the γ-alumina support, cyclohexane selectivity was 16% at 220°C for 60 minutes, equivalent to what was observed for δ-alumina at the same conditions, yet cyclohexanol was present for the former with 8% selectivity. Interestingly, cyclohexane selectivity doubled to 32% with γ-alumina when the reaction time was doubled, which was not observed with the other supports. When the reaction temperature was further increased to 280°C, 100% cyclohexane selectivity was achieved.

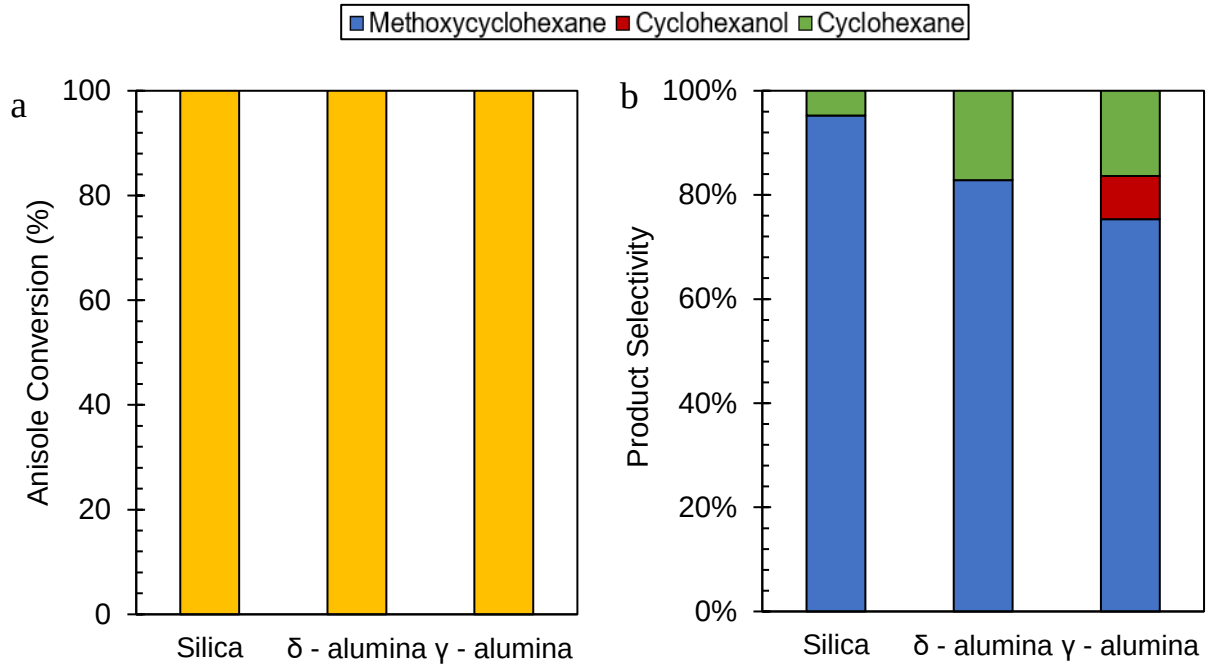

Figure 2.6. a) Conversion and b) product selectivity with varied supports at 220°C for 60 minute, an initial hydrogen pressure of 3.5MPa, and 0.1g of 10 wt.% Ni (reduced at 400°C for 2h).

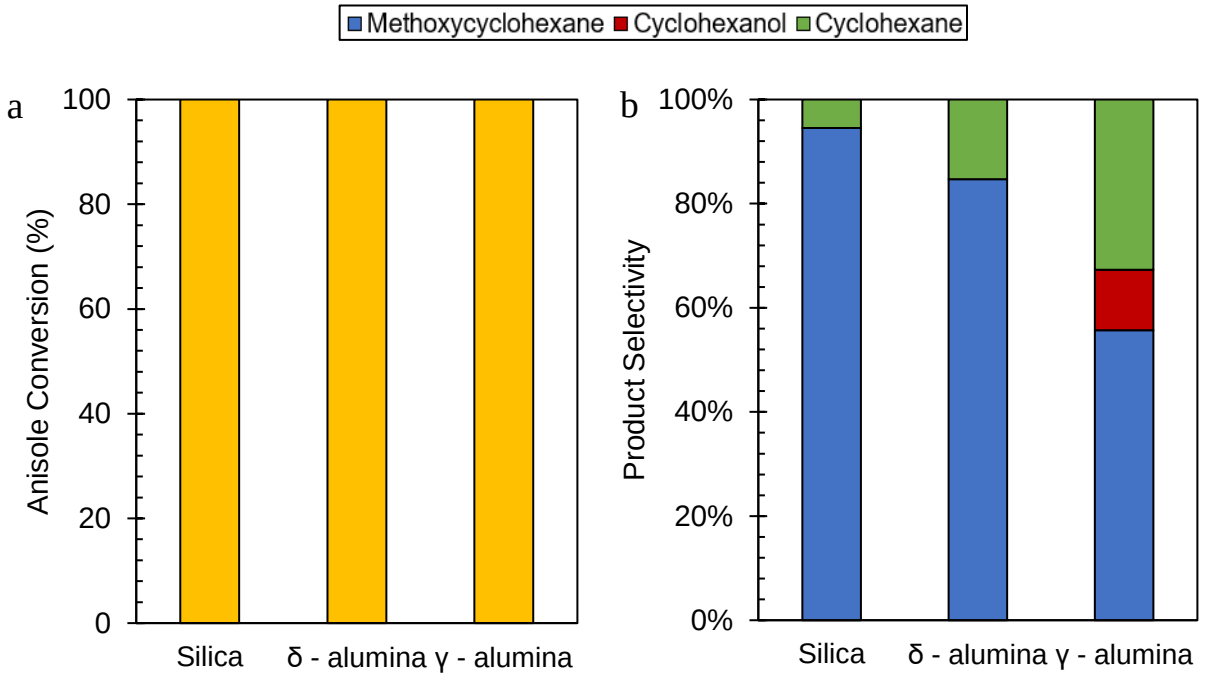

Figure 2.7. a) Conversion and b) product selectivity with varied support at 220°C for 120 minute, an initial hydrogen pressure of 3.5MPa, and 0.1g of 10 wt.% Ni (reduced at 400°C for 2h).

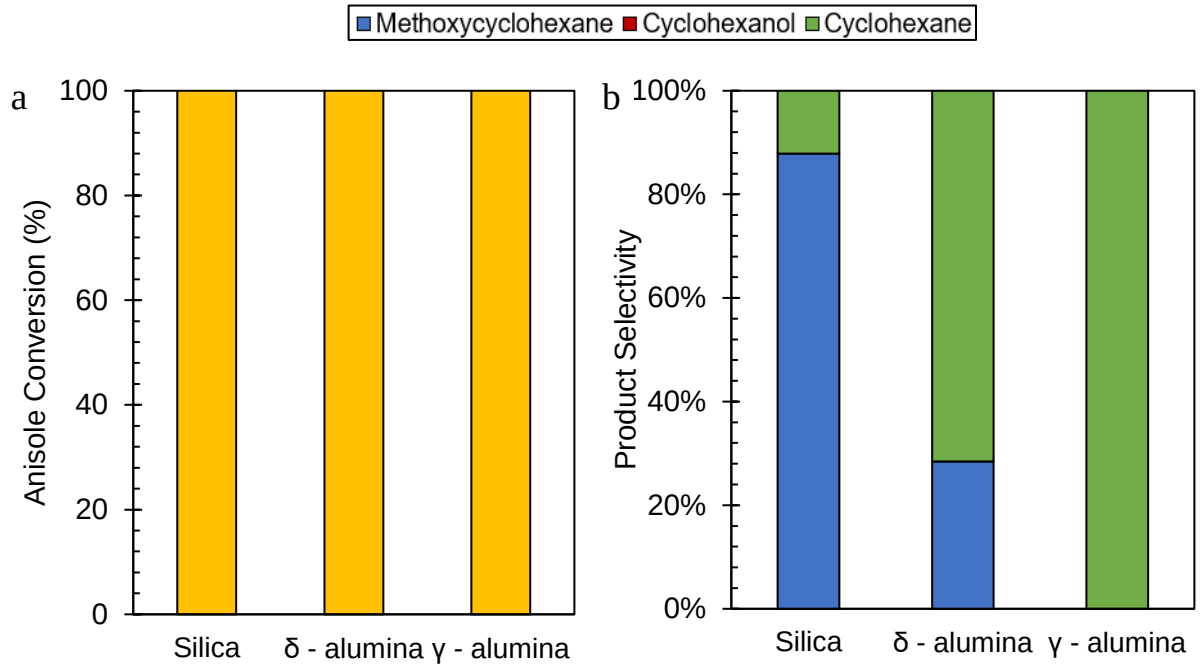

Figure 2.8. a) Conversion and b) product selectivity with varied support at 280°C for 60 minutes, an initial hydrogen pressure of 3.5MPa, and 0.1g of 10 wt.% Ni (reduced at 400°C for 2h).

2.4 Discussion

The catalyst support can play an important role in activity and product selectivity. Previous studies have shown that strong acid sites on the support are necessary for deoxygenation activity of transition metal catalysts, but also are directly related to coke formation and thus catalyst deactivation (Ghampson et al., 2016; Kwak et al., 2011; Robinson et al., 2016; Busca et al., 2007). Alumina is a common support for transition metal catalysts for its relative cheap cost and wide availability; however, due to its high acidity, several studies have investigated more neutral materials such as silica, zirconia, and activated carbon in attempt to limit coking reactions (Gandarias & Arias, 2013; Huuska & Rintala, 1985). This increased support aciditiy has been reported to be facilitate coke formation on catalysts (Wu et al., 2013).

The use of the silica support promoted the hydrogenation activity based on the observed methoxycyclohexane selectivity; however, limited deoxygenation activity was observed when increasing reaction temperature, time, and catalyst amount. The γ- and δ-alumina supports had comparable anisole conversion when compared to silica, while having a higher selectivity towards deoxygenated products (i.e., cyclohexane), with γ-alumina producing the highest cyclohexane

yields. The support acidity has been previously reported as follows: SiO_2 < δ-Al_2O_3 < γ-Al_2O_3 (Huuska & Rintala, 1985; Carre et al., 2008). The observed selectivity towards cyclohexane for the studied supports demonstrate that the deoxygenation is dependent on the support acid sites, while the hydrogenation of anisole's benzene ring is due to the impregnated Ni (Foster et al., 2012; Lee et al., 2012). Previous studies have confirmed active sites for C-O bond cleavage on alumina supports, which are required for the deoxygenation step (Hindin & Weller, 1956; Yakovlev et al., 2009; Tang et al., 2016).

Liquid products included exclusively methoxycyclohexane, cyclohexanol, and cyclohexane. The reaction pathway for the studied conditions, shown in Figure 2.9, consisted of the following steps: (i) an initial hydrogenation of the aromatic ring in anisole to form methoxycyclohexane, (ii) demethylation forming cyclohexanol and methane, and (iii) deoxygenation by dehydration to form cyclohexane and water. This specific reaction pathway has been identified in previous anisole HDO studies using nickel based catalysts (Khromova et al., 2014; Jin et al., 2014; Khromova et al., 2014). Support material and/or operating conditions was not observed to influence the reaction pathway.

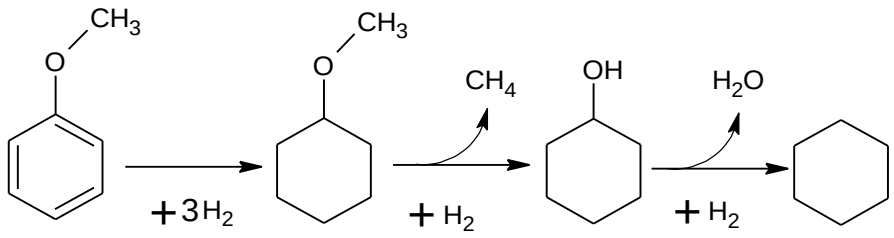

Figure 2.9. Anisole HDO reaction pathway based on identified liquid products.

A similar anisole HDO study using 10 wt.% Ni supported on γ-alumina also observed ~100% conversion and 74% deoxygenation, though requiring operating conditions of 300°C, 5 MPa of hydrogen, and a longer reaction time of 16 hours (Tang et al., 2016). Mortensen et al. reported 100% phenol conversion of phenol and 46% deoxygenation with 10 wt.% Ni on γ – alumina with reaction conditions of 275°C, 10 MPa of hydrogen, and a reaction time of 5 hours (Mortensen et al., 2013). Direct comparisons with the previous studies are difficult due to differences in catalyst material, operating conditions, and catalyst preparation methods. Nonetheless, the EA reactor demonstrated comparable anisole conversion rates at shorter reaction times, milder operating conditions, and lower metal loading when compared to similar studies

using mechanically stirred batch reactors. For example, guaiacol HDO using 10 wt.% Ni catalysts reported conversion rates of approximately 87% at operating conditions of 300^{o}C and 4MPa of hydrogen for 8 hours (Zhang et al., 2014). Complete anisole conversion (100%) was observed with a reaction time of 20 minutes at 280^{o}C and 6 MPa of hydrogen; however, bimetallic catalyst loadings upwards of 85 wt.% Ni and 5 wt.% Cu were required (Smirnov et al., 2014). Bykova et al. reported 80% conversion and 71% of deoxygenation of guaiacol with 14wt.% Ni/ 6wt.% Cu on γ-alumina in a batch reactor, with operating conditions of 320^{o}C, 11MPa of hydrogen for 1 hour (Bykova et al., 2011). A similar study of anisole HDO carried out with 10wt.% Ni on γ-alumina was also stated to have ~100% conversion with approximately 74% deoxygenation rate, yet operating conditions were again much harsher with 300^{o}C, 5 MPa of hydrogen, and relatively long reaction time of 16 hours (W. Tang et al., 2016). A study using 5 wt.% noble metal catalysts containing Pd, Pt, Rh, and Ru supported on activated carbon demonstrated between 70-90% conversion of phenol at 250^{o}C, 4 MPa of hydrogen, and a reaction time of 2 hours (Mu et al., 2014).

HDO results in the EA reactor were highly dependent on support material and operating conditions. Silica supported catalyst resulted in 100% conversion in 30 minute reaction time, demonstrating efficient hydrogenation activity but deoxygenation was limited, even at elevated temperatures and reaction times. Catalyst supported by γ-alumina resulted in 100% conversion and complete deoxygenation in 60 minutes at 280°C, demonstrating to be very effective for HDO of anisole. Finally, γ-alumina catalyst obtained 100% anisole conversion with 20% deoxygenation at milder operating conditions of 220°C and 3.5MPa of H_2 after 45 minutes, using 10 wt.% Ni/ γ-Al_2O_3.

2.5 Comparison with mechanically stirred batch reactor

The EA reactor conversion rates at shorter reaction times, lower metal loadings, and milder operating conditions relative to previous studies were further investigated by conducting experiments in a mechanically stirred batch reactor. The general experimental setup and operating conditions, previously explained in Section 2.2.3, were kept constant. The maximum impeller speed of ~800 rpm was used for the entire reaction time. An initial test with no catalyst (not shown) was performed under the same experimental conditions and resulted in no observable anisole

conversion. All subsequent catalyst experiments were carried out in duplicates under identical conditions to guarantee reproducibility of the data.

2.5.1 Results and Discussion

Figures 2.10 and 2.11 present anisole conversion and liquid product selectivity for Ni and Ni-Cu catalysts in the EA reactor and the mechanically stirred reactor, respectively. Anisole conversion was reduced for the stirred reactor compared to the EA reactor for all catalyst samples. Interestingly, 12% anisole conversion was observed in the EA reactor with the blank Al_2O_3, while there was no indication of anisole conversion in the stirred reactor. Product selectivity towards deoxygenated products (i.e. cyclohexane) were comparable for all catalysts except for the Ni4/Cu1 catalyst, which increased from 19% to 36% with the stirred reactor. Product selectivity to demethylated products (i.e. cyclohexanol) generally increased in the mechanically stirred reactor. Cyclohexanol selectivity was 22% for the Ni5 catalyst in the stirred reactor, while not detected in the EA reactor. Anisole conversion was enhanced in the EA reactor relative to experiments conducted in the stirred reactor with similar product selectivity, therefore, both hydrogenated products (methoxycyclohexane) and deoxygenated products (cyclohexane) had greater yields in the EA reactor.

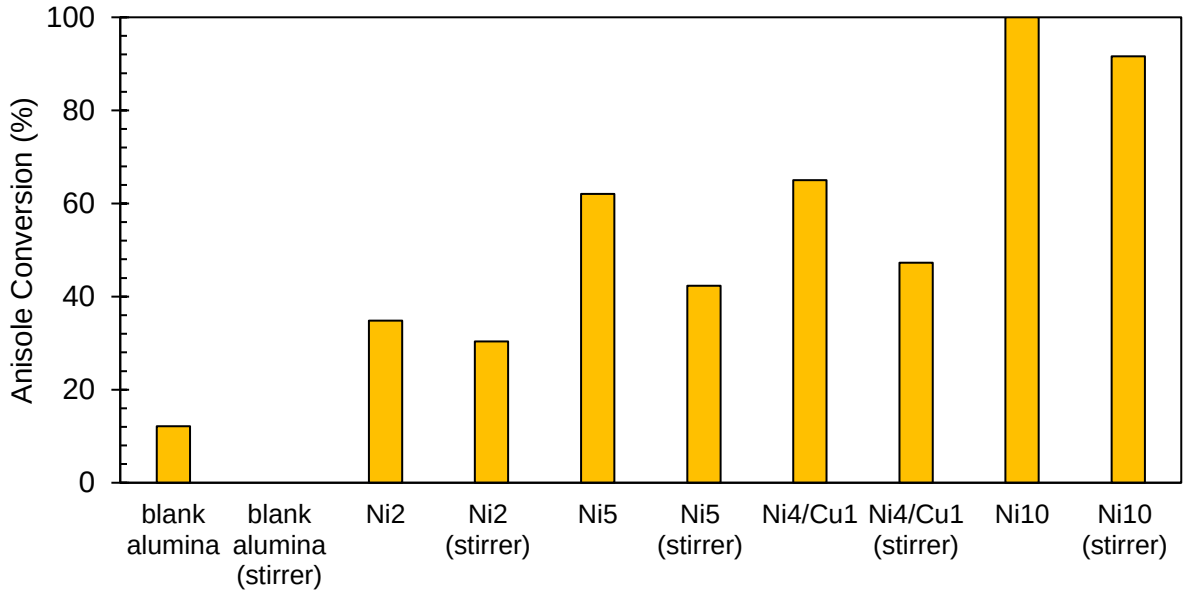

Figure 2.10. Comparison of anisole conversion Ni and Ni-Cu experiments between EA reactor and mechanically stirred reactor, performed at 220°C, an initial hydrogen pressure of 3.5MPa, 0.1g of catalyst (reduced at 400°C for 1h) and a reaction time of 45 minutes.

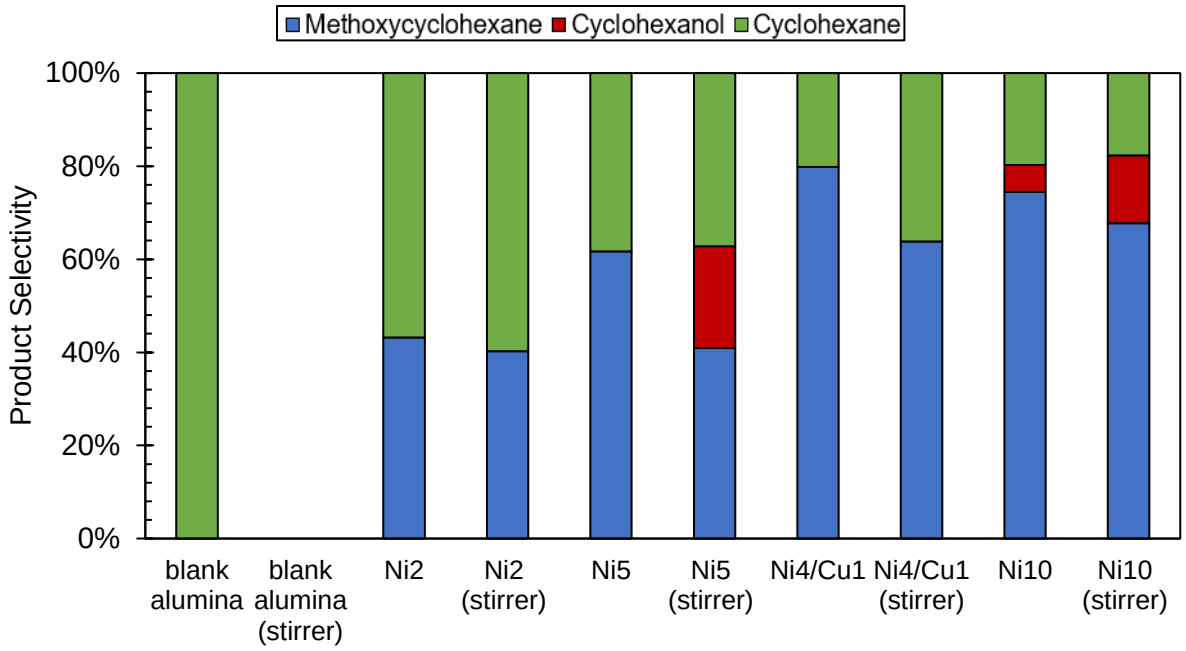

Figure 2.11. Comparison of product selectivity Ni and Ni-Cu experiments of between EA reactor and mechanically stirred reactor, performed at 220°C, an initial hydrogen pressure of 3.5MPa, 0.1g of catalyst (reduced at 400°C for 1h) and a reaction time of 45 minutes.

2.6 Conclusion

Hydrodeoxygenation of anisole as a bio-oil model compound was studied in a novel externally agitated batch reactor to validate its use and to generate baseline data for subsequent catalyst performance optimization studies. Silica, γ-alumina, and δ-alumina supports impregnated with 10 wt.% Ni were measured at varying reaction temperatures and times to determine their impact on anisole conversion and deoxygenation activity. Furthermore, comparative experiments were conducted in the EA reactor and a batch reactor mechanically stirred with an impeller to investigate the actual improvements, if any, the EA reactor may have on the HDO of anisole. Conclusions are summarized as follows:

1) The EA reactor was capable of anisole HDO with comparable conversion rates at shorter reaction times, milder operating conditions, and lower metal loadings when compared to similar HDO studies using mechanically stirred batch reactors.

2) Deoxygenation activity between supports was directly related to the acidity of the support implemented, in the order of SiO_2 < δ-Al_2O_3 < γ-Al_2O_3. Silica demonstrated limited deoxygenation activity relative to alumina supports, even with longer reaction times and higher reaction temperatures.

3) γ-alumina demonstrated the highest deoxygenation activity between supports while cyclohexane selectivity significantly from 17% to 100% when reaction temperature was increased from 160°C to 280°C.

4) γ-alumina was chosen as the support material for subsequent catalyst experiments with a reaction time of 45 minutes, reaction temperature 220°C, and an initial hydrogen pressure of 3.5MPa.

5) Hydrogenation and deoxygenation activity was improved when HDO was conducted in the EA reactor compared to the mechanically stirred batch reactor.

References

Absi-Halabi, M., Stanislaus, A., & Trimm, D. L. (1991). Coke formation on catalysts during the hydroprocessing of heavy oils. *Applied Catalysis*, *72*(2), 193–215. https://doi.org/10.1016/0166-9834(91)85053-X

Ardiyanti, A. R., Khromova, S. A., Venderbosch, R. H., Yakovlev, V. A., & Heeres, H. J. (2012). Catalytic hydrotreatment of fast-pyrolysis oil using non-sulfided bimetallic Ni-Cu catalysts on a δ-Al2O3 support. *Applied Catalysis B: Environmental*, *117–118*, 105–117. https://doi.org/10.1016/j.apcatb.2011.12.032

Bridgwater, a. V. (2012). Review of fast pyrolysis of biomass and product upgrading. *Biomass and Bioenergy*, *38*, 68–94. https://doi.org/10.1016/j.biombioe.2011.01.048

Busca, G., Kennedy, P., & Genova, I. (2007). Acid Catalysts in Industrial Hydrocarbon Chemistry, 5366–5410. *Chem. Rev.*, 107, 5366-5410. http://doi.org/10.1021/cr068042e

Bykova, M. V., Bulavchenko, O. a., Ermakov, D. Y., Lebedev, M. Y., Yakovlev, V. a., & Parmon, V. N. (2011). Guaiacol hydrodeoxygenation in the presence of Ni-containing catalysts. *Catalysis in Industry*, *3*(1), 15–22. https://doi.org/10.1134/S2070050411010028

Calles, J. A., Carrero, A., & Vizcaíno, A. J. (2009). Ce and La modification of mesoporous Cu-Ni/SBA-15 catalysts for hydrogen production through ethanol steam reforming. *Microporous and Mesoporous Materials*, *119*(1–3), 200–207. https://doi.org/10.1016/j.micromeso.2008.10.028

Carre, S., Gnep, N. S., Revel, R., & Magnoux, P. (2008). Characterization of the acid-base properties of transition aluminas by model reaction. *Applied Catalysis A: General*, *348*(1), 71–78. https://doi.org/10.1016/j.apcata.2008.06.024

de Miguel Mercader, F., Groeneveld, M. J., Kersten, S. R. a., Geantet, C., Toussaint, G., Way, N. W. J., Hogendoorn, K. J. a. (2011). Hydrodeoxygenation of Pyrolysis Oil Fractions: Process Understanding and Quality Assessment Through Co-processing in Refinery Units. *Energy & Environmental Science*, *4*, 985. https://doi.org/10.1039/c0ee00523a

Dickey, D. S. (2015). Tackling difficult mixing problems. *Chemical Engineering Progress*, *111*(8), 35–42.

Elliott, D. C. (2013). Transportation fuels from biomass via fast pyrolysis and hydroprocessing. *Wiley Interdisciplinary Reviews: Energy and Environment*, *2*(5), 525–533. https://doi.org/10.1002/wene.74

Foster, A. J., Do, P. T. M., & Lobo, R. F. (2012). The synergy of the support acid function and the metal function in the catalytic hydrodeoxygenation of m-cresol. *Topics in Catalysis*, *55*(3–4), 118–128. https://doi.org/10.1007/s11244-012-9781-7

Gandarias, I., & Arias, P. L. (2013). Hydrotreating Catalytic Processes for Oxygen Removal in the Upgrading of Bio-Oils and Bio-Chemicals. *Liquid, Gaseous, and Solid Biofuels-Conversion Techniques*, 327–356. https://doi.org/10.5772/50479

Ghampson, I. T., Sepúlveda, C., Dongil, A. B., Pecchi, G., García, R., Fierro, J. L. G., Escalona, N. (2016). Phenol hydrodeoxygenation: Effect of support and Re promoter on the reactivity of Co catalysts. *Catalysis Science & Technology*, *6*, 7289–7306. https://doi.org/10.1039/C6CY01038E

Hindin, S. G., & Weller, S. W. (1956). The Effect of Pretreatment on the Activity of Gamma-Alumina. I. Ethylene Hydrogenation. *The Journal of Physical Chemistry*, *60*, 1501–1506. https://doi.org/10.1021/j150545a008

Huuska, M., & Rintala, J. (1985). Effect of catalyst acidity on the hydrogenolysis of anisole. *Journal of Catalysis*. https://doi.org/10.1016/0021-9517(85)90099-5

Huynh, T., Armbruster, U., Kreyenschulte, C., Nguyen, L., Phan, B., Nguyen, D., & Martin, A. (2016). Understanding the Performance and Stability of Supported Ni-Co-Based Catalysts in Phenol HDO. *Catalysts*, *6*(11), 176. https://doi.org/10.3390/catal6110176

Huynh, T. M., Armbruster, U., Phan, B. M. Q., Nguyen, D. A., & Martin, A. (2013). Effect of second metal (Cu, Co) on catalytic performance of bimetallic Ni-based catalyst for phenol HDO, *Green Chemistry*. 1–2.

Jin, S., Xiao, Z., Li, C., Chen, X., Wang, L., Xing, J., Liang, C. (2014). Catalytic hydrodeoxygenation of anisole as lignin model compound over supported nickel catalysts. *Catalysis Today*, *234*, 125–132. https://doi.org/10.1016/j.cattod.2014.02.014

Khromova, S. A., Smirnov, A. A., Bulavchenko, O. A., Saraev, A. A., Kaichev, V. V., Reshetnikov, S. I., & Yakovlev, V. A. (2014). Anisole hydrodeoxygenation over Ni-Cu bimetallic catalysts: The effect of Ni/Cu ratio on selectivity. *Applied Catalysis A: General*, *470*(JANUARY 2014), 261–270. https://doi.org/10.1016/j.apcata.2013.10.046

Kwak, J. H., Mei, D., Peden, C. H. F., Rousseau, R., & Szanyi, J. (2011). (100) facets of γ-Al2O3: The active surfaces for alcohol dehydration reactions. *Catalysis Letters*, *141*(5), 649–655. https://doi.org/10.1007/s10562-010-0496-8

Latifi, M., Berruti, F., & Briens, C. (2015). Thermal and catalytic gasification of bio-oils in the Jiggle Bed Reactor for syngas production. *International Journal of Hydrogen Energy*, *40*(17), 5856–5868. https://doi.org/10.1016/j.ijhydene.2015.02.088

Lee, C. R., Yoon, J. S., Suh, Y. W., Choi, J. W., Ha, J. M., Suh, D. J., & Park, Y. K. (2012). Catalytic roles of metals and supports on hydrodeoxygenation of lignin monomer guaiacol. *Catalysis Communications*, *17*, 54–58. https://doi.org/10.1016/j.catcom.2011.10.011

Mahamulkar, S., Yin, K., Davis, R. J., Shibata, H., Malek, A., Jones, C. W., & Agrawal, P. K. (2016). In Situ Generation of Radical Coke and the Role of Coke-Catalyst Contact on Coke Oxidation. *Industrial and Engineering Chemistry Research*, *55*(18), 5271–5278. https://doi.org/10.1021/acs.iecr.6b00556

Mortensen, P. M., Grunwaldt, J. D., Jensen, P. A., & Jensen, A. D. (2013). Screening of catalysts for hydrodeoxygenation of phenol as a model compound for bio-oil. *ACS Catalysis*, *3*(8), 1774–1785. https://doi.org/10.1021/cs400266e

Navalikhina, M. D., & Krylov, O. V. (2001). Hydrogenating activity and adsorption capacity of supported nickel catalysts modified by heteropoly compounds. *Kinetics and Catalysis*. https://doi.org/10.1023/A:1010429804739

Pandey, M. P., & Kim, C. S. (2011). Lignin Depolymerization and Conversion: A Review of Thermochemical Methods. *Chemical Engineering and Technology*, *34*(1), 29–41. https://doi.org/10.1002/ceat.201000270

Rana, M. S., Sámano, V., Ancheyta, J., & Diaz, J. A. I. (2007). A review of recent advances on process technologies for upgrading of heavy oils and residua. *Fuel*, *86*(9 SPEC. ISS.), 1216–1231. https://doi.org/10.1016/j.fuel.2006.08.004

Robinson, A. M., Hensley, J. E., & Will Medlin, J. (2016). Bifunctional Catalysts for Upgrading of Biomass-Derived Oxygenates: A Review. *ACS Catalysis*, *6*(8), 5026–5043. https://doi.org/10.1021/acscatal.6b00923

Smirnov, a. a., Khromova, S. a., Bulavchenko, O. a., Kaichev, V. V., Saraev, a. a., Reshetnikov, S. I., Yakovlev, V. a. (2014). Effect of the Ni/Cu ratio on the composition and catalytic properties of nickel-copper alloy in anisole hydrodeoxygenation. *Kinetics and Catalysis*, *55*(1), 69–78. https://doi.org/10.1134/S0023158414010145

Sobieszuk, P., Pohorecki, R., Cygański, P., & Grzelka, J. (2011). Determination of the interfacial area and mass transfer coefficients in the Taylor gas-liquid flow in a microchannel. *Chemical Engineering Science*, *66*(23), 6048–6056. https://doi.org/10.1016/j.ces.2011.08.029

Sotowa, K. I. (2014). Fluid behavior and mass transport characteristics of gas-liquid and liquid-liquid flows in microchannels. *Journal of Chemical Engineering of Japan*, *47*(3), 213–224. https://doi.org/10.1252/jcej.13we141

Sugai, Y., Babadagli, T., & Sasaki, K. (2014). Consideration of an effect of interfacial area between oil and CO2 on oil swelling. *Journal of Petroleum Exploration and Production Technology*, *4*(1), 105–112. https://doi.org/10.1007/s13202-013-0085-7

Tang, W., Zhang, X., Zhang, Q., Wang, T., & Ma, L. (2016). Hydrodeoxygenation of Anisole over Ni/α-Al_2O_3 Catalyst. *Chinese Journal of Chemical Physics*, *29*(5), 617–622. https://doi.org/10.1063/1674-0068/29/cjcp1603062

Venderbosch, R. H., Ardiyanti, A. R., Wildschut, J., Oasmaa, A., & Heeres, H. J. (2010). Stabilization of biomass-derived pyrolysis oils. *Journal of Chemical Technology and Biotechnology*, *85*(5), 674–686. https://doi.org/10.1002/jctb.2354

Wildschut, J., Mahfud, F. H., Venderbosch, R. H., & Heeres, H. J. (2009). Hydrotreatment of Fast Pyrolysis Oil Using Heterogeneous Noble-Metal Catalysts. *Industrial & Engineering Chemistry Research*, *48*(23), 10324–10334. https://doi.org/10.1021/ie9006003

Wu, S.-K., Lai, P.-C., Lin, Y.-C., Wan, H.-P., Lee, H.-T., & Chang, Y.-H. (2013). Atmospheric Hydrodeoxygenation of Guaiacol over Alumina - , Zirconia - , and Silica-Supported Nickel Phosphide Catalysts. *Sustainable Chemical Engineering*, *1*, 349–358.

Yakovlev, V. A., Khromova, S. A., Sherstyuk, O. V., Dundich, V. O., Ermakov, D. Y., Novopashina, V. M., Parmon, V. N. (2009). Development of new catalytic systems for upgraded bio-fuels production from bio-crude-oil and biodiesel. *Catalysis Today*, *144*(3–4), 362–366. https://doi.org/10.1016/j.cattod.2009.03.002

Zarchin, R., Rabaev, M., Vidruk-Nehemya, R., Landau, M. V., & Herskowitz, M. (2015). Hydroprocessing of soybean oil on nickel-phosphide supported catalysts. *Fuel*, *139*, 684–691. https://doi.org/10.1016/j.fuel.2014.09.053

Chapter 3

Anisole hydrodeoxygenation over low loading
Ni-Cu/γ-Al_2O_3 catalysts in a novel externally agitated reactor

3.1 Introduction

Reliable renewable energy sources are required due to increasing global energy demands and diminishing fossil fuel reserves, including coal, natural gas, and oil which supply upwards of 86% of current world energy demands (Huynh et al., 2015). In addition to energy supply, climate change triggered by green house gas and CO_2 emissions, for which fossil fuels are a main contributor, hastens the necessity for improved carbon neutral energy sources and chemical production. Lignocellulosic biomass has recently been considered a promising renewable feedstock for energy production and transportation biofuels. It has been shown as a reliable feedstock due to its abundance, its non-competitive with food production, and its relatively low cost (Kumar & Reetu, 2015; Saini et al., 2015). Converting lignocellulosic biomass to liquid fuels is desirable due to compatibility with current petroleum hydrotreating infrastructure as well as advantages to storage, transportation, and processing. (Lewis, 2007). Fast pyrolysis has been recognized as an effective method to convert biomass to a liquid product, commonly known as bio-oil (D. C. Elliott, 2013).

Fast pyrolysis involves thermal decomposition of biomass at temperatures of approximately 500^{o}C, in the absence of oxygen, high heating rates of >1000^{o}C/s, followed by rapid cooling to maximize liquid yields (Inaki et al., 2013; Chheda et al., 2007). The resulting crude pyrolysis oil is of poor quality compared to traditional transportation fuels and contains undesirable properties due to high oxygen and water content (30-40%) (Zhong et al., 2012). Effective upgrading techniques are thus essential to reduce the oxygen content to convert the bio-oil into a suitable transportation fuel (Mortensen et al., 2011). Catalytic hydrodeoxygenation (HDO) of crude pyrolysis bio-oil is an effective upgrading route to diminish the high oxygen content and improve its overall properties. HDO involves heating the oil feedstock to high temperatures (200-400^{o}C), under high hydrogen pressures (10-30 MPa), and in the presence of a heterogenous

catalyst. The oxygen moieties in the substrate are removed as water, thus converting the oxygenated compounds to a feedstock more similar to petroleum oil (Bridgwater, 2012). Generally, HDO can be written in its most simplified version as:

$$CH_{1.4}O_{0.4} + 0.7H_2 \rightarrow \text{“}CH_2\text{”} + 0.4H_2O \quad (1)$$

Where “CH_2” represents an undetermined hydrocarbon product (Mortensen et al., 2013).

Extensive research has focused on discovering effective catalysts with adequate HDO activity, low cost, and long lifespans, resisting catalyst deactivation by coke formation (Absi-Halabi et al., 1991; Furimsky, 1999). Initial experiments investigated sulfided CoMo and NiMo catalysts commonly used for hydrodesulfurization (HDS) in petroleum hydrotreating; however, they were found to be ineffective for HDO. Without the addition of an external sulfur source, sulfided catalysts quickly deactivated through sulfur stripping, resulting in contamination of the upgraded bio-oil product (Gonçalves et al., 2016). Noble metal catalysts such as Pd, Rh, Ru, and Pt have shown high efficiency for hydrogenation and HDO activity, although their cost and poor longevity makes them unattractive (Mu et al., 2014).

Non-sulfided transition metals are promising catalysts and have demonstrated ability to carry out HDO of both model compounds and pyrolysis bio-oils. Their relatively low cost and high availability makes them more desirable in comparison to noble metals (Wildschut et al., 2009). Nickel-based catalysts specifically have been broadly studied and have been shown to be effective in hydrogenation reactions; however, rapid catalyst deactivation due to elevated coke formation has been proven to be problematic (Navalikhina & Krylov, 2001; Yakovlev et al., 2012). Furthermore, nickel-based catalysts typically require high metal loadings such as 20 wt.% (Ardiyanti et al., 2012), 60 wt.% (Bykova et al., 2011) with some studies even reporting loadings as high as 90 wt.% (Khromova et al., 2014; Smirnov et al., 2014). Improving transition metal catalysts has thus been a major focus to enhance their capacity for pyrolysis bio-oil hydrotreatment.

The addition of a second metal, referred as a promoter, has also been studied to improve catalyst activity, selectivity, and/or stability. Reports indicate that copper addition to nickel-based catalysts can enhance catalytic performance for HDO. Copper addition from 0 – 7 wt.% to 20 wt.% of nickel supported on γ-Al_2O_3 demonstrated reduced nickel particle size and weakened the interaction between Ni and the support, improving reducibility, and thus catalytic performance, when compared to monometallic Ni/γ-Al_2O_3 (Youn et al., 2006). Enhanced nickel dispersion

across the support surface was also observed when copper was added to nickel-based catalysts (Vizcaíno et al., 2007). Lastly, several studies report reduced coke deposition during HDO reactions with Ni-Cu catalysts compared to monometallic Ni catalysts (Y. Li et al., 2017). This effect has been also observed in steam reforming catalysts (Lee et al., 2004).

This study compares the performance of low metal loading (<10 wt.%) Ni and bimetallic Ni-Cu catalysts on a γ-alumina support for HDO of anisole, a pyrolytic bio-oil model compound. This study also establishes the capability of a novel externally agitated (EA) reactor for HDO-type reactions. Low metal loadings (2-10 wt.%) were implemented to demonstrate catalyst cost reductions for transition metal catalysts to minimize current economic challenges for bio-oil upgrading methods. Mild HDO conditions (220^{o}C and 3.5MPa) were chosen to reduce thermal cracking and catalyst coking, preventing catalyst deactivation. Reaction products and carbon deposits were examined to further understand the reaction mechanisms.

3.2 Materials and Methods

3.2.1 Catalyst preparation

All catalysts were prepared by incipient wetness impregnation using aqueous solutions of $Ni(NO_3)_2 \cdot 6H_2O$ and $Cu(NO_3)_2 \cdot 3H_2O$ obtained from Sigma-Aldrich (Steinheim, Germany). Spherical γ-alumina particles with a diameter of 1.7mm were obtained from provided by Sasol (K2476, Hamburg, Germany). The alumina spheres were crushed, sieved, and the 75-150μm particle size fraction was used for impregnation. Metal precursor amounts were calculated to achieve the desired Ni and Ni-Cu compositions and dissolved in a volume of water equal to the pore volume of the support. Catalyst formulations presented in this study indicate the weight fraction of the impregnated metal (e.g., Ni5 refers to 5 wt.% Nickel on γ-alumina). Monometallic Ni and bimetallic Ni-Cu catalysts had a total metal loading of 5.0 wt.% and 10 wt.% for comparison, except for the case of a 2.0 wt.% Ni catalyst. Following impregnation, catalyst samples were dried overnight in an oven at 100^{o}C, then calcined in dry air (Praxair, Ultra-Zero) at 400^{o}C for 3 hours with a heating rate of 10^{o}C/min and a flowrate of 10mL/min. Catalysts were reduced with 3.5MPa of hydrogen (Praxair, Ultra-High Purity (UHP)) at 400^{o}C for 1 hour in the reactor prior to HDO reaction.

3.2.2 Catalyst Characterization

Temperature programmed reduction (H_2 – TPR)

A catalyst mass of 0.1g was placed in a 0.25 inch ID quartz tube and treated in a 40ml/min mixture of H_2 in Argon (5 vol% H_2, Praxair, UHP)) at atmospheric pressure with a constant heating rate of 10^{o}C/min until a maximum temperature of 1000^{o}C. The temperature was raised in the system at a rate 10 K/min to 1073K. The amount of hydrogen consumption was measured using a SRI 110 TCD detector. Hydrogen consumption in the TPR system was calibrated using known amounts of CuO.

Texture Characteristics from N_2 Physiorption.

Specific surface area (S_{BET}), mesopore volume (V_p), and average pore diameter (d_p) of the blank support and Ni/Cu catalysts were determined from nitrogen adsorption-desorption isotherms at 77K using a Tristar II 3020. The catalysts were degassed prior to measurements at 453K for 24 hours.

Thermogravimetric Analysis (TGA)

Spent catalyst samples (10mg) were first vacuum dried over night at room temperature to remove volatile remnants. Samples were analyzed using a PerkinElmer Pyris 1 TGA using an air flowrate of 30mL/min with a heating rate of 10^{o}C/min until a maximum temperature of 800^{o}C (10 Hz, two-point calibration, alumel and iron for reference).

3.2.3 Experimental Setup and Catalyst Testing Procedure

Catalytic hydrodeoxygenation reactions of anisole were carried out in a 100mL stainless steel high-pressure and temperature batch reactor (model 4793 Parr) attached to a pneumatic actuator providing external agitation. A schematic of the reactor and the surrounding components is provided in Figure 3.1. A catalyst mass of 0.1g was added to the reactor, sealed, and vacuum purged with nitrogen three times to ensure removal of air. The reactor was then pressurized with hydrogen gas at room temperature to 3.5 MPa prior to the reduction. Catalysts were reduced for a total of 1 hour (t = 0 when heater was turned on at room temperature) using a heating rate of

12°C/min to a final temperature of 400°C. After 1 hour, the reactor was cooled in hydrogen atmosphere at an approximate rate of 5°C/min to 40°C. A summary of the operating conditions implemented for HDO of anisole is presented in Section 2.2.3.

Table 3.1 Operating conditions implemented for HDO of anisole.

Parameter	**Value**	**Units**
Reduction time	60	minutes
Reduction temperature	400	°C
Initial Hydrogen Pressure (at 25°C)	3.5	MPa
Reaction Temperature	220	°C
Reaction Time	45	minutes

The liquid reactant mixture was composed of 1.2ml of anisole (99%, Fischer Scientific), 20ml of n-decane (99%, Fischer Scientific), and 0.4ml of n-dodecane (99%, Fischer Scientific, used as internal standard for chromatographic analysis). After the catalyst reduction and cooling step, the reactor was depressurized and the liquid reactant was injected into the reactor using a syringe through a septum to prevent exposing the reactor to air. Hydrogen was then flowed through the reactor for 5 minutes to ensure no residual air was present. The reactor was then pressurized to 3.5 MPa of hydrogen at 40°C. This amount of hydrogen corresponds to a H:O ratio of approximately 10:1 for anisole. Reaction time started from 40°C (t = 0), when the heater was initiated, the reactor was heated to 220°C at a heating rate of 12°C/min and then held at the reaction temperature for 45minutes. External agitation was also initiated at t = 0. The reactor was then fan cooled to 40°C, then opened and gas products captured in a 10L gas sampling bag for analysis.

3.2.4 Product Analysis

Gas products captured in a gas sampling bag and were analyzed on a Micro-GC (Agilent 490) for H_2, CO, CO_2, and CH_4 content using CP-MolSieve 5A and PoraPLOT U columns and a TCD detector. The system was calibrated using a standard gas mixture (Praxair, UHP). Liquid samples were collected and identified by Gas Chromatography (Agilent 7890A) using a HP-5MS

column (Agilent, 30m x 0.250mm x 0.25µm film thickness) coupled to a MS detector (Agilent 5975C MSD) and quantified using Flame Ionization Detector (FID). The GC-MS system was calibrated using liquid standards of methoxycyclohexane (99%, Alfa Aesar), cyclohexanol (99%, Alfa Aesar), and cyclohexane (99%, Alfa Aesar). The anisole conversion was determined as:

$$x = \left(1 - \frac{C_A}{C_A^0}\right) \cdot 100\% \quad (2)$$

where C_A represents the concentration of anisole in the product and C_A^0 is the concentration of anisole initially introduced into the reactor. Liquid product selectivity was calculated as:

$$s_i(mol\%) = \frac{n_{product\ i}}{n_{anisole\ converted}} \cdot 100\% \quad (3)$$

where $n_{product\ i}$ is the number of moles of product i and $n_{anisole\ converted}$ is the number of moles of converted anisole. Liquid product selectivity is normalized based on the total liquid products formed, and does not consider anisole that was not converted.

All catalyst experiments were carried out in duplicates or triplicates to verify reproducibility of the data. Data is presented as the average of the duplicates or triplicates. Three triplicates were performed in this chapter, with an average standard deviation of 6.8 (conversion) and 4.6 (selectivity). The carbon balance for all runs was always above 88%.

3.3 Results and Discussion

3.3.1 H_2-TPR

Temperature-programmed reduction (TPR) analysis provides details on metal-support interactions as well as the impact promoters (Cu) can have on the reduction process and the relative proportion of nickel species (Zhang et al., 2005). The H_2-TPR profiles of the fresh catalyst samples are presented in Figure 3.1. For comparison purposes, the reduction profile of 2 wt.% Cu/ $\gamma - Al_2O_3$ is included in Figure 3.1b. An initial test with bare γ – alumina support showed no reduction temperature peaks, indicating negligible hydrogen uptake from the support surface.

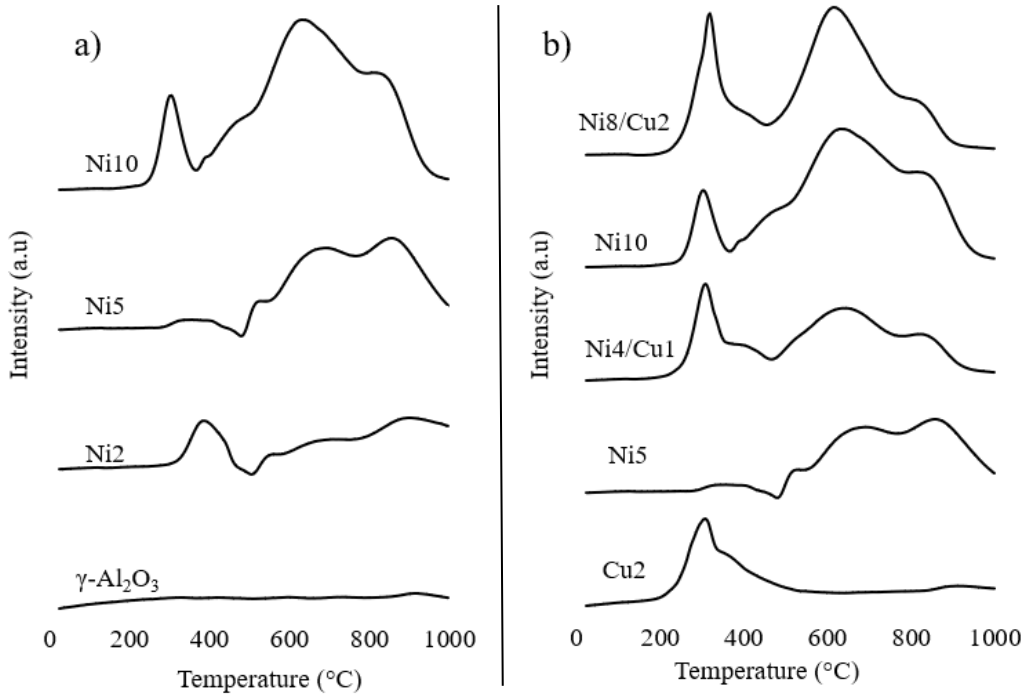

Figure 3.1 H_2-TPR Profiles for a) bare γ-alumina support, 2, 5 and 10 wt.% of Ni and b) Ni and Ni-Cu catalysts with total metal loadings of 5 and 10 wt.%

H_2-TPR profiles of monometallic Ni catalysts (Fig. 3.1 a) show a broad reduction area between 300ºC – 1000ºC with three key reduction peaks centered at approximately 350ºC, 620ºC, and 810ºC (Figure 3.1a). Previous TPR studies on nickel-based catalysts have reported that Ni^{2+} directly reduces to Ni^0 without any intermediates, thus each peak is expected to represent individual Ni species (Molina & Poncelet, 1998). As nickel metal loading increased from 2 wt.% to 10 wt.%, all three reduction peaks shifted gradually to lower temperatures, suggesting a weaker interaction with the support. For example, the first reduction peak shifted from 405ºC in Ni 2% to 315ºC in Ni10%. This first reduction peak is assigned to what is commonly referred to as crystal NiO, that weakly interact with the alumina support and are much more readily reduced (Mattos et al., 2004). Although easier to reduce, NiO species, located on the alumina surface, are highly susceptible to particle growth, agglomeration, and migration at elevated temperatures that can cause reduced nickel dispersion and increases in particle size (Xu et al., 2001). Reduction peaks above 500ºC are associated with spinal $NiAl_2O_4$ species that strongly interact with the support, and are more difficult to reduce (Bartholomew & Farrauto, 1976). Spinel $NiAl_2O_4$ are known to

comprise two different orientations, an easier reducible octahedral geometry and a tetrahedral geometry which is more difficult to reduce, owing to the two separate TPR peaks at ~620^{o}C and ~810^{o}C, respectively (Kirumakki et al., 2006; Yang et al., 2009). Alternatively to NiO, $NiAl_2O_4$ spinels are embedded into the alumina lattice and even though they are more difficult to reduce, are typically more stable, better dispersed, and more resistant to coking (Hu et al., 1997).

Hydrogen consumption derived from the TPR profiles is provided in Table 3.2. Hydrogen consumption was divided into a low temperature (<400°C) and high temperature (400 - 1000°C) region due to the limitations of the band heater used in the experimental setup which had a maximum temperature of 400^{o}C. Catalysts were reduced at 400°C and therefore were not completely reduced prior to HDO experiments, NiO species were thus mostly reduced. TPR profiles demonstrate that as nickel loading increased from 2 wt.% to 10 wt.%, total hydrogen consumption increased; however, NiO and $NiAl_2O_4$ species did not proportionally increase. For example, the reduction profile of the Ni2 catalyst resulted in the highest proportion (17%) of NiO species and was the most reducible at 400°C relative to the Ni5 and Ni10 catalysts, indicating a weak interaction with the support and less nickel dispersion. Interestingly, when Ni loading was increased to 5 wt.%, total hydrogen consumption increased; however, there was a major shift towards reduction peaks associated with $NiAl_2O_4$ spinels with only 4% hydrogen consumption occurring below 400°C, suggesting that there was a much stronger interaction with the support and nickel dispersion. As nickel loading was further increased to 10 wt.%, both NiO and $NiAl_2O_4$ phases increased with a greater proportion of hydrogen consumption occurring below 400°C compared to the Ni5 catalyst with 11%. These results indicate that depending on reduction temperature, the proportion of NiO species does not necessarily improve relative to increasing metal loadings.

Table 3.2 Quantitative TPR data for Ni and Ni-Cu catalysts. Hydrogen consumption is presented as a function of reduction temperature.

Catalyst	Total H_2 Consumption (mmol)	H_2 Consumption (%)	
		Low Temperature (<400^{o}C)	High Temperature (400 – 1000^{o}C)
Ni2	0.142	17	83
Ni5	0.218	4	96
Ni10	0.412	11	89
Ni4/Cu1	0.261	26	74
Ni8/Cu2	0.370	23	77

Bimetallic catalyst profiles produced the same relative three reduction peaks, demonstrating that nickel species were present in both NiO and $NiAl_2O_4$ phases. The substitution of nickel metal loading with copper improved the degree of reducibility below 400°C and significantly increased the proportion of NiO relative to monometallic Ni catalysts of equal loading; however, the effect on total hydrogen consumption up to 1000°C varied depending on metal loading. For example, the Ni4/Cu1 catalyst resulted in a drastic improvement in total hydrogen consumption, specifically below 400°C, compared to the Ni5 catalyst. The reduction profile of Ni4/Cu1 also indicates a shift in the first reduction peak to lower temperatures (320ºC) in comparison to the 5Ni sample (380°C). The Ni8/Cu2 catalyst, however, did not have a shift in peak reduction temperature relative to Ni10. Furthermore, although a clear improvement in reducibility below 400°C and increase in NiO species is present with the Ni8/Cu2 catalyst relative to Ni10, total hydrogen consumption declined slightly.

The general improvement in reducibility with the addition of Cu to Ni/Al_2O_3 catalysts has been widely reported in literature (Yakovlev et al., 2009; Youn et al., 2006). As indicated in the reduction profile of $Cu/\gamma - Al_2O_3$, as well as in other studies, copper is more easily reduced than nickel with a narrower reduction temperature (Figure 3.3b) (Tavares et al., 1996; Kang et al., 2002). Studies have also shown that copper can have a strong interaction with nickel, resulting in the formation of Ni-Cu alloys which has been shown to be more easily reduced than CuO or NiO separately (Smirnov et al., 2014). This would explain the improved reducibility below 400°C for bimetallic Ni-Cu catalysts relative to the monometallic Ni catalysts with equivalent loading. Furthermore, the presence of Ni-Cu alloys may cause incomplete NiO reduction due to copper species typically positioned closer to the surface, potentially blocking some Ni particles (Cangiano et al., 2010). This may explain the decrease in total hydrogen consumption for the Ni8/Cu2 catalyst in relation to the Ni10 catalyst.

3.3.2 Surface Area Measurements

Table 3.3 presents the textural characteristics of the catalysts and bare alumina support determined by the BET method following calcination to investigate possible changes in the catalyst texture following impregnation. Specifically, changes in porosity can affect reactant and product diffusion into and out of the catalyst (Zhang et al., 2014). Incorporation of metal precursors (Ni or

Cu) slightly reduced specific surface area (A_{BET}), pore volume, and average pore diameter with increasing metal loadings. There were negligible differences between monometallic Ni and bimetallic Ni-Cu catalysts with equal metal loadings. The observed gradual decrease in surface area was expected and has been reported in other studies as a result of the Ni or Cu dispersion across the support surface, partially blocking pores (Yang et al., 2014). The reduced pore volume and diameter also indicates that metal particles are dispersed within the support pore channels (Sankaranarayanan et al., 2015). Generally, high surface area is desired to improve metal dispersion and thermal stability, thus providing more active metal sites for hydrogenation and decreasing sintering and migration effects during calcination (Newnham et al., 2012; García-Diéguez et al., 2010).

Table 3.3 Surface area, pore volume, and average pore diameter of the calcined catalysts determined by BET method

Catalyst	A_{BET} (m^2/g)	V_{pores} (cm^3/g)	Average pore diameter (Å)
γ-Al_2O_3	201	0.505	76
Ni2	190	0.468	74
Ni5	182	0.443	73
Ni4/Cu1	184	0.438	72
Ni10	172	0.414	71
Ni8/Cu2	168	0.412	72

3.3.3 Catalyst Activity in Anisole Hydrodeoxygenation

Figures 3.2 and 3.3 present anisole conversion and liquid product selectivity following anisole HDO experiments, respectively. Figures 3.2a and 3.3a compare anisole conversion and liquid product selectivity for increasing nickel loadings. Figure 3.2b and 3.3b compare anisole conversion and liquid product selectivity between Ni and Ni-Cu catalysts with equal metal loadings of 5 wt.% and 10 wt.%.

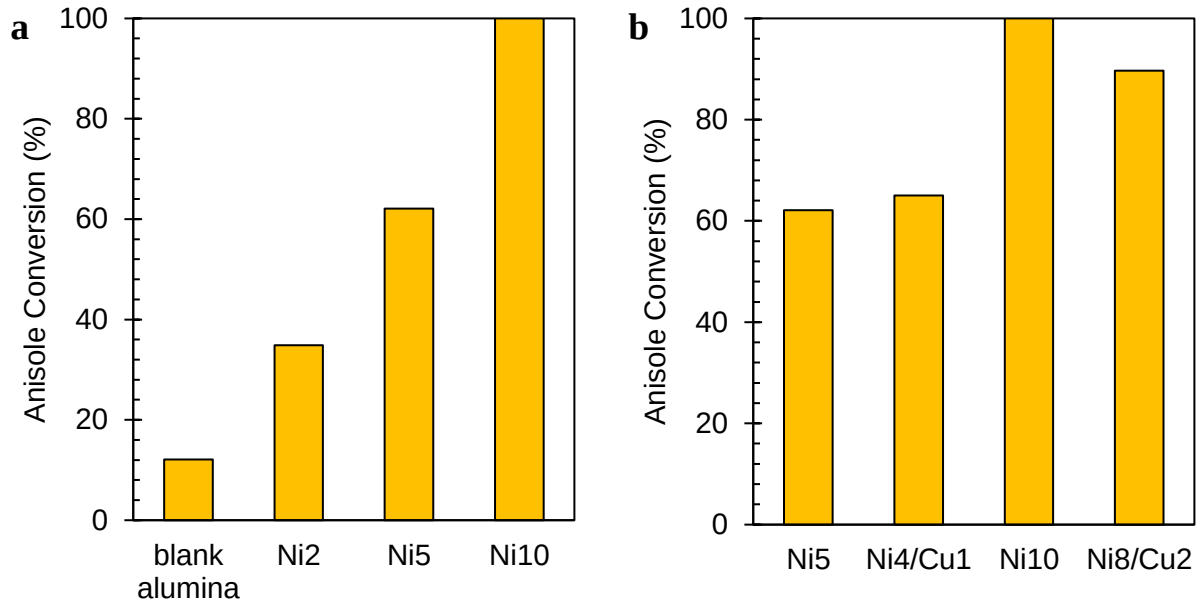

Figure 3.2. (a) Ni and (b) Ni-Cu experiments performed at 220°C, an initial hydrogen pressure of 3.5MPa, 0.1g of catalyst (reduced at 400°C for 1h) and a reaction time of 45 minutes.

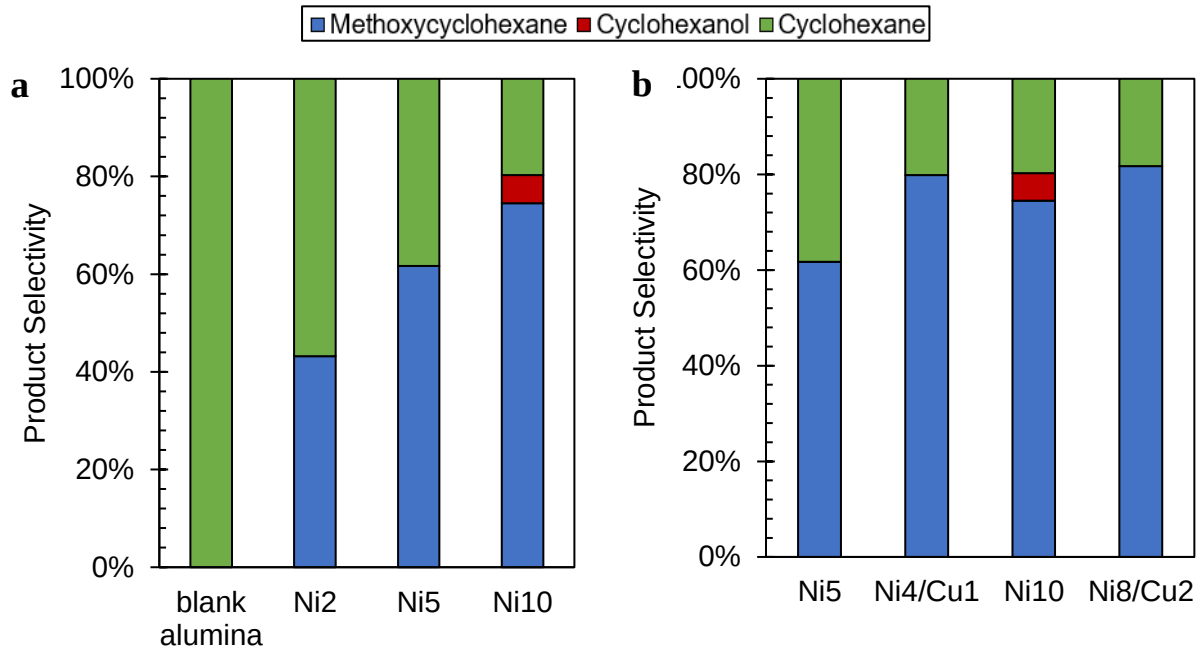

Figure 3.3. (a) Ni and (b) Ni-Cu experiments performed at 220°C, an initial hydrogen pressure of 3.5MPa, 0.1g of catalyst (reduced at 400°C for 1h) and a reaction time of 45 minutes.

A test with no catalyst (not shown) was initially performed under the same experimental conditions and resulted in no observable anisole conversion, verifying that the reactor itself was not catalytically active and had no impact on anisole HDO. Bare γ-Al_2O_3 support experiments resulted in 11% anisole conversion with 100% cyclohexane selectivity (Figure 3.2a and 3.3a). Tests conducted with bare SiO_2 support in Chapter 2 resulted in zero anisole conversion, verifying that this bare γ-Al_2O_3 support was responsible for both hydrogenation and deoxygenation activity. Alumina supports generally only contain active sites for C-O bond cleavage, relevant in deoxygenation; however, other studies have also reported evidence for minor hydrogenation activity with bare alumina supports (Hindin et al., 1956; Yakovlev et al., 2009; Tang et al., 2016).

Anisole conversion increased from 35% to 100% as nickel metal loading was increased from 2 to 10 wt%, whereas selectivity towards deoxygenated products (i.e. cyclohexane) decreased from 57% to 20% (Figures 3.2a and 3.3a). Cyclohexanol in the liquid product was only observed for the 10Ni catalyst. Although in this case HDO selectivity towards cyclohexane decreased steadily from 57% to 20%, cyclohexane yield increased from 14% with Ni2% to 18% with Ni10. Similar studies have observed increasing anisole conversion as nickel metal loadings increased (Zhang et al., 2016; Smirnov et al., 2014). As nickel loading increased, active sites for hydrogenation increased proportionately, shown by the higher methoxycyclohexane selectivity from 43% to 74% with Ni2 and Ni10 catalysts, respectively. This agrees with the TPR profiles where total hydrogen consumption also increased with increasing nickel loadings. Interestingly, cyclohexane yields were similar at 2 wt.% nickel loading compared to 10 wt.% in the EA reactor, even though methoxycyclohexane yields were almost seven times as much for the latter with 70% for Ni10 compared to 11% for Ni2. This suggests that increasing nickel loading enhances hydrogenation of the aromatic ring, improving conversion, while the rate of deoxygenation is kinetically limited.

Bimetallic Ni-Cu and monometallic Ni catalyst comparisons varied depending on the total metal loadings (Figures 3.2b and 3.3b). Bimetallic Ni4/Cu1 had a slight improvement in anisole conversion relative to monometallic Ni5 from 62% to 65%; however, cyclohexane selectivity was reduced from 38% to 20%. Conversely, Ni8/Cu2 catalyst had a reduced anisole conversion from 100% to 90% when compared to the Ni10 catalyst. Cyclohexane selectivity was relatively unchanged between Ni8/Cu2 and Ni10 catalysts with 18% and 20%, respectively. Although cyclohexane selectivity was similar between Ni8/Cu2 and Ni10 catalysts, 11% cyclohexanol

selectivity was present, which was not observed for Ni8/Cu2 or any other studied catalyst. Monometallic 10Ni was shown to be the most effective catalyst with the highest anisole conversion and cyclohexane yield.

Previous studies conflict when comparing monometallic Ni or bimetallic Ni-Cu catalyst performance for HDO or hydrogenation reactions. Studies have suggested that monometallic Ni catalysts are more active for benzene hydrogenation at reaction temperatures between 200^{o}C – 220^{o}C, where above 220^{o}C bimetallic Ni-Cu catalysts are thought to be more active (Khromova et al., 2014). It was predicted that fewer cracking reactions, facilitated by nickel, occurred at lower temperatures, forming methane and coke while leading to faster catalyst deactivation (Smirnov et al., 2014). Similar findings of decreased conversion with copper addition where reported for HDO of phenol with a significant decrease in conversion when substituting 20 wt.% nickel metal loading with 4 wt.% and 10 wt.% of copper (Huynh et al., 2013). An increase in anisole HDO was also seen using Ni-Cu catalyst with a total metal loading of 38 wt.% when compared to monometallic nickel catalysts of equal loading (Yakovlev et al., 2009). Some studies have suggested that the reduced performance following copper addition is due to the strong interaction between nickel and alumina, favouring copper species to arrange themselves closer to the catalyst surface and nickel species below the surface (Yao & Goodman, 2014; Kang et al., 2002). Copper may thus block available active sites on nickel particles. A related study on anisole HDO described higher conversion but lower deoxygenation with bimetallic 16 wt.% Ni/ 2 wt.% Cu catalyst relative to monometallic 20 wt.% Ni (Ardiyanti et al., 2012). The authors suggested that the added copper impacted the nickel-alumina interaction by reducing the formation of Ni-alumina spinels that are difficult to reduce.

Liquid products identified by GC-MS included exclusively methoxycyclohexane, cyclohexanol, and cyclohexane for all catalyst samples. The observed compounds suggest that the reaction pathway under the studied conditions included an initial hydrogenation of the anisole aromatic ring to form methoxycyclohexane, followed by demethylation of the C_{methyl}-O bond yielding cyclohexanol and methane, then lastly, deoxygenation of cyclohexanol via the C-O bond by intramolecular dehydration of the hydroxyl group to ultimately form cyclohexane and water. This reaction pathway has been reported in other studies using similar catalysts (Figure 3.4, Khromova et al., 2014; Jin et al., 2014; Sankaranarayanan et al., 2015).

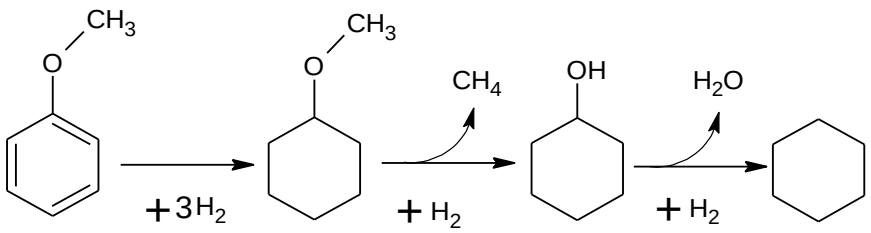

Figure 3.4 Observed reaction pathway of anisole conversion.

A previously reported alternative to the observed reaction pathway in this study involves an initial demethylation to phenol, followed by direct HDO to form benzene and methanol, which may be further hydrogenated to form cyclohexane (Viljava et al., 2000; Smirnov et al., 2014). No benzene was detected by GC-MS in this study, which has been reported as high as 50% product selectivity when using similar Ni/γ-Al_2O_3 and Ni-Cu/δ-Al_2O_3 catalysts for anisole HDO (Yang et al., 2014; Ardiyanti et al., 2012). Methanol and phenol were also not detected in the liquid phase, further confirming that the alternative reaction route involving direct HDO was not present. Another anisole HDO study with similar alumina-supported nickel catalysts reported phenol selectivity as high as 21% (W. Tang et al., 2016).

It is not fully understood which operating parameters influence the dominate reaction pathway. Some reports have suggested that direct anisole HDO to form benzene is more favoured at temperatures above 230°C compared to HDO following an initial aromatic ring hydrogenation (Centeno et al., 1995; Lee et al., 2014; Zhao et al., 2011). This is due to the oxygen bond to aromatic carbon (bond enthalpy -422 kJ/mol) being more difficult to break than the oxygen bond to sp^3 carbon (bond enthalpy -385 kJ/mol) (Sankaranarayanan et al., 2015). The first scenario describes direct HDO. Although aromatic ring hydrogenation is not necessarily desired as this consumes more hydrogen, it can be beneficial at lower temperatures to promote deoxygenation by weakening neighbouring C-O bonds, lowering the energy required to break it (Robinson et al., 2016). For example, the general C-O bond dissociation energy of an aromatic alcohol (i.e. phenol) is 469 kJ/mol, whereas in secondary alcohols (i.e. cyclohexanol) is only 385 kJ/mol (Venderbosch et al., 2010). Other reports have explained the presence of two separate reaction pathways on the existence of two types of nickel active sites on the alumina support. One active site is thought to facilitate aromatic ring hydrogenation via electron-accepting properties, where the reactant adsorbs planarly via the π-system of the aromatic ring. The second electron-donating active site is believed to adsorb the reactant vertically via the oxygen atom, allowing the cleavage of the $C_{aromatic}$-O bond for deoxygenation (Khromova et al., 2014; Gevert et al., 1986; Vogelzang et al., 1983).

3.3.4 Gas Phase Analysis

Micro-GC analysis of gas phase products are presented in Figure 3.5. Methane was the only detectable gas product besides hydrogen. Methanol, which was not observed in the liquid phase for any catalyst, was also undetected in the gas phase. This last result is consistent with the suggested reaction pathway that does not include direct HDO to benzene. As nickel loading increased in the monometallic Ni catalysts, methane increased from 0.63 mol% with bare γ-Al_2O_3 support to 2.20 mol% with the Ni10% catalyst (Figure 3.5a). Copper addition to the nickel-based catalysts lowered methane production from 0.94 mol% to 0.70 mol% for the Ni5 and Ni4/Cu1 catalysts, respectively, and from 2.20 mol% to 0.82 mol% for the Ni10 and Ni8/Cu2 catalysts, respectively (Figure 3.5b). Methane production of monometallic catalysts was directly proportional to the cyclohexanol and cyclohexane yield, which increased with nickel loading. Methane production of bimetallic catalysts was also directly proportional to cyclohexanol and cyclohexane yield. This is consistent with the proposed reaction pathway, where methane is released following demethylation of methoxycyclohexane, forming cyclohexanol.

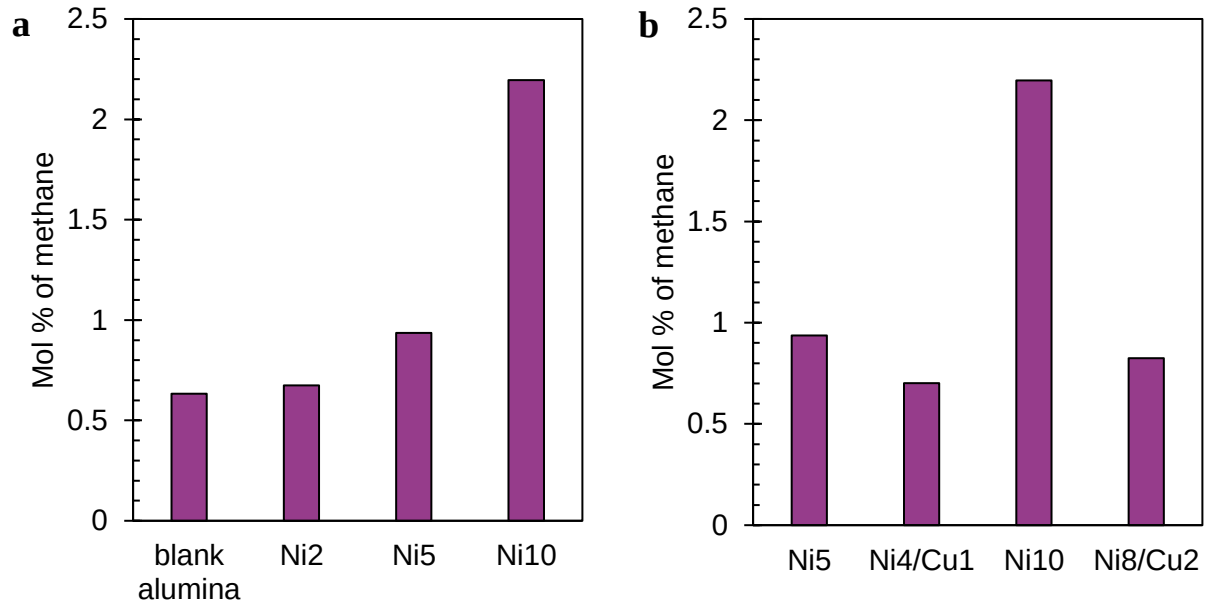

Figure 3.5. Methane mole fraction based on the initial anisole carbon for (a) Ni and (b) Ni-Cu experiments performed at 220^{o}C, an initial hydrogen pressure of 3.5MPa, 0.1g of catalyst (reduced at 400^{o}C for 1h) and a reaction time of 45 minutes.

3.3.5 Coke Analysis

Coke formation from TGA analysis of spent catalysts are presented in Figure 3.6. As nickel loading increased, coke production decreased from 0.66 mol% with bare γ-Al_2O_3 support to 0.37 mol% with the Ni10 catalyst (Figure 3.6a). On the other hand, the impact of copper addition on coke production varied with total metal loading. For example, coke deposits decreased from 0.37 mol% to 0.22 mol% for the Ni5 and Ni4/Cu1 catalysts, respectively, but increased from 0.37 mol% to 0.49 mol% for the Ni10 and Ni8/Cu2 catalysts, respectively (Figure 3.6b). Studies have suggested that coke formation is directly related to the support acidity and take place on the acid sites (Marecot et al., 1992; Bu et al., 2012). Lewis acid sites, which are known to be highly present on alumina, have been shown to bind species to the catalyst surface, with Brønsted acid sites donating protons to form carbocations thought to be responsible for coke formation (Furimsky et al., 1999; Popov et al., 2010). This would explain that as nickel loading increased, more acid sites located on the support would be blocked by dispersed nickel species, reducing coke formation.

The change in coke formation with the addition of copper can be related to the particle size of the nickel. Literature has reported that the addition of copper to nickel-based catalysts can lower nickel particle size while improving dispersion across the support (Vizcaíno et al., 2007; Dongil et al., 2016). It is thought that smaller Ni particles and increased dispersion can limit the formation of large Ni clusters, which facilitate the formation of coke (Ruckenstein & Hul, 1999). A study reported bimetallic Ni-Cu catalysts to be less susceptible to coking in comparison to monometallic Ni during HDO of bio-oil, and attributed it to the enhanced nickel dispersion and reduced particle size when copper was added (Y. Li et al., 2017). Although, other studies have indicated that increased nickel loadings can lead to enlarged nickel particle size on the supports surface, diminishing the blocking of acid sites on the alumina (Sánchez-Cárdenas et al., 2016). This may explain the distinct behaviour of coke formation at different nickel loadings. Lee et al. reported similar results during CO_2 reforming of methane, where the addition of 1 wt.% of Cu to 10 wt.% Ni/γ-Al_2O_3 lead to reduced coke formation relative to monometallic Ni, however, the addition of 5 wt.% of Cu increased coke formation (Lee et al., 2004).

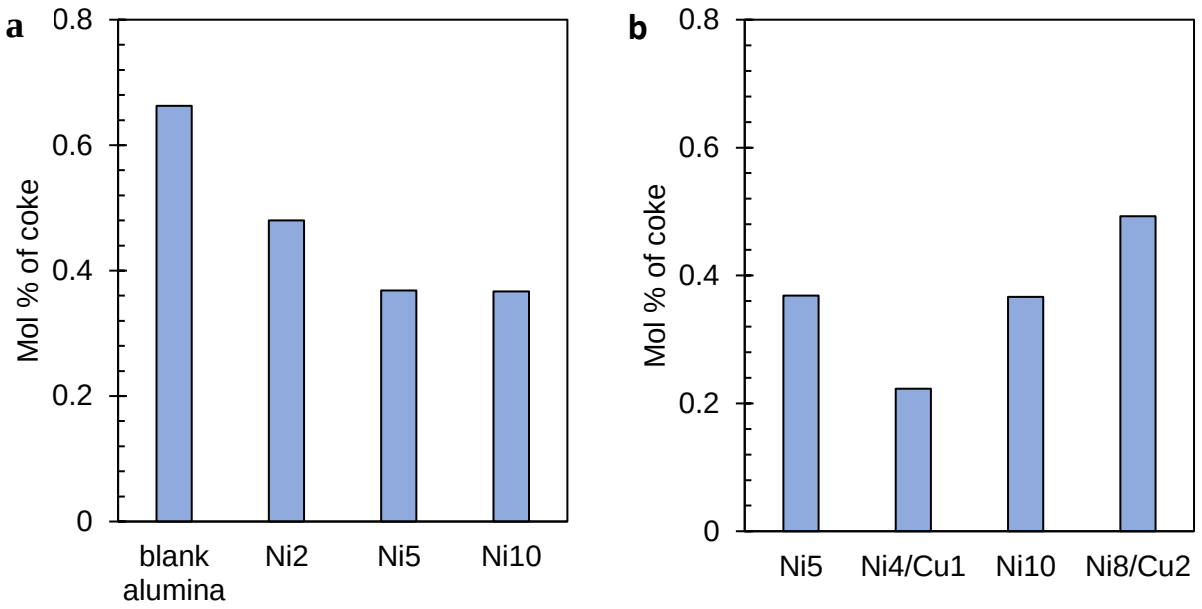

Figure 3.6. Coke mole fraction based on the initial anisole carbon for (a) Ni and (b) Ni-Cu experiments performed at 220^{o}C, an initial hydrogen pressure of 3.5MPa, 0.1g of catalyst (reduced at 400^{o}C for 1h) and a reaction time of 45 minutes.

3.4 Conclusion

Hydrodeoxygenation of anisole as a bio-oil model compound was studied in a novel externally agitated batch reactor at mild operating conditions of 220^{o}C, an initial hydrogen pressure of 3.5MPa, and a reaction time of 45 minutes. Monometallic Ni and bimetallic Ni-Cu catalysts were compared with total metal loadings of 5 wt.% and 10 wt.%. It was expected that the addition of copper as a promoter would increase the degree of reducibility of the nickel catalyst, thus allowing more hydrogen to be available, resulting in an increase in HDO activity. Conclusions are summarized as follows:

1) As nickel loading increased, total hydrogen consumption increased but the proportion of nickel species varied depending on nickel loadings. The substitution of nickel with copper improved the degree of reducibility relative to monometallic Ni catalysts, even at low metal loadings.

2) The observed reaction pathway based on gas and liquid products consists of a single reaction pathway; an initial hydrogenation of the aromatic ring to form methoxycyclohexane, followed by demethylation to form cyclohexanol, then finally deoxygenation via a dehydration reaction to form cyclohexane.

3) Monometallic Ni catalysts had higher cyclohexane yields than bimetallic Ni-Cu catalysts at both metal loadings whereas conversion differences varied based on total metal loading. As nickel loading increased, hydrogenation of the aromatic ring increased, however, deoxygenation yields (i.e. cyclohexane) remained relatively constant.

4) Coke formation decreased as nickel loading increased, although coke formation varied with the addition of copper depending on total metal loading.

References

Absi-Halabi, M., Stanislaus, A., & Trimm, D. L. (1991). Coke formation on catalysts during the hydroprocessing of heavy oils. *Applied Catalysis*, *72*(2), 193–215. https://doi.org/10.1016/0166-9834(91)85053-X

Ardiyanti, A. R., Khromova, S. A., Venderbosch, R. H., Yakovlev, V. A., & Heeres, H. J. (2012). Catalytic hydrotreatment of fast-pyrolysis oil using non-sulfided bimetallic Ni-Cu catalysts on a δ-Al2O3 support. *Applied Catalysis B: Environmental*, *117–118*, 105–117. https://doi.org/10.1016/j.apcatb.2011.12.032

Bartholomew, C. H., & Farrauto, R. J. (1976). Chemistry of nickel-alumina catalysts. *Journal of Catalysis*, *45*(1), 41–53. https://doi.org/10.1016/0021-9517(76)90054-3

Bridgwater, a. V. (2012). Review of fast pyrolysis of biomass and product upgrading. *Biomass and Bioenergy*, *38*, 68–94. https://doi.org/10.1016/j.biombioe.2011.01.048

Bu, Q., Lei, H., Zacher, A., Wang, L., Ren, S., Liang, J., Ruan, R. (2012). A Review of Catalytic HDO of Lignin-Derived Phenols from Biomass Pyrolysis. *Biosource Tech.*, *124*, 470–477.

Bykova, M. V., Bulavchenko, O. a., Ermakov, D. Y., Lebedev, M. Y., Yakovlev, V. a., & Parmon, V. N. (2011). Guaiacol hydrodeoxygenation in the presence of Ni-containing catalysts. *Catalysis in Industry*, *3*(1), 15–22. https://doi.org/10.1134/S2070050411010028

Centeno, A., Laurent, E., & Delmon, B. (1995). Influence of the Support of CoMo Sulfide Catalysts and of the Addition of Potassium and Platinum on the Catalytic Performances for the Hydrodeoxygenation of Carbonyl, Carboxyl, and Guaiacol-Type Molecules. *Journal of Catalysis*. https://doi.org/10.1006/jcat.1995.1170

Furimsky, E. (1999). Deactivation of hydroprocessing catalysts. *Catalysis Today*, *52*(4), 381–495. https://doi.org/10.1016/S0920-5861(99)00096-6

García-Diéguez, M., Herrera, M. C., Pieta, I. S., Larrubia, M. A., & Alemany, L. J. (2010). NiBa catalysts for CO2-reforming of methane. *Catalysis Communications*, *11*(14), 1133–1136. https://doi.org/10.1016/j.catcom.2010.06.008

Gevert, B., Otterstedt, J., Massoth, F. (1986). Kinetics of the HDO of Methyl-Substitituted Phenols. *Applied Catalysis*. 13, 119-131.

Gonçalves, V. O. O., Brunet, S., & Richard, F. (2016). Hydrodeoxygenation of Cresols Over Mo/Al2O3 and CoMo/Al2O3 Sulfided Catalysts. *Catalysis Letters*, *146*(8), 1562–1573. https://doi.org/10.1007/s10562-016-1787-5

Jin, S., Xiao, Z., Li, C., Chen, X., Wang, L., Xing, J., Liang, C. (2014). Catalytic hydrodeoxygenation of anisole as lignin model compound over supported nickel catalysts. *Catalysis Today*, *234*, 125–132. https://doi.org/10.1016/j.cattod.2014.02.014

Kang, M., Song, M. W., Kim, T. W., & Kim, K. L. (2002). y-Alumina Supported Cu-Ni Bimetallic Catalysts: Characterization and Selective Hydrogenation of 1,3-Butadiene. *The Canadian Journal of Chemical Engineering.* 80 (Feb), 63–70.

Khromova, S. A., Smirnov, A. A., Bulavchenko, O. A., Saraev, A. A., Kaichev, V. V., Reshetnikov, S. I., & Yakovlev, V. A. (2014). Anisole hydrodeoxygenation over Ni-Cu bimetallic catalysts: The effect of Ni/Cu ratio on selectivity. *Applied Catalysis A: General*, *470*(JANUARY 2014), 261–270. https://doi.org/10.1016/j.apcata.2013.10.046

Kirumakki, S. R., Shpeizer, B. G., Sagar, G. V., Chary, K. V. R., & Clearfield, A. (2006). Hydrogenation of Naphthalene over NiO/SiO2-Al2O3 catalysts: Structure-activity correlation. *Journal of Catalysis*, *242*(2), 319–331. https://doi.org/10.1016/j.jcat.2006.06.014

Kumar, J., & Reetu, S. (2015). Lignocellulosic agriculture wastes as biomass feedstocks for second-generation bioethanol production : concepts and recent developments. *Biotech.* 5(4), 337–353. https://doi.org/10.1007/s13205-014-0246-5

Lee, J. H., Lee, E. G., Joo, O. S., & Jung, K. D. (2004). Stabilization of Ni/Al2O3 catalyst by Cu addition for CO2 reforming of methane. *Applied Catalysis A: General*, *269*(1–2), 1–6. https://doi.org/10.1016/j.apcata.2004.01.035

Lee, W. S., Wang, Z., Wu, R. J., & Bhan, A. (2014). Selective vapor-phase hydrodeoxygenation of anisole to benzene on molybdenum carbide catalysts. *Journal of Catalysis*, *319*, 44–53. https://doi.org/10.1016/j.jcat.2014.07.025

Lewis, N. S. (2007). Powering the Planet. *Materials Research Society Bulletin*, *32*, 808.

Li, Y., Zhang, C., Liu, Y., Tang, S., Chen, G., Zhang, R., & Tang, X. (2017). Coke formation on the surface of Ni/HZSM-5 and Ni-Cu/HZSM-5 catalysts during bio-oil hydrodeoxygenation. *Fuel*, *189*, 23–31. https://doi.org/10.1016/j.fuel.2016.10.047

Marecot, P., Martinez, H., & Barbier, J. (1992). Coking Reaction by Anthracene on Acidic Aluminas and Silica-Aluminas. *Journal of Catalysis*, *138*, 474–481.

Mattos, A. R. J. M., Probst, S. H., Afonso, J. C., & Schmal, M. (2004). Hydrogenation of 2-ethyl-hexen-2-al on Ni/Al2O3 catalysts. *Journal of the Brazilian Chem. Society*, *15*(5), 760–766.

Molina, R., & Poncelet, G. (1998). α-Alumina-Supported Nickel Catalysts Prepared from Nickel Acetylacetonate: A TPR Study. *Journal of Catalysis*, *173*(2), 257–267. https://doi.org/10.1006/jcat.1997.1931

Mortensen, P. M., Grunwaldt, J. D., Jensen, P. A., & Jensen, A. D. (2013). Screening of catalysts for hydrodeoxygenation of phenol as a model compound for bio-oil. *ACS Catalysis*, *3*(8), 1774–1785. https://doi.org/10.1021/cs400266e

Mortensen, P. M., Grunwaldt, J. D., Jensen, P. A., Knudsen, K. G., & Jensen, A. D. (2011). A review of catalytic upgrading of bio-oil to engine fuels. *Applied Catalysis A: General*, *407*(1–2), 1–19. https://doi.org/10.1016/j.apcata.2011.08.046

Mu, W., Ben, H., Du, X., Zhang, X., Hu, F., Liu, W., Deng, Y. (2014). Noble metal catalyzed aqueous phase hydrogenation and hydrodeoxygenation of lignin-derived pyrolysis oil and related model compounds. *Bioresource Technology*. 173, 6-10 https://doi.org/10.1016/j.biortech.2014.09.067

Navalikhina, M. D., & Krylov, O. V. (2001). Hydrogenating activity and adsorption capacity of supported nickel catalysts modified by heteropoly compounds. *Kinetics and Catalysis*. 42(2) 264-274. https://doi.org/10.1023/A:1010429804739

Newnham, J., Mantri, K., Amin, M. H., Tardio, J., & Bhargava, S. K. (2012). Highly stable and active Ni-mesoporous alumina catalysts for dry reforming of methane. *International Journal of Hydrogen Energy*, *37*(2), 1454–1464. doi.org/10.1016/j.ijhydene.2011.10.036

Robinson, A. M., Hensley, J. E., & Will Medlin, J. (2016). Bifunctional Catalysts for Upgrading of Biomass-Derived Oxygenates: A Review. *ACS Catalysis*, *6*(8), 5026–5043. https://doi.org/10.1021/acscatal.6b00923

Sankaranarayanan, T. M., Berenguer, A., Ochoa-Hernández, C., Moreno, I., Jana, P., Coronado, J. M., Pizarro, P. (2015). Hydrodeoxygenation of anisole as bio-oil model compound over supported Ni and Co catalysts: Effect of metal and support properties. *Catalysis Today*, *243*(C), 163–172. https://doi.org/10.1016/j.cattod.2014.09.004

Smirnov, a. a., Khromova, S. a., Bulavchenko, O. a., Kaichev, V. V., Saraev, a. a., Reshetnikov, S. I., Yakovlev, V. a. (2014). Effect of the Ni/Cu ratio on the composition and catalytic properties of nickel-copper alloy in anisole hydrodeoxygenation. *Kinetics and Catalysis*, *55*(1), 69–78. https://doi.org/10.1134/S0023158414010145

Tang, W., Zhang, X., Zhang, Q., Wang, T., & Ma, L. (2016). Hydrodeoxygenation of Anisole over Ni/α-Al_2O_3 Catalyst. *Chinese Journal of Chemical Physics*, *29*(5), 617–622. https://doi.org/10.1063/1674-0068/29/cjcp1603062

Venderbosch, R., Ardiyanti, A. R., Wildschut, J., Oasmaa, A., & Heeres, H. (2010). Stabilisation of Biomass derived Pyrolysis Oils by Catalytic Hydrotreatment. *J Chem Technol Biotechnol*, *85*, 674–686.

Viljava, T.-R., Komulainen, R. S., & Krause, A. (2000). Effect of H_2S on the stability of $CoMo/Al_2O_3$ catalysts during hydrodeoxygenation. *Catalysis Today*, *60*(1–2), 83–92. https://doi.org/http://dx.doi.org/10.1016/S0920-5861(00)00320-5

Vizcaíno, A. J., Carrero, A., & Calles, J. A. (2007). Hydrogen production by ethanol steam reforming over Cu-Ni supported catalysts. *International Journal of Hydrogen Energy*, *32*(10–11), 1450–1461. https://doi.org/10.1016/j.ijhydene.2006.10.024

Vogelzang, M. W., Li, C. L., Schuit, G. C. A., Gates, B. C., & Petrakis, L. (1983). Hydrodeoxygenation of 1-naphthol: Activities and stabilities of molybdena and related catalysts. *Journal of Catalysis*, *84*(1), 170–177. https://doi.org/10.1016/0021-9517(83)90095-7

Wildschut, J., Mahfud, F. H., Venderbosch, R. H., & Heeres, H. J. (2009). Hydrotreatment of Fast Pyrolysis Oil Using Heterogeneous Noble-Metal Catalysts. *Industrial & Engineering Chemistry Research*, *48*(23), 10324–10334. https://doi.org/10.1021/ie9006003

Yakovlev, V. A., Bykova, M. V, & Khromova, S. A. (2012). Stability of nickel-containing catalysts for hydrodeoxygenation of biomass pyrolysis products. *Catalysis in Industry*, *4*(4), 324–339. https://doi.org/10.1134/S2070050412040204

Yakovlev, V. A., Khromova, S. A., Sherstyuk, O. V., Dundich, V. O., Ermakov, D. Y., Novopashina, V. M., Parmon, V. N. (2009). Development of new catalytic systems for upgraded bio-fuels production from bio-crude-oil and biodiesel. *Catalysis Today*, *144*(3–4), 362–366. https://doi.org/10.1016/j.cattod.2009.03.002

Yang, R., Li, X., Wu, J., Zhang, X., & Zhang, Z. (2009). Promotion effects of copper and lanthanum oxides on nickel/gamma-alumina catalyst in the hydrotreating of crude 2-ethylhexanol. *Journal of Physical Chemistry C*, *113*(41), 17787–17794. https://doi.org/10.1021/jp9053296

Yang, Y., Ochoa-Hernández, C., de la Peña O'Shea, V. A., Pizarro, P., Coronado, J. M., & Serrano, D. P. (2014). Effect of metal-support interaction on the selective hydrodeoxygenation of anisole to aromatics over Ni-based catalysts. *Applied Catalysis B: Environmental, 145,* 91–100. https://doi.org/10.1016/j.apcatb.2013.03.038

Yao, Y., & Goodman, D. W. (2014). Direct evidence of hydrogen spillover from Ni to Cu on Ni-Cu bimetallic catalysts. *Journal of Molecular Catalysis A: Chemical, 383–384,* 239–242. https://doi.org/10.1016/j.molcata.2013.12.013

Youn, M. H., Seo, J. G., Kim, P., Kim, J. J., Lee, H. I., & Song, I. K. (2006). Hydrogen production by auto-thermal reforming of ethanol over Ni/ γ-Al2O3 catalysts: Effect of second metal addition. *Journal of Power Sources, 162,* 1270–1274. https://doi.org/10.1016/j.jpowsour.2006.08.015

Zhang , X., Chen, X., Jin, S., Peng, Z., & Liang, C. (2016). Ni/Al_2O_3 Catalysts Derived from Layered Double Hydroxide and Their Applications in Hydrodeoxygenation of Anisole. *ChemistrySelect, 1*(3), 577–584. https://doi.org/10.1002/slct.201600161

Zhang, X., Long, J., Kong, W., Zhang, Q., Chen, L., Wang, T., Li, Y. (2014). Catalytic upgrading of bio-oil by Ni-based catalysts supported on mixed oxides, *28,* 2562–2570.

Chapter 4

Effect of lanthanum promotion on Ni and Ni-Cu catalysts
for HDO of Anisole in a novel externally agitated reactor

4.1 Introduction

It is crucial to develop new technologies for more sustainable energy source from renewable feedstocks due to the issues associated with fossil fuels such as pollution, global warming, and availability. Lignocellulosic biomass has recently been considered a likely feedstock that has the potential to substitute fossil fuels for transportation biofuels and chemical production (Alonso et al., 2010). Pyrolysis has been identified as a promising method to convert biomass to biofuels or chemicals; however, the resulting crude pyrolysis oil contains high oxygen content (30-40%) (Furimsky, 2000; Mohan et al., 2006). This high oxygen content leads to poor heating values and makes it unsuitable as a fuel, requiring upgrading techniques that effectively remove oxygen to convert bio-oil into a more appropriate transportation fuel (Adjaye & Bakhshi, 1995; He & Wang, 2012).

Catalytic hydrodeoxygenation (HDO) has been recognized as an effective bio-oil upgrading method to reduce oxygen content, which occurs at temperatures between 200-400^{o}C, hydrogen pressures between 10-30MPa, and with a heterogenous catalyst (Zacher et al., 2014). Research into HDO catalysts has received considerable attention to find catalysts that exhibit high HDO activity, are relatively low cost, and are resistant to catalyst deactivation via coke formation (Absi-Halabi et al., 1991; Furimsky, 1999). Nickel-based catalysts supported on metal oxides such as alumina have been tested extensively and demonstrate effective HDO activity, though highly susceptible to coke formation and thus deactivate quickly due to the high acidity of alumina (Kim et al., 2011; Xu et al., 2001). Methods to improve the performance and longevity of these transition metal catalysts has received attention to improve their performance for bio-oil hydrotreating.

Studies have shown that the addition of a promoter to transition metal catalysts can enhance its activity, selectivity, and/or stability. Magnesium promotion has been demonstrated to reduce metal particle size and support acidity in alumina-supported catalysts, resulting in decreased coke

formation and increased activity (Basagiannis & Verykios, 2008; Li et al., 2011). The addition of potassium has shown to improve metal dispersion, reducibility, and prevention of carbon deposits by reducing the number of acid sites on alumina (Siahvashi & Adesina, 2013; Wang et al., 2013). Cerium-doped alumina catalysts also can reduce catalyst deactivation by coking by reducing the available acid sites (Alvarez-Galvan et al., 2008).

Several reports have demonstrated lanthanum promotion to improve catalytic performance of nickel-based catalysts in other chemical applications. La addition has been shown to improve hydrogenation activity of amorphous Ni-Mo-B catalysts through increasing surface area and improving the reducibility of Ni species (Wang et al., 2010). The incorporation of an initial lanthanum impregnation to Ni/γ-Al_2O_3 catalysts further demonstrated the ability to improve the reducibility of nickel by influencing the metal-support interaction by preventing the formation of nickel-aluminate species that are difficult to reduce (Hossain et al., 2009). The basicity of lanthanum has also been shown to reduce the acidity of alumina-supported catalysts, lowering coking during ethanol steam reforming and gasification (Sánchez-Sánchez et al., 2007; Mazumder et al., 2014).

This study aims to investigate the promotion effects of lanthanum addition on Ni and Ni-Cu/γ-alumina catalyst for HDO of anisole as a bio-oil model compound. Lanthanum has not yet been considered for Ni and Ni-Cu on γ-Al_2O_3 catalysts in HDO of anisole as a bio-oil model compound. The basic nature of lanthanum is anticipated to reduce the number of available acid sites to limit coke formation and thus, catalyst deactivation. Furthermore, lanthanum is projected to improve the reducibility of nickel, enhancing catalytic activity. Reaction products and carbon deposits were examined to further understand the reaction mechanisms and to obtain a reaction carbon balance.

4.2 Materials and Methods

4.2.1 Catalyst preparation

All catalysts were prepared by incipient wetness impregnation using aqueous solutions of $Ni(NO_3)_2{\cdot}6H_2O$, $Cu(NO_3)_2{\cdot}3H_2O$, and $La(NO_3)_3{\cdot}6H_2O$ obtained from Sigma-Aldrich (Steinheim, Germany). Ni and Ni-Cu catalysts containing lanthanum were first impregnated with 1 wt.% lanthanum, then dried and calcined under the same conditions as previously mentioned before then

being impregnated with Ni and Ni-Cu compositions. Refer to Section 3.2.1 for the detailed catalyst preparation method. Catalyst formulations presented in this study indicate the weight fraction of the impregnated metal (e.g., Ni5/La1 refers to 5 wt.% nickel and 1 wt.% lanthanum on γ-alumina). Monometallic Ni and bimetallic Ni-Cu catalysts had a total metal loading of 5 wt.% and 10 wt.% for comparison, except for the additional 2 wt.% Ni catalyst. Catalysts were reduced with 3.5MPa of hydrogen at 400^{o}C for 1 hour in the reactor prior to HDO reactions.

4.2.2 Catalyst Characterization

Refer to Section 3.2.2 for the detailed catalyst characterization methods for temperature programmed reduction (H_2 – TPR), N_2 Physiorption, and thermosgravimetric analysis (TGA).

4.2.3 Experimental Setup and Catalyst Testing Procedure

Refer to Section 3.2.3 for the experimental setup and protocol used for catalyst testing.

4.2.4 Product Analysis

Refer to Section 3.2.4 for the detailed method used for product analysis.

All catalyst experiments were carried out in duplicates or triplicates under identical conditions to guarantee reproducibility of the data. Data is presented as the average of the duplicates or triplicates. Five triplicates were performed in this chapter, with an average standard deviation of 7.1 (conversion) and 4.6 (selectivity). The carbon balance was always above 88%.

4.3 Results and Discussion

4.3.1 H_2-TPR

Temperature-programmed reduction (TPR) analysis shows the interaction between metals and the support, as well as the influence promoters (La) can have on reduction and the relative proportion of nickel species (Zhang et al. 2005). The H_2-TPR profiles of the catalyst samples are presented in Figure 4.1. For comparison purposes, the reduction profile of 1 wt.% La/γ – Al_2O_3 is

included in Figure 4.1a. An initial test with bare γ – alumina support showed no reduction temperature peak indicating negligible hydrogen uptake from the support surface.

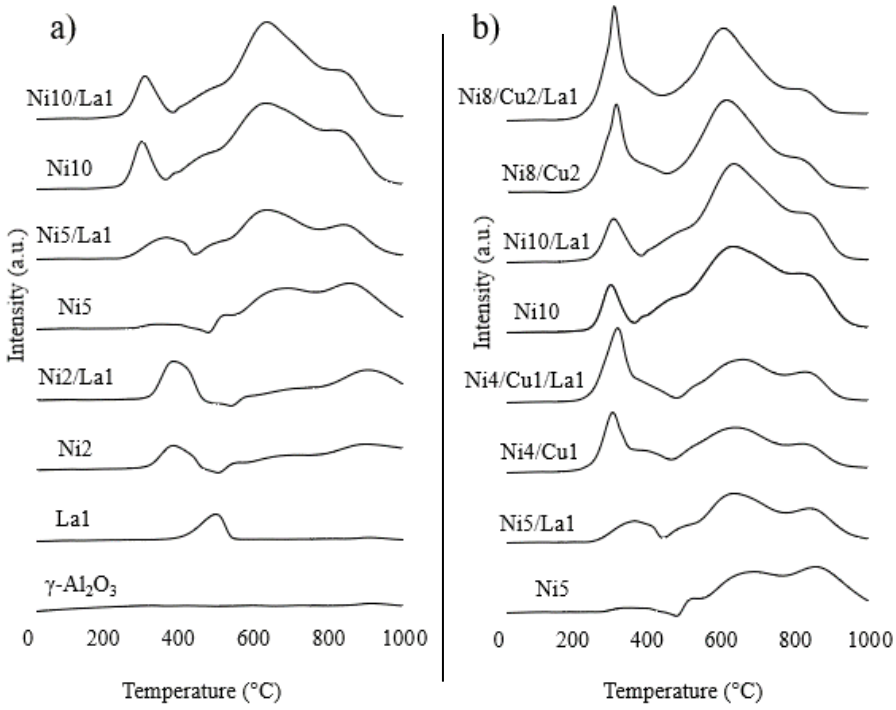

Figure 4.1 H_2-TPR Profiles for a) bare γ-alumna support, 2, 5, and 10 wt.% of Ni with and without 1 wt.% La and b) Ni and Ni-Cu catalyst with total metal loadings of 5 and 10 wt.% with and without 1 wt.% La

H_2-TPR profiles of Ni and Ni-Cu catalysts with and without 1 wt.% La showed a broad reduction area between 300°C – 1000°C with three key reduction peaks centered at approximately 350°C, 620°C, and 810°C (Figure 4.1a and 4.1). TPR studies on nickel-based catalysts have reported that Ni^{2+} directly reduces to Ni^0 without any intermediates, indicating that each reduction peak represents an individual nickel species (Molina & Poncelet, 1998). Bare γ-alumina with 1 wt.% La demonstrated a sharp reduction peak at approximately 500°C, demonstrating that lanthanum has some hydrogen uptake and is reducible, while requiring a higher temperature than Ni. The addition of 1 wt.% La to any monometallic Ni or bimetallic Ni-Cu catalyst did not appear to shift the temperature of any reduction peak, but did increase the proportion of reducible species below 400°C for all catalysts as shown in Table 4.1. Related literature has reported that La and Ni can interact strongly together, reducing the interaction between Ni and alumina, causing a higher

amount of NiO species to form, and thus improving the degree of reducibility (Calles et al., 2009; Mazumder et al., 2014). Reports have indicated that NiO species are more easily sintered during reduction, leading to enlarged nickel particle size (Melchor-Hernández et al., 2013). This could explain the reduced total hydrogen consumption observed for some catalysts as larger particles would have less exposed active nickel sites to adsorb hydrogen. Furthermore, a report has suggested the possibility of lanthanum to redistribute following a second impregnation with nickel, which could settle on top of nickel particles, blocking active sites, which could also explain the reduced total hydrogen consumption with lanthanum promoted catalysts (Damyanova et al., 1996).

Table 4.1 Quantitative TPR data for Ni and Ni-Cu catalysts with and without the promotion of lanthanum. Hydrogen consumption is presented as a function of reduction temperature.

Catalyst	Total H_2 Consumption (mmol)	H_2 Consumption (%)	
		Low Temperature (<400°C)	High Temperature (400 – 1000°C)
Ni2	0.142	17	83
Ni2/La1	0.143	23	77
Ni5	0.218	4	96
Ni5/La1	0.235	13	87
Ni10	0.412	11	89
Ni10/La1	0.382	12	88
Ni4/Cu1	0.261	26	74
Ni4/Cu1/La1	0.249	32	67
Ni8/Cu2	0.370	23	77
Ni8/Cu2/La1	0.406	27	73

4.3.2 Surface Characteristics

Table 4.2 presents the surface characteristics of the catalysts and bare alumina support determined by the BET method following calcination. The addition of 1 wt.% lanthanum prior to Ni or Ni-Cu impregnation had negligible affect on average pore diameter or specific surface area (A_{BET}). Although minor, incorporation of La consistently reduced pore volume for all catalysts, which could indicate that lanthanum species are dispersed within the support pore channels (Hossain et al., 2009).

Table 4.2 Surface area, pore volume, and average pore diameter of the calcined catalysts determined by BET method

Catalyst	A_{BET} (m^2/g)	V_{pores} (cm^3/g)	Average pore diameter (Å)
Ni2	190	0.468	74
Ni2/La1	187	0.457	74
Ni5	182	0.443	73
Ni5/La1	182	0.433	73
Ni4/Cu1	184	0.438	72
Ni4/Cu1/La1	185	0.433	71
Ni10	172	0.414	71
Ni10/La1	174	0.411	72
Ni8/Cu2	168	0.412	72
Ni8/Cu2/La1	164	0.400	72

4.3.3 Catalytic Activity in Anisole Hydrodeoxygenation

Figures 4.2 and 4.3 present anisole conversion and liquid product selectivity for monometallic Ni catalysts with and without La following anisole HDO, respectively. Anisole conversion was completely inhibited from 11% to 0% when lanthanum was impregnated on the bare γ-Al_2O_3 support (Figure 4.2). Furthermore, lanthanum addition also noticeably reduced anisole conversion for all monometallic Ni catalysts, regardless of metal loading. Product selectivity towards deoxygenated products (i.e. cyclohexane) also decreased for all monometallic Ni catalysts with lanthanum promotion, but was much more prominent at lower loadings.

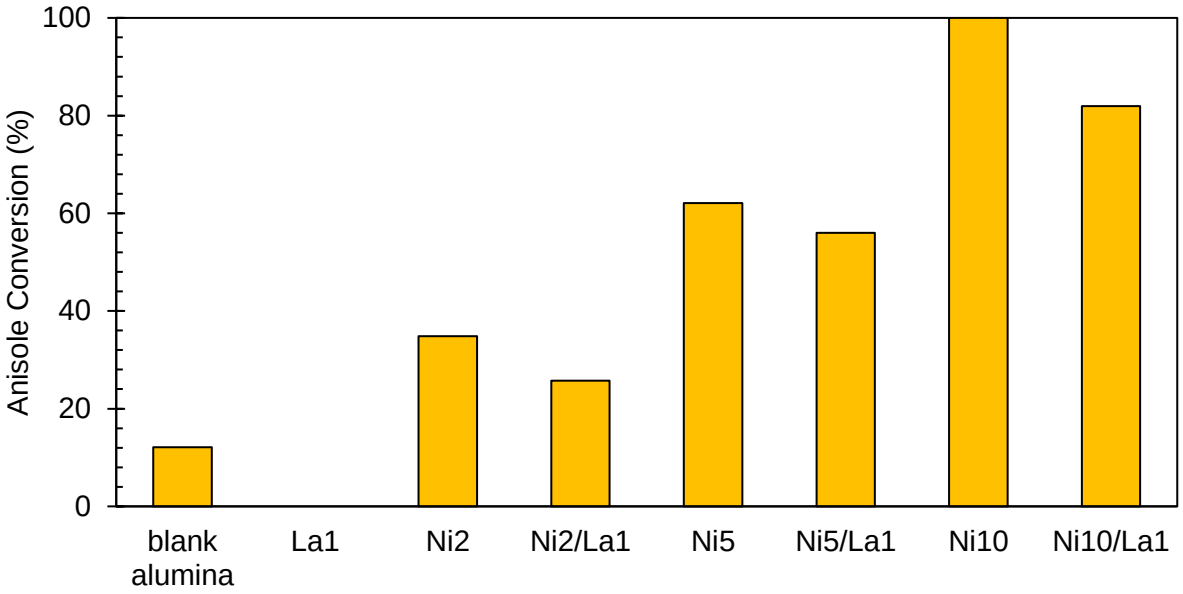

Figure 4.2. Ni and Ni-La experiments performed at 220°C, an initial hydrogen pressure of 3.5MPa, 0.1g of catalyst (reduced at 400°C for 1h) and a reaction time of 45 minutes.

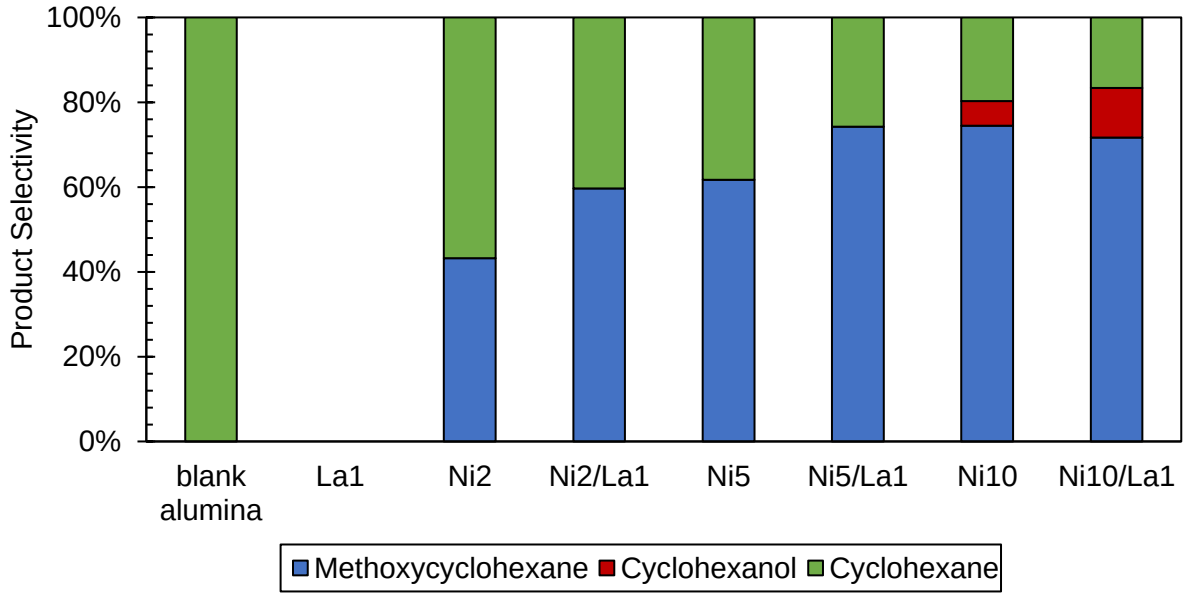

Figure 4.3. Ni and Ni-La experiments performed at 220°C, an initial hydrogen pressure of 3.5MPa, 0.1g of catalyst (reduced at 400°C for 1h) and a reaction time of 45 minutes.

Figures 4.4 and 4.5 present anisole conversion and liquid product selectivity for bimetallic Ni-Cu catalysts with and without La promotion following anisole HDO experiments, respectively. Bimetallic Ni-Cu catalysts resulted in similar reductions in anisole conversion as was observed for monometallic Ni catalysts (Figure 4.4). Product selectivity towards cyclohexane slightly decreased for Ni-Cu catalysts with lanthanum promotion, more so at lower loadings (Figure 4.5).

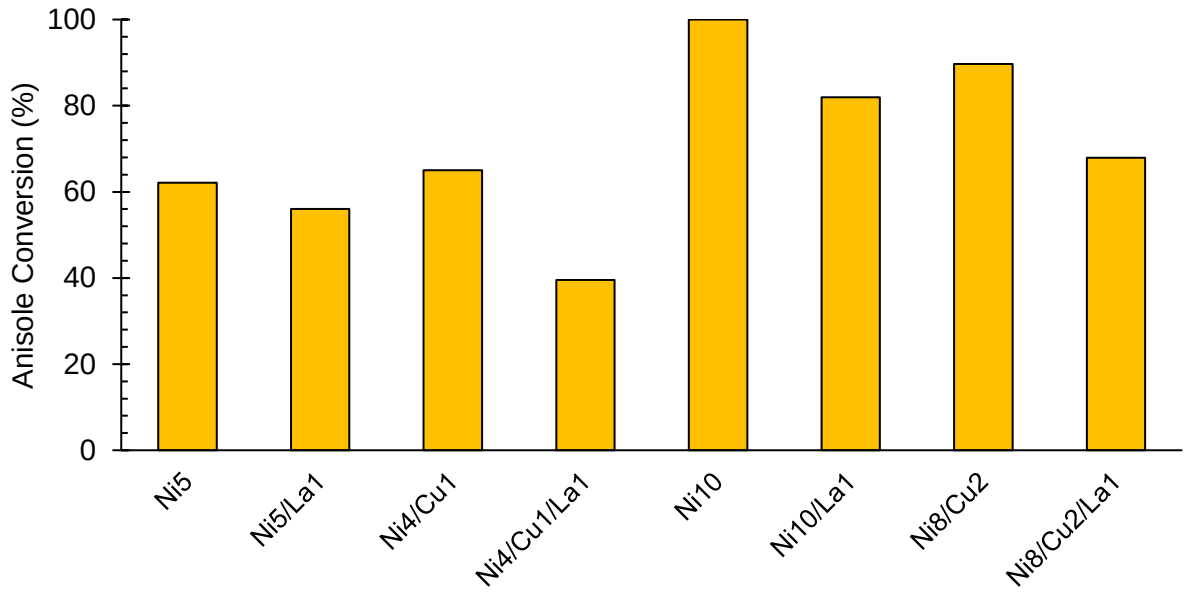

Figure 4.4. Ni-Cu and Ni-Cu-La experiments performed at 220°C, an initial hydrogen pressure of 3.5MPa, 0.1g of catalyst (reduced at 400°C for 1h) and a reaction time of 45 minutes.

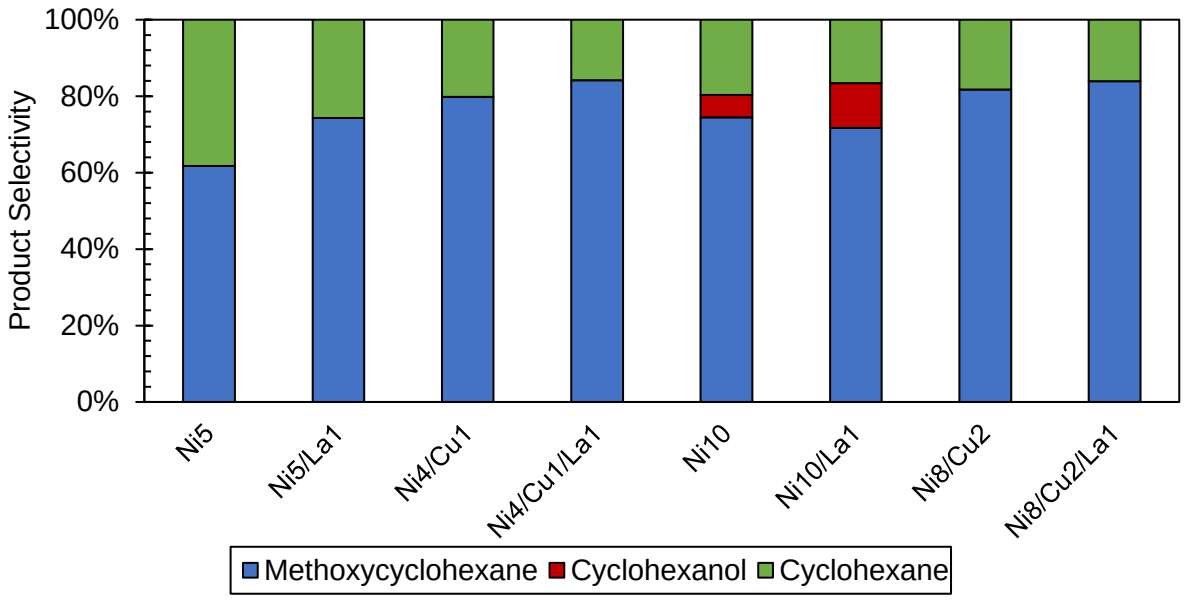

Figure 4.5. Ni-Cu and Ni-Cu-La experiments performed at 220°C, an initial hydrogen pressure of 3.5MPa, 0.1g of catalyst (reduced at 400°C for 1h) and a reaction time of 45 minutes.

Liquid products identified remained exclusively methoxycyclohexane, cyclohexanol, and cyclohexane, as lanthanum promotion did not seem to affect the reaction route previously described in Figure 3.5. Cyclohexanol remained detectable in the liquid product only for Ni10 and Ni10/La1 catalysts.

The promotion of 1 wt.% of lanthanum to both monometallic Ni and bimetallic Ni-Cu catalysts resulted in lower anisole conversion for all conditions. Several reports have demonstrated that lanthanum addition can reduce the acidity of alumina supports due to the basic nature of lanthanum (Sánchez-Sánchez et al., 2007; Montini et al., 2010). This would explain the reduced deoxygenation activity and decrease in cyclohexane selectivity with lanthanum promotion, even at a low loading of 1 wt.%. Although TPR analysis indicated that lanthanum promotion improved the degree of reducibility of nickel and increased the proportion of NiO species, hydrogenation interestingly did not increase proportionately. Methoxycyclohexane selectivity was instead marginally unaffected at higher loadings with Ni10 and Ni8/Cu2 catalysts with lanthanum promotion, and methoxycylohexane yields decreased. This result could be due to a previously reported phenomena where La molecules acted as centres for nickel species to gravitate towards during the second impregnation, and then redistribute on top of nickel species, thus blocking

available nickel species (Damyanova et al., 1996). The previous study also reported a similar reduction in styrene hydrogenation with La impregnation with increasing loadings from 2.3 to 8.7 wt.% on sepiolite catalysts prior to 5 wt.% nickel loading. On the other hand, hydrogenation of 2-ethylhexanol exhibited better activity when 1.5 wt.% La was added to 6 wt.% Ni/γ-Al_2O_3 catalysts, which was based on increased available active sites. When La loading increased to 2 wt.%, however, hydrogenation activity dropped and was attributed to excessive blocking of active sites (Yang et al., 2009). This suggests that the amount of lanthanum loading could be factor in the ability to effect hydrogenation activity. Carbon deposits, discussed in Section 4.4.4, could have also contributed to the reduction in anisole conversion and deoxygenation activity by physically blocking active sites on both the support and nickel particles. Furthermore, the greater amount of NiO species in the lanthanum promoted catalysts, which are more readily sintered during reduction to form larger Ni ensembles, could also lower hydrogenation activity.

4.3.4 Gas Phase Analysis

Micro-GC analysis of gas phase products are presented in Figure 4.6. Methane remained the only detectable product besides hydrogen, consistent with the previously proposed reaction pathway. Methane production remained approximately constant with lanthanum addition for catalysts with low metal loadings (Ni2, Ni5, and Ni4/Cu1), even though cyclohexanol and cyclohexane yields were lower than without lanthanum promotion. Catalysts with higher metal loadings (Ni10 and Ni8/Cu2) led to reduced methane production after lanthanum promotion, directly proportional to their corresponding cyclohexanol and cyclohexane yields.

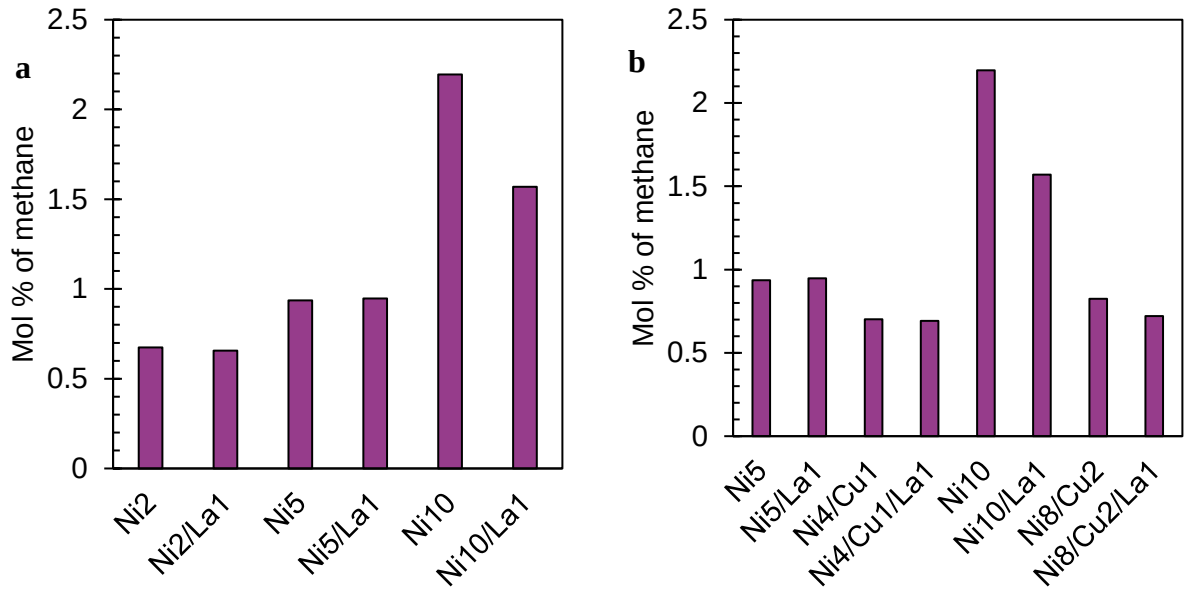

Figure 4.6. (a) Ni-La and (b) Ni-Cu-La experiments performed at 220°C, an initial hydrogen pressure of 3.5MPa, 0.1g of catalyst (reduced at 400°C for 1h) and a reaction time of 45 minutes.

4.3.5 Coke Analysis

Formation of coke obtained from TGA analysis of spent catalysts are presented in Figure 4.7. The addition of 1 wt.% of La increased coke formation for all catalysts except Ni8/Cu2, being most prominent for Ni5 and Ni4/Cu1 catalysts (Figure 4.7a and 4.7b). This result is inconsistent with most literature involving lanthanum promotion of nickel-based catalysts, where several studies report carbon deposit declines on the catalyst. Coke formation was reduced significantly during ethanol steam reforming when 3-15 wt.% La was incorporated into Ni/γ-Al_2O_3 catalysts (Sánchez-Sánchez et al., 2007). The addition of 10 wt.% La to 10 wt.% Ni/α-Al_2O_3 catalysts during steam reforming of the aqueous fraction of bio-oil resulted in reduced coke content (Aguayo et al., 2016). Lanthanum promotion also reduced coke deposits on Ni/γ-Al_2O_3 catalysts in dry reforming of methane (Al-Fatesh et al., 2014).

The ability of lanthanum addition to reduce coke formation has been attributed to several factors. The high acidity and number of acid sites for alumina supports is thought to facilitate coke deposition on catalysts (Popov et al., 2010). Incorporating a basic promoter such as lanthanum is believed to help partially neutralize the acidity of alumina, lowering the number of acid sites and reduce coke deposits (Marecot et al., 1992; Sugunan & Sherly, 1993). Several studies have

nonetheless determined that coke formation may be highly influenced by nickel dispersion and particle size. For example, reports have indicated that carbon deposits are more prevalent in the presence of larger Ni clusters, compared to smaller and more dispersed nickel particles (Zhang et al., 2007; Tang et al., 2000; Da Silva et al., 2014). This may explain the variations in coke formation at the studied metal loadings. Studies have also shown that the reduction of NiO to Ni^0 can cause nickel particles to increase in size through sintering and agglomeration (Richardson et al., 2003; Du & Chen, 2007; Jeangros et al., 2013). The addition of lanthanum did increase the NiO content of catalysts based on the TPR profiles when compared to those without lanthanum, and therefore, could enlarge the nickel particle size during reduction. Copper addition to nickel based catalysts has been shown to reduce nickel particle size and limit large Ni clusters by improving dispersion and preventing sintering (Vizcaíno et al., 2007; Chen et al., 2004). This could explain the smaller coke formation increase for bimetallic Ni-Cu catalysts when compared to monometallic Ni catalysts, in addition to the reduced coke formation for the Ni8/Cu2 when compared to the Ni10 catalyst.

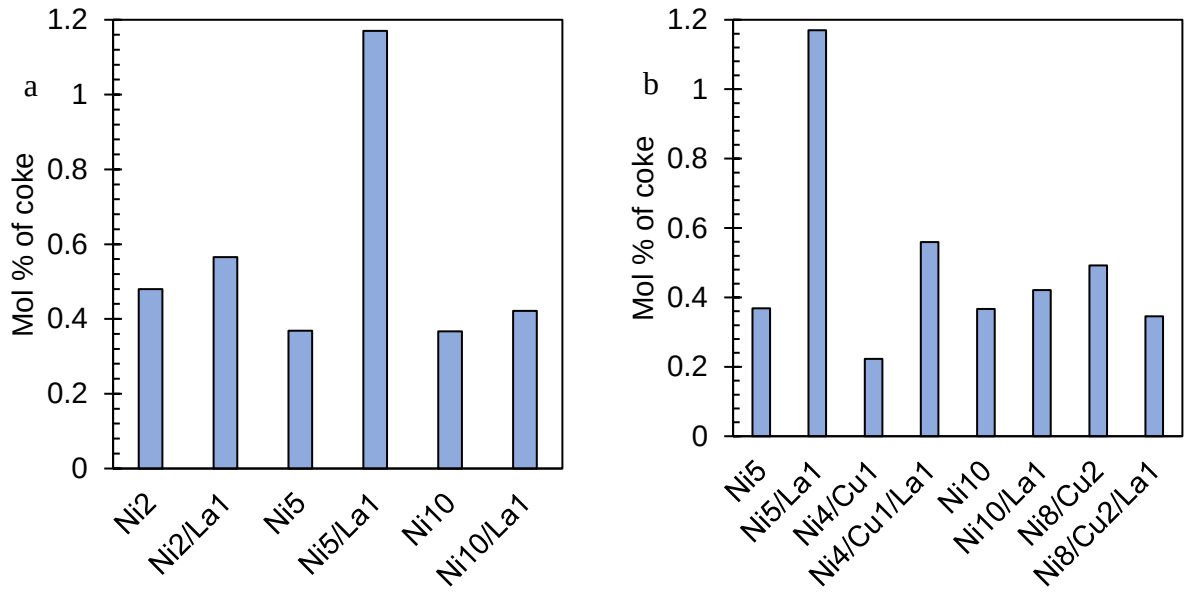

Figure 4.7. (a) Ni-La and (b) Ni-Cu-La experiments performed at 220°C, an initial hydrogen pressure of 3.5MPa, 0.1g of catalyst (reduced at 400°C for 1h) and a reaction time of 45 minutes.

4.4 Conclusion

This study investigated lanthanum promotion of Ni and Ni-Cu catalysts for hydrodeoxygenation of anisole as a model compound in a novel externally agitated batch reactor at mild operating conditions of 220°C and an initial hydrogen pressure of 3.5MPa with a reaction time of 45 minutes. Ni and Ni-Cu catalysts were compared with and without prior impregnation of 1 wt.% lanthanum. It was expected that by adding a basic promoter such as lanthanum to the Ni and Ni-Cu catalysts, that the support acidity would decrease, resulting in reduced coke formation and an increase in anisole conversion and deoxygenation from more exposed active sites to carry out hydrogenation and HDO. Major conclusions are summarized as follows:

1) Lanthanum promotion increased the proportion of NiO species for all Ni and Ni-Cu catalysts, enhancing their degree of reducibility below 400°C.

2) Lanthanum addition decreased anisole conversion for all Ni and Ni-Cu catalysts. Cyclohexane selectivity was reduced, being more prominent at lower loadings. Contrary to the TPR results, methoxycylohexane yields were also reduced with the promotion of lanthanum.

3) Coke formation generally increased with the addition of lanthanum, counter to most previous studies and the anticipated reduction of the Al_2O_3 support acidity.

4) The influence of La on hydrogenation and/or deoxygenation activity is believed to be highly dependant on the dispersion and particle size of nickel species on the catalyst.

References

Absi-Halabi, M., Stanislaus, A., & Trimm, D. L. (1991). Coke formation on catalysts during the hydroprocessing of heavy oils. *Applied Catalysis*, *72*(2), 193–215. https://doi.org/10.1016/0166-9834(91)85053-X

Adjaye, J., & Bakhshi, N. (1995). Catalytic conversion of a biomass-derived oil to fuels and chemicals I: model compound studies and reaction pathways. *Biomass and Bioenergy*. 8(3) 131-149.

Aguayo, T., Bilbao, J., Gayubo, A. G., Valle, B., & Remiro, A. (2016). Catalysts of Ni / alpha-Al 2O3 and Ni / La2O3 - alpha Al2O3 for hydrogen production by steam reforming of bio-oil aqueous fraction with pyrolytic lignin retention, *International Journal of Hydrogen Energy*. 38, 1307-1318. https://doi.org/10.1016/j.ijhydene.2012.11.014

Al-Fatesh, A. S., Naeem, M. A., Fakeeha, A. H., & Abasaeed, A. E. (2014). Role of La2O3 as promoter and support in Ni/ γ-Al2O3 catalysts for dry reforming of methane. *Chinese Journal of Chemical Engineering*, *22*(1), 28–37. https://doi.org/10.1016/S1004-9541(14)60029-X

Alonso, D. M., Bond, J. Q., & Dumesic, J. A. (2010). Catalytic conversion of biomass to biofuels. *Green Chemistry*. 12, 1493–1513. https://doi.org/10.1039/c004654j

Alvarez-Galvan, M. C., Navarro, R. M., Rosa, F., Briceño, Y., Gordillo Alvarez, F., & Fierro, J. L. G. (2008). Performance of La,Ce-modified alumina-supported Pt and Ni catalysts for the oxidative reforming of diesel hydrocarbons. *International Journal of Hydrogen Energy*, *33*(2), 652–663. https://doi.org/10.1016/j.ijhydene.2007.10.023

Basagiannis, A. C., & Verykios, X. E. (2008). Influence of the carrier on steam reforming of acetic acid over Ru-based catalysts. *Applied Catalysis B: Environmental*, *82*(1–2), 77–88. https://doi.org/10.1016/j.apcatb.2008.01.014

Calles, J. A., Carrero, A., & Vizcaíno, A. J. (2009). Ce and La modification of mesoporous Cu-Ni/SBA-15 catalysts for hydrogen production through ethanol steam reforming. *Microporous and Mesoporous Materials*, *119*(1–3), 200–207. https://doi.org/10.1016/j.micromeso.2008.10.028

Chen, H.-W., Wang, C.-Y., Yu, C.-H., Tseng, L.-T., & Liao, P.-H. (2004). Carbon dioxide reforming of methane reaction catalyzed by stable nickel copper catalysts. *Catalysis Today*, *97*(2–3), 173–180. https://doi.org/10.1016/j.cattod.2004.03.067

Da Silva, A. L. M., Den Breejen, J. P., Mattos, L. V., Bitter, J. H., De Jong, K. P., & Noronha, F. B. (2014). Cobalt particle size effects on catalytic performance for ethanol steam reforming - Smaller is better. *Journal of Catalysis*, *318*, 67–74. https://doi.org/10.1016/j.jcat.2014.07.020

Damyanova, S., Daza, L., & Fierro, J. L. G. (1996). Surface and Catalytic Properties of Lanthanum-Promoted Ni / Sepiolite Catalysts for Styrene Hydrogenation. *Journal of Catalysis*, *159*(74), 150–161.

Du, Y., & Chen, R. (2007). Effect of Nickel Particle Size on Alumina Supported Nickel Catalysts for p-Nitrophenol Hydrogenation. *Construction*, *21*(3), 251–255.

Furimsky, E. (1999). Deactivation of hydroprocessing catalysts. *Catalysis Today*, *52*(4), 381–495. https://doi.org/10.1016/S0920-5861(99)00096-6

Furimsky, E. (2000). Catalytic hydrodeoxygenation. *Applied Catalysis A: General*, *199*(2), 147–190. https://doi.org/10.1016/S0926-860X(99)00555-4

He, Z., & Wang, X. (2012). Hydrodeoxygenation of model compounds and catalytic systems for pyrolysis bio-oils upgrading. *Catalysis for Sustainable Energy*, *Versita*, *1*, 28–52. https://doi.org/10.2478/cse-2012-0004

Hossain, M. M., Lopez, D., Herrera, J., & de Lasa, H. I. (2009). Nickel on lanthanum-modified gamma- Al2O3 oxygen carrier for CLC: Reactivity and stability. *Catalysis Today*, *143*(1–2), 179–186. https://doi.org/10.1016/j.cattod.2008.09.006

Jeangros, Q., Hansen, T. W., Wagner, J. B., Damsgaard, C. D., Dunin-Borkowski, R. E., Hebert, C., Hessler-Wyser, A. (2013). Reduction of nickel oxide particles by hydrogen studied in an environmental TEM. *Journal of Materials Science*, *48*(7), 2893–2907. https://doi.org/10.1007/s10853-012-7001-2

Kim, H. W., Kang, K. M., Kwak, H. Y., & Kim, J. H. (2011). Preparation of supported Ni catalysts on various metal oxides with core/shell structures and their tests for the steam reforming of methane. *Chemical Engineering Journal*, *168*(2), 775–783. https://doi.org/10.1016/j.cej.2010.11.045

Li, X., Liu, S., Zhu, X., Wang, Y., Xie, S., Xin, W., Xu, L. (2011). Effects of zinc and magnesium addition to ZSM-5 on the catalytic performances in 1-hexene aromatization reaction. *Catalysis Letters*, *141*(10), 1498–1505. https://doi.org/10.1007/s10562-011-0677-0

Marecot, P., Martinez, H., & Barbier, J. (1992). Coking Reaction by Anthracene on Acidic Aluminas and Silica-Aluminas. *Journal of Catalysis*, *138*, 474–481.

Mazumder, J., & De Lasa, H. (2014). Fluidizable Ni/La2O3-Al2O3 catalyst for steam gasification of a cellulosic biomass surrogate. *Applied Catalysis B: Environmental*, *160–161*(1), 67–79. https://doi.org/10.1016/j.apcatb.2014.04.042

Melchor-Hernández, C., Gómez-Cortés, A., & Díaz, G. (2013). Hydrogen production by steam reforming of ethanol over nickel supported on La-modified alumina catalysts prepared by sol-gel. *Fuel*, *107*, 828–835. https://doi.org/10.1016/j.fuel.2013.01.047

Mohan, D., Pittman, C. U., & Steele, P. H. (2006). Pyrolysis of wood/biomass for bio-oil: A critical review. *Energy and Fuels*, *20*(3), 848–889. https://doi.org/10.1021/ef0502397

Molina, R., & Poncelet, G. (1998). α-Alumina-Supported Nickel Catalysts Prepared from Nickel Acetylacetonate: A TPR Study. *Journal of Catalysis*, *173*(2), 257–267. https://doi.org/10.1006/jcat.1997.1931

Montini, T., Singh, R., Das, P., Lorenzut, B., Bertero, N., Riello, P., Fornasiero, P. (2010). Renewable H2 from Glycerol Steam Reforming: Effect of La2O3 and CeO2 Addition to Pt/Al2O3 catalysts. *ChemSusChem*, *3*(5), 619–628. https://doi.org/10.1002/cssc.200900243

Ogawa, Y., Toba, M., & Yoshimura, Y. (2003). Effect of lanthanum promotion on the structural and catalytic properties of nickel-molybdenum/alumina catalysts. *Applied Catalysis A: General*, *246*(2), 213–225. https://doi.org/10.1016/S0926-860X(03)00049-8

Popov, A., Kondratieva, E., Goupil, J. M., Mariey, L., Bazin, P., Gilson, J. P., Maugé, F. (2010). Bio-oils hydrodeoxygenation: Adsorption of phenolic molecules on oxidic catalyst supports. *Journal of Physical Chemistry C*, *114*(37), 15661–15670. https://doi.org/10.1021/jp101949j

Richardson, J. T., Scates, R., & Twigg, M. V. (2003). X-ray diffraction study of nickel oxide reduction by hydrogen. *Applied Catalysis A: General*, *246*(1), 137–150. https://doi.org/10.1016/S0926-860X(02)00669-5

Sánchez-Sánchez, M. C., Navarro, R. M., & Fierro, J. L. G. (2007). Ethanol steam reforming over Ni/La-Al2O3 catalysts: Influence of lanthanum loading. *Catalysis Today*, *129*(3–4), 336–345. https://doi.org/10.1016/j.cattod.2006.10.013

Siahvashi, A., & Adesina, A. A. (2013). Synthesis gas production via propane dry (CO2) reforming: Influence of potassium promotion on bimetallic Mo-Ni/Al2O3. *Catalysis Today*, *214*, 30–41. https://doi.org/10.1016/j.cattod.2012.12.005

Sugunan, S., & Sherly, K. B. (1993). Basicity and electron donor properties oflanthanum oxide and its mixed oxides with alumina. *Indian Journal of Chemistry*, *32A*(August), 689–692.

Tang, S., Ji, L., Lin, J., Zeng, H. C., Tan, K. L., & Li, K. (2000). CO2 Reforming of Methane to Synthesis Gas over Sol–Gel-made Ni/γ-Al2O3 Catalysts from Organometallic Precursors. *Journal of Catalysis*, *194*(2), 424–430. https://doi.org/10.1006/jcat.2000.2957

Vizcaíno, A. J., Carrero, A., & Calles, J. A. (2007). Hydrogen production by ethanol steam reforming over Cu-Ni supported catalysts. *International Journal of Hydrogen Energy*, *32*(10–11), 1450–1461. https://doi.org/10.1016/j.ijhydene.2006.10.024

Wang, J., Chernavskii, P. A., Wang, Y., & Khodakov, A. Y. (2013). Influence of the support and promotion on the structure and catalytic performance of copper-cobalt catalysts for carbon monoxide hydrogenation. *Fuel*, *103*, 1111–1122. https://doi.org/10.1016/j.fuel.2012.07.055

Wang, W. yan, Yang, Y. quan, Luo, H. an, & Liu, W. ying. (2010). Effect of additive (Co, La) for Ni-Mo-B amorphous catalyst and its hydrodeoxygenation properties. *Catalysis Communications*, *11*(9), 803–807. https://doi.org/10.1016/j.catcom.2010.02.019

Wang, W., Yang, Y., Luo, H., Peng, H., & Wang, F. (2011). Effect of La on Ni-W-B Amorphous Catalysts in Hydrodeoxygenation of Phenol. *Ind. Eng. Chem. Res.* 50, 10936–10942.http://dx.doi.org/10.1021/ie201272d.

Xu, Z., Li, Y., Zhang, J., Chang, L., Zhou, R., & Duan, Z. (2001). Bound-state Ni species - a superior form in Ni-based catalyst for CH4/CO2 reforming. *Applied Catalysis A: General*, *210*(1–2), 45–53. https://doi.org/10.1016/S0926-860X(00)00798-5

Yang, R., Li, X., Wu, J., Zhang, X., Xi, X., & Zhang, Z. (2009). Promotion effects of la and Ce on Ni/Al2O3 catalysts in hydrotreating of crude 2-ethylhexanol. *Catalysis Letters*, *132*(1–2), 275–280. https://doi.org/10.1007/s10562-009-0111-z

Yang, R., Li, X., Wu, J., Zhang, X., & Zhang, Z. (2009). Promotion effects of copper and lanthanum oxides on nickel/gamma-alumina catalyst in the hydrotreating of crude 2-ethylhexanol. *Journal of Physical Chemistry C*, *113*(41), 17787–17794. https://doi.org/10.1021/jp9053296

Zacher, A., Olarte, M., & Santosa, D. (2014). A review and perspective of recent bio-oil hydrotreating research. *Green Chemistry*, *16*(2), 491. https://doi.org/10.1039/c3gc41382a

Zhang, J., Wang, H., & Dalai, A. K. (2007). Development of stable bimetallic catalysts for carbon dioxide reforming of methane. *Journal of Catalysis*, *249*(2), 300–310. https://doi.org/10.1016/j.jcat.2007.05.004

Zhang, J., Xu, H., & Li, W. (2005). Kinetic study of NH3 decomposition over Ni nanoparticles: The role of la promoter, structure sensitivity and compensation effect. *Applied Catalysis A: General*, *296*(2), 257–267. https://doi.org/10.1016/j.apcata.2005.08.046

Chapter 5

5.1 Conclusions

Hydrodeoxygenation of anisole, a bio-oil model compound, was successfully carried out in the EA reactor with comparable conversion rates at relatively shorter reaction times when compared to previous HDO studies in the literature with stirred reactors. The EA reactor was initially validated for catalytic hydrodeoxygenation of anisole at varying reaction times (30 – 120min) and temperatures (160^oC – 280^oC) using 10 wt%. nickel supported on 3 different supports, including γ – alumina, δ – alumina, and silica. Anisole conversions of 100% were obtained with all three supports at 220°C after 30 minutes, though silica supported catalysts demonstrated limited deoxygenation activity, even when reaction temperature was increased to 280°C. The γ-alumina support demonstrated the highest degree of deoxygenation out of all 3 supports, with cyclohexane selectivity varying significantly from 17% to 100% when reaction temperatures varied from 160°C to 280°C. The 10 wt.% Ni/ γ-alumina at 220°C and 45 minutes was thus selected as a baseline for subsequent catalyst optimization experiments.

Comparisons were made between the EA reactor and a mechanically stirred batch reactor operating at equivalent conditions and catalyst compositions. The EA reactor demonstrated improved anisole conversion relative to the mechanically stirred reactor with all Ni and Ni-Cu catalysts tested. The increase in anisole conversion was a result of an increase in hydrogenation, and thus methoxycylohexane, and deoxygenation towards cyclohexane. This would suggest that the EA reactor influences the mass transfer between the gas-liquid phases, likely a result of the greater interfacial area.

Monometallic Ni and bimetallic Ni-Cu of low metal loading were compared at the established operating conditions. Total hydrogen consumption for the TPR profiles increased when nickel loading was increased from 2 wt.% to 10 wt.% for monometallic Ni catalysts, but the proportion of reducible NiO species that were present did not increase uniformly. This non-linear increase in NiO species relative to increasing metal loading is likely due to varying nickel particle size and dispersion that interact with the support differently. Copper addition to the nickel-based catalysts improved reducibility and increased the proportion of NiO species relative to catalysts without copper of equal total loading. The improved reducibility with copper addition is believed

to be a result of the strong interaction between nickel and copper species, reducing the metal-support interaction. Based on detectable liquid and gas products, the reaction pathway included an initial hydrogenation of the aromatic ring in anisole to form methoxycylohexane, then a demethylation to form cyclohexanol, and finally deoxygenation to form cyclohexane. Deoxygenation yields remained relatively constant when nickel loading was increased from 2 wt.% to 10 wt.%, even though methoxycyclohexane yields were seven times greater in the latter. Monometallic Ni catalysts resulted in higher cyclohexane yields relative to bimetallic Ni-Cu catalysts of equal metal loading. Catalyst coke formation following HDO tests decreased as nickel loading increased for monometallic Ni catalysts. The effects of copper promotion on coke formation was dependent on total metal loading, where coke deposits were greater for the bimetallic Ni-Cu catalyst at 5 wt.% total metal loading, but was greater for the monometallic Ni catalyst at 10 wt.% total metal loading. The differences in coke formation is thought to be influenced by varying nickel particle size and dispersion, where smaller, more dispersed Ni particles reduce the prevalence of coke formation.

Lanthanum promotion was then studied on the monometallic Ni and bimetallic Ni-Cu catalysts. When 1 wt.% of La was initially impregnated, the degree of reducibility below 400°C for all catalysts was improved and the proportion of NiO species increased. This was believed to be due to the strong interaction between nickel and lanthanum, weakening the Ni-Al interaction to form more easily reducible NiO species on the catalyst surface. Lanthanum addition also reduced anisole conversion for all catalysts, independent of total metal loading or the presence of copper, where both methoxycyclohexane and cyclohexane yields decreased. Contrary to the expected lower coke formation due to the basic nature of lanthanum, coke formation generally increased relative to unpromoted Ni and Ni-Cu catalysts. This once again was thought to be the result of larger nickel particle size and less dispersion, facilitating coke formation.

5.2 Recommendations

Results demonstrated that the Externally Agitated (EA) reactor is an effective mixing method for catalytic hydrodeoxygenation using a model compound. The EA reactor showed possible enhancements over mechanically stirred batch reactors, but the comparisons were limited in terms of catalyst and operating conditions. Future experiments should compare the EA reactor and a mechanically stirred reactor at different operating conditions to better demonstrate potential

gas-liquid mass transfer improvements with the EA reactor. Performing experiments at higher temperatures, increasing the hydrogen consumption in the liquid and at the catalyst surface, would result in gas-liquid mass transfer limitations, potentially demonstrating improved mixing in the EA reactor when compared to impeller systems.

Adding a basic promoter like lanthanum was observed to reduce overall conversion and deoxygenation activity and increased coke production. It is recommended to investigate an acidic promoter's impact on conversion, selectivity, and coke production with varying support materials. For example, niobium oxide has been previously demonstrated as a potential acidic promoter in other related studies.

Since nickel dispersion and particle size is expected to influence several factors regarding catalytic activity, reducibility, and coke formation, analytical techniques should be implemented to effectively measure dispersion and particle size on the support. This would include x-ray diffraction (XRD) and transmission electron microscopy (TEM) which could provide more information on crystalline structure and particle size distribution of metals located on the catalysts surface. To better characterize support acid sites, ammonia TPD could be performed as well.

The experimental setup could be improved with the addition of a sampling attachment, where small fractions of liquid products would be extracted as the reaction is proceeding, allowing conversion, product selectivity, and yields to be analyzed as a function of reaction time. This would provide important information for reaction pathways while also improving reaction kinetic measurements.

Finally, although the EA reactor has successfully demonstrated HDO of a model compound, further studies must ultimately investigate the HDO of a real pyrolysis bio-oil where coke formation, and thus catalyst deactivation, is much more susceptible. This would certainly determine if the EA reactor is an acceptable system for bio-oil HDO and display its applicability as a promising novel reactor configuration for these studies.

Title: An overview of fast pyrolysis of biomass

Author: A.V. Bridgwater,D. Meier,D. Radlein

Publication: Organic Geochemistry

Publisher: Elsevier

Date: December 1999

Order Completed

Thank you for your order.

This Agreement between Western University -- Brett Pomeroy ("You") and Elsevier ("Elsevier") consists of your license details and the terms and conditions provided by Elsevier and Copyright Clearance Center.

Your confirmation email will contain your order number for future reference.

printable details

License Number	4251690812311
License date	Dec 17, 2017
Licensed Content Publisher	Elsevier
Licensed Content Publication	Organic Geochemistry
Licensed Content Title	An overview of fast pyrolysis of biomass
Licensed Content Author	A.V. Bridgwater,D. Meier,D. Radlein
Licensed Content Date	Dec 1, 1999
Licensed Content Volume	30
Licensed Content Issue	12
Licensed Content Pages	15
Type of Use	reuse in a thesis/dissertation
Portion	figures/tables/illustrations
Number of figures/tables/illustrations	2
Format	both print and electronic
Are you the author of this Elsevier article?	No
Will you be translating?	No
Original figure numbers	Figure 1, 2
Title of your thesis/dissertation	Hydrodeoxygenation of Anisole in a Novel Externally Agitated Reactor
Expected completion date	Dec 2017
Estimated size (number of pages)	101
Requestor Location	Western University 1151 Richmond St. London, ON N6G 5A4 Canada Attn: Western University
Total	0.00 CAD

ORDER MORE CLOSE WINDOW

Title: A review of catalytic upgrading of bio-oil to engine fuels

Author: P.M. Mortensen,J.-D. Grunwaldt,P.A. Jensen,K.G. Knudsen,A.D. Jensen

Publication: Applied Catalysis A: General

Publisher: Elsevier

Date: 4 November 2011

Order Completed

Thank you for your order.

This Agreement between Western University -- Brett Pomeroy ("You") and Elsevier ("Elsevier") consists of your license details and the terms and conditions provided by Elsevier and Copyright Clearance Center.

Your confirmation email will contain your order number for future reference.

printable details

License Number	4251690353062
License date	Dec 17, 2017
Licensed Content Publisher	Elsevier
Licensed Content Publication	Applied Catalysis A: General
Licensed Content Title	A review of catalytic upgrading of bio-oil to engine fuels
Licensed Content Author	P.M. Mortensen,J.-D. Grunwaldt,P.A. Jensen,K.G. Knudsen,A.D. Jensen
Licensed Content Date	Nov 4, 2011
Licensed Content Volume	407
Licensed Content Issue	1-2
Licensed Content Pages	19
Type of Use	reuse in a thesis/dissertation
Portion	figures/tables/illustrations
Number of figures/tables/illustrations	1
Format	both print and electronic
Are you the author of this Elsevier article?	No
Will you be translating?	No
Original figure numbers	Figure 1
Title of your thesis/dissertation	Hydrodeoxygenation of Anisole in a Novel Externally Agitated Reactor
Expected completion date	Dec 2017
Estimated size (number of pages)	101
Requestor Location	Western University 1151 Richmond St. London, ON N6G 5A4 Canada Attn: Western University
Total	0.00 USD

ORDER MORE CLOSE WINDOW

Title: Screening of Catalysts for Hydrodeoxygenation of Phenol as a Model Compound for Bio-oil

Author: Peter M. Mortensen, Jan-Dierk Grunwaldt, Peter A. Jensen, et al

Publication: ACS Catalysis

Publisher: American Chemical Society

Date: Aug 1, 2013

PERMISSION/LICENSE IS GRANTED FOR YOUR ORDER AT NO CHARGE

This type of permission/license, instead of the standard Terms & Conditions, is sent to you because no fee is being charged for your order. Please note the following:

- Permission is granted for your request in both print and electronic formats, and translations.
- If figures and/or tables were requested, they may be adapted or used in part.
- Please print this page for your records and send a copy of it to your publisher/graduate school.
- Appropriate credit for the requested material should be given as follows: "Reprinted (adapted) with permission from (COMPLETE REFERENCE CITATION). Copyright (YEAR) American Chemical Society." Insert appropriate information in place of the capitalized words.
- One-time permission is granted only for the use specified in your request. No additional uses are granted (such as derivative works or other editions). For any other uses, please submit a new request.

If credit is given to another source for the material you requested, permission must be obtained from that source.

Curriculum Vitae

Post-secondary Education and Degrees:

Master of Engineering Science **2015 - 2017**
Reaction and Process Systems
Western University, London, Ontario, Canada

Honours Bachelor of Science **2010 - 2015**
Biochemistry
Wilfrid Laurier University, Waterloo, Ontario, Canada

Honours and Awards:

FOSSA Research Assistant Scholarship **2015**
Wilfrid Laurier University, Waterloo, Ontario, Canada

Related Work Experience:

Teaching Assistant, Chemical and Biochemical Engineering **2015 - 2017**
Western University, London, Ontario Canada

Research Assistant **2014 - 2015**
Centre for Cold Regions and Water Science
Wilfrid Laurier University, Waterloo, Ontario, Canada

Instructional Assistant **2014**
Wilfrid Laurier University, Waterloo, Ontario, Canada